The role of hepatoma derived growth factor in tissue injury and repair

Anastasia Ardasheva

Supervised by
Professor Tonia Vincent
Professor Philippa Hulley
Professor Adrien Hallou

Harris Manchester College
University of Oxford

A thesis submitted in fulfilment of the requirements
of the degree of *Doctor of Philosophy*

Abstract

The role of hepatoma derived growth factor in tissue injury and repair

Connective tissues, including skin and cartilage, utilise several mechanisms to respond to injury. In cartilage, one such mechanism is through the release of heparin-bound growth factors from the extracellular matrix. These include fibroblast growth factor (FGF)-2 and connective tissue growth factor (CTGF) which are pro-regenerative in both skin and cartilage. Another growth factor is hepatoma derived growth factor (HDGF), about which little is known. We hypothesised that HDGF, like FGF2 and CTGF, plays a role in tissue injury and repair.

Medium conditioned by injured skin and cartilage (pig and mouse) confirmed an injury-dependent release of HDGF protein in normal wild-type (WT) tissues, but not in HDGF-knockout (*Hdgf*$^{-/-}$). Bulk RNA sequencing analysis showed similar responses to injury at 4 hours in WT and *Hdgf*$^{-/-}$ cartilage. Five genes, including *Hdgf* itself, were differentially expressed at baseline in both skin and cartilage. Three of these were genes encoding ribosomal subunits leading to further investigation of HDGF's role in protein translation. *Ex vivo* SILAC labelling of newly synthesised proteins in injured skin (at 48 hours) revealed a global decrease in protein synthesis in *Hdgf*$^{-/-}$ tissue as well as a strong reduction in proteins involved in translation.

In vivo, murine, studies revealed a delay in skin wound healing in 15- and 26-week-old, but not 10-week-old, *Hdgf*$^{-/-}$ male mice when compared with age-matched WT animals. Histological analysis of wounds confirmed features of delayed healing (delayed re-epithelialization and increased granulation tissue) in 15-week-old *Hdgf*$^{-/-}$ males. This work demonstrates for the first time the injury-

induced nature of HDGF release in skin and cartilage and its role in skin repair. The mechanism for HDGF's effects after tissue injury does not appear to be through early transcriptional regulation, but through control of protein translation.

Declaration

I hereby declare that the experimental work and the thesis are my own work. I have appropriately acknowledged people who assisted me in experimental work and analysis within each chapter. All experimental work was undertaken in line with the regulations of the Kennedy Institute of Rheumatology and the University of Oxford. All material is appropriately cited and acknowledged in the relevant sections throughout this thesis.

Acknowledgements

I would like to thank my supervisor, Professor Tonia Vincent, for taking me under her wing for the last three years and for helping me navigate my project during its highs and lows. Tonia helped me hit the ground running from day one, pushed me out of my comfort zone, and always encouraged me to be brave and creative with my science. I would also like to thank my co-supervisors, Professors Philippa Hulley and Adrien Hallou, for providing helpful input at various points throughout my project and for their willingness and availability to always support me whenever I needed them. I would also like to thank my college tutor Dr Gina Hadley for supporting my decision to pursue a DPhil in the middle of graduate-entry medicine course and for her continued pastoral support over the last five years. Lastly, I want to thank every single person at the Vincent group, the wider Kennedy Institute, and Botnar Research Centre that I have crossed paths with for their help, large or small, with experimental work and data analysis and, most importantly, for their friendship and encouragement. It truly takes a village to complete a DPhil in 3 years, and I would have never been able to do it without them.

On a personal note, I would like to thank my parents and sisters for their continuous emotional support during my lengthy academic journey. Every phone call and meme on Instagram brightened my mood on days when my experiments failed. I want to thank Jakub and my cats Rembrandt and Motya for being my immediate support network on a daily basis, especially during the write-up period, and for making sure I eat and sleep well. I also thank Geert for supporting my career aspirations and my decision to pursue medicine and a PhD at Oxford. Lastly, I thank all my Oxford friends for their unwavering support throughout my PhD and for the fun memories we have created together.

Table of Contents

Chapter 1: Introduction.

1.1. Tissue injury and repair

Tissue injury is defined as a disruption to the normal architecture or function of bodily tissues that activates multiple overlapping processes, including inflammation, tissue formation and remodelling, aimed to repair the tissue and restore its original function.[1] Understanding the mechanisms behind tissue repair and regeneration have always been important in medicine, as they can determine patient outcomes following different types of trauma (e.g. mechanical, burns, bleeding, etc.), surgery, and various diseases that affect the architecture and/or function of tissues. In Europe and the USA, high incidence of common causes that are associated with poorer tissue healing (e.g. ageing population, diabetes mellitus, cancer, more surgical procedures) make it especially important to understand better the processes of tissue repair to improve patients' quality of life.[2]

When mammalian tissues are injured, they deploy a multitude of processes aiming to restore structural and functional integrity of the damaged tissue. Regardless of the tissue type (e.g. bone, skin, or internal organs), the cascade of events triggered by injury to vascularised tissues generally consists of four phases: 1) haemostasis (platelets adhere to exposed collagen and von Willebrand factor, forming a temporary fibrin clot), 2) inflammation (activation of inflammatory and immune cells in response to "damage" signals), 3) proliferation (formation of granulation tissue, new vessels and tissue deposition), and 4) remodelling (progressive restoration of original structure and function).[3] In the context of tissue response to injury, the term "repair" is generally defined as the restoration of tissue continuity and is broadly differentiated into two subtypes: regeneration and replacement (also sometimes referred to as "repair"). Regeneration is the process

by which injured tissue is replaced with new tissue identical in structure and function to the original, leaving no evidence of prior damage.[1] This requires the proliferation of surviving cells, activation and differentiation of tissue stem cells, and occasionally the de-differentiation of mature cells into precursor cells. Notable examples of tissue regeneration in humans include regrowth of the liver after partial removal and ongoing renewal of the epidermis and gut lining, which benefit from high rates of cellular turnover and stem cells embedded within the tissue.[2 4]

Replacement (or repair), however, is a type of response to injury that leads to "imperfect" tissue restoration that often fails to re-establish the original function and/or architecture of the damaged tissue.[5] For the purposes of this work, I will further refer to "replacement" as "repair". When the regenerative capacities of the tissue are limited - due to extensive loss of extracellular matrix (ECM), a shortage of stem cells, a lack of vasculature, or predominance of mature and non-dividing cells - the tissue often cannot be fully regenerated.[1] Repair is thus often characterised by proliferation and migration of fibroblasts, influx of inflammatory debris-removing cells, and deposition of new collagen, resulting in formation of fibrous (scar) tissue. Oftentimes, this newly formed fibrous tissue provides necessary strength but lacks the specialised properties of the original tissue, often resulting in compromised tissue function, as seen following heart attacks or deep skin wounds.[3] Several key factors distinguish regeneration from repair. Tissues with abundant and accessible stem cells and rapid cell turnover, such as epithelium, regenerate better, while those with fewer stem cells and a lack of vasculature may repair primarily through fibroblast activity leading to fibrotic tissue formation.[1-3] Several factors can shift the balance towards scar formation. For instance, preservation of the ECM scaffold facilitates regeneration, whereas its degradation

promotes fibrosis. A persistent inflammatory response is another factor that can contribute to excessive fibrosis, delayed healing, and suppressed tissue regeneration.[3]

Connective tissues, including skin, ligaments, tendons, cartilage, and bone, heal through proliferation of endogenous mesenchymal cells. Following injury, these tissues progress through an inflammatory phase which is at least in part regulated by the connective tissue cells themselves. The activated cells are capable of secreting cytokines and growth factors like transforming growth factor β (TGF-β).[6 7] In the proliferative phase, connective tissue cells expand and synthesise ECM, notably collagen and elastin, according to tissue type.[8-10] Finally, the remodelling phase aims to remodel the collagenous architecture and restore shape and function albeit often imperfectly.[3 11 12] The final outcome is typically a fibrotic scar that does not fully recapitulate the biomechanical or physiological properties of the original connective tissue. Both human and animal studies confirm that regeneration is limited to select organs and circumstances (e.g. liver regeneration, human oral mucosa, the endometrium), while repair by fibrosis is the dominant response in most mature connective tissues. Additionally, other factors such as microbiome, age, and hormones can affect how tissue responds to injury.[2] In this thesis, I will examine the response to injury in two connective tissues - cartilage and skin - with the aim to understand better the biology of connective tissue repair.

1.2. Unmet clinical needs: cartilage degradation, chronic skin wounds, and scars

Osteoarthritis (OA) is a disease of cartilage degradation, low grade synovitis, and bone remodelling, and is one of the most common diseases worldwide, estimated to affect nearly 600 million people worldwide.[13] [14] OA poses a rapidly growing clinical and public health challenge worldwide, driven by ageing population, obesity, and increased sports-related injuries. According to most recent estimates, the incidence of OA is projected to increase 75% for knee, 49% for hand, 79% for hip, and 95% for other types of OA by 2050.[14] OA comes with a great cost, as, in the US alone, where over 30 million people live with OA, its estimated yearly economic burden stands at more than $136 billion.[15] This disease results in progressive cartilage degradation, pain, disability, and diminished quality of life, contributing to nearly 12 million disability-adjusted life years (DALYs) among working-age individuals globally.[16] Despite its devastating effects, there is currently no cure for OA and its management consists mainly of pain relief, often including opioids, and joint replacement surgery. As articular cartilage is an avascular tissue and has limited intrinsic healing capacity, current clinical approaches include autologous chondrocyte implantation and minimally invasive surgeries, which generally fail to restore hyaline cartilage structure or to halt disease progression.[17] OA was originally described as a “wear-and-tear” disease, and only more recently it has been re-defined as a disease of balance between mechano-inflammatory and pro-regenerative responses driven by the acute injury response.[18] [19] These limitations highlight an unmet clinical need for improved understating of cartilage response to injury that could lead to the development of innovative treatments

capable of promoting cartilage repair and restoring joint function to mitigate the global burden of OA.

Chronic skin wounds represent a similarly significant clinical challenge affecting an estimated 10.5 million Medicare beneficiaries in the US, costing the healthcare system approximately $22.5 billion annually.[20] Chronic wounds are skin defects that have not gone through orderly repair following injury, resulting in failure of structural and functional reconstruction of the tissue. Chronic wounds are classified based on the underlying cause, such as vascular insufficiency, diabetes mellitus, pressure ulcers, immunocompromised status, age, and other comorbidities.[2] In the US alone, chronic wounds affect approximately 6.5 million people annually, with diabetic foot ulcers, venous leg ulcers, and pressure ulcers among leading causes.[20] Despite advances in both diagnostics and therapy, resources remain insufficient to match the scale and complexity of the problem, resulting in high rates of incomplete healing, persistent pain, and risk of serious complications like infection and possible amputation. Most chronic wounds fail to restore the skin's barrier function, making the skin susceptible to further tissue breakdown and resulting in ongoing healthcare utilisation and diminished quality of life for millions of patients.[20] The lack of effective and universally adopted strategies for prevention, diagnosis, and management means that many wounds remain untreated or suboptimally managed, resulting in increasing incidence of chronic wounds alongside other contributing factors such as ageing population, diabetes, and vascular disease. Recent policy changes, such as extended wound care packages introduced into clinical practice, legislation aimed at improving access to wound care, and emerging technologies, such as telemonitoring of wounds and incorporation of bioengineered skin, show promise, but the scale and impact of the

problem highlight the need for wound care research.[20] Understanding biology of skin wound healing can help identify potential new therapeutic targets and provide better care for millions of patients.

While chronic wounds are characterised by "under-healing", the other end of the spectrum is scarring or "over-healing". Similar to chronic wounds, scars constitute another major unmet need in regenerative medicine. While scar formation is essential for initial wound closure, fibrotic scars differ markedly from native tissue: unlike uninjured skin, they lack any of the appendages such as hair follicles and sweat/sebaceous glands, have denser extracellular matrix, and are mechanically weaker and less elastic. These deficits can impair thermoregulation, limit mobility (e.g. if a stiff scar tissue is located over a joint), potentially necessitating surgical intervention to prevent functional loss. Pathological scarring, including hypertrophic scars (affecting over 90% of burn patients) and keloids (benign fibrotic tumours which extend beyond the original wound boundaries), adds to this burden, often causing pruritus (itching), discomfort, and pain.[21] [22] Globally, rising rates of burns, surgery, trauma, and comorbidities such as diabetes and vascular disease contribute to increased scar prevalence, with the global scar treatment market valued at $20 billion in 2020 and projected to reach $60 billion within 10 years. Despite this significant burden, current treatments, such as silicone dressings, topical agents, and surgical revision, often fail to restore the native architecture and/or function of the skin.[22] More research on scarring will help to deepen understanding of the cellular and molecular mechanisms driving fibrosis and can lead to development of innovative therapies that can minimise or prevent scarring and transform patient outcomes. This work addresses an important unmet

clinical need of understanding the mechanisms behind tissue response to injury and its further repair by using cartilage and skin as model tissues.

1.3. The cartilage

1.3.1. Cartilage anatomy and function

Cartilage is a specialised connective tissue fundamental to joint and skeletal function. There are three distinct types of cartilage: hyaline, fibrocartilage, and elastic cartilage. Hyaline cartilage is the most abundant type in the human body, found on articular surfaces of bones, the trachea, nose, epiphyseal growth plate, and ventral segments of the ribs. Its smooth surface enables low-friction articulation, playing a crucial role in joint movement and shock absorption. Main components of hyaline cartilage are collagen type II and proteoglycans. Fibrocartilage is the toughest and least flexible type, consists mainly of type I collagen, and is enriched with dense collagen fibres, giving it ability to withstand high degrees of tension and compression. It is present in intervertebral discs, menisci, and ligament-tendon interfaces. Elastic cartilage, containing networks of elastin and collagen fibres, is highly flexible, enabling structural support in areas requiring repeated bending such as the ear, larynx, and epiglottis.[23]

Microscopically, cartilage is an avascular tissue that can be divided into three zones: a superficial zone (containing flattened chondrocytes and collagen fibres aligned parallel to the joint surface), a thick middle zone (home to sparsely located chondrocytes surrounded by the proteoglycan-rich extracellular matrix (ECM)), and a deep zone (housing large collagen fibrils and chondrocytes organised in columns), which contains a “tidemark” separating hyaline and calcified cartilage, which, in turn, borders the subchondral bone.[24] Healthy articular cartilage is comprised of chondrocytes surrounded by a pericellular matrix (PCM), containing heparan sulfate proteoglycan perlecan, growth factors, hyaluronic acid, and type VI

collagen, and an aggrecan- and hyaluronan-rich territorial/inter territorial matrix that together form the ECM (Figure 1.1).[25]

Cartilage can be affected by a wide range of diseases that impair its structure and function, often leading to pain, disability, and joint degeneration. OA is the most common disease of cartilage degradation that results in pain, stiffness, and reduced mobility.[14] Rheumatoid arthritis damages cartilage through autoimmune inflammation, while rare type II collagen disorders such as achondrogenesis or spondyloepimetaphyseal dysplasia impair cartilage development and cause skeletal abnormalities.[26] [27] Other diseases affecting cartilage include osteochondritis dissecans, which primary affects children and adolescents and is characterised by focal cartilage and subchondral bone lesions, relapsing polychondritis that causes recurrent inflammation of cartilage in the ears, nose, and airways, and chondrocalcinosis (also known as pseudogout) that provokes acute inflammation and joint damage via deposition of calcium pyrophosphate crystals.[28-30] Cartilage can also develop benign or malignant tumours, including osteochondromas and chondrosarcomas, which can also impair tissue architecture and/or function.[31]

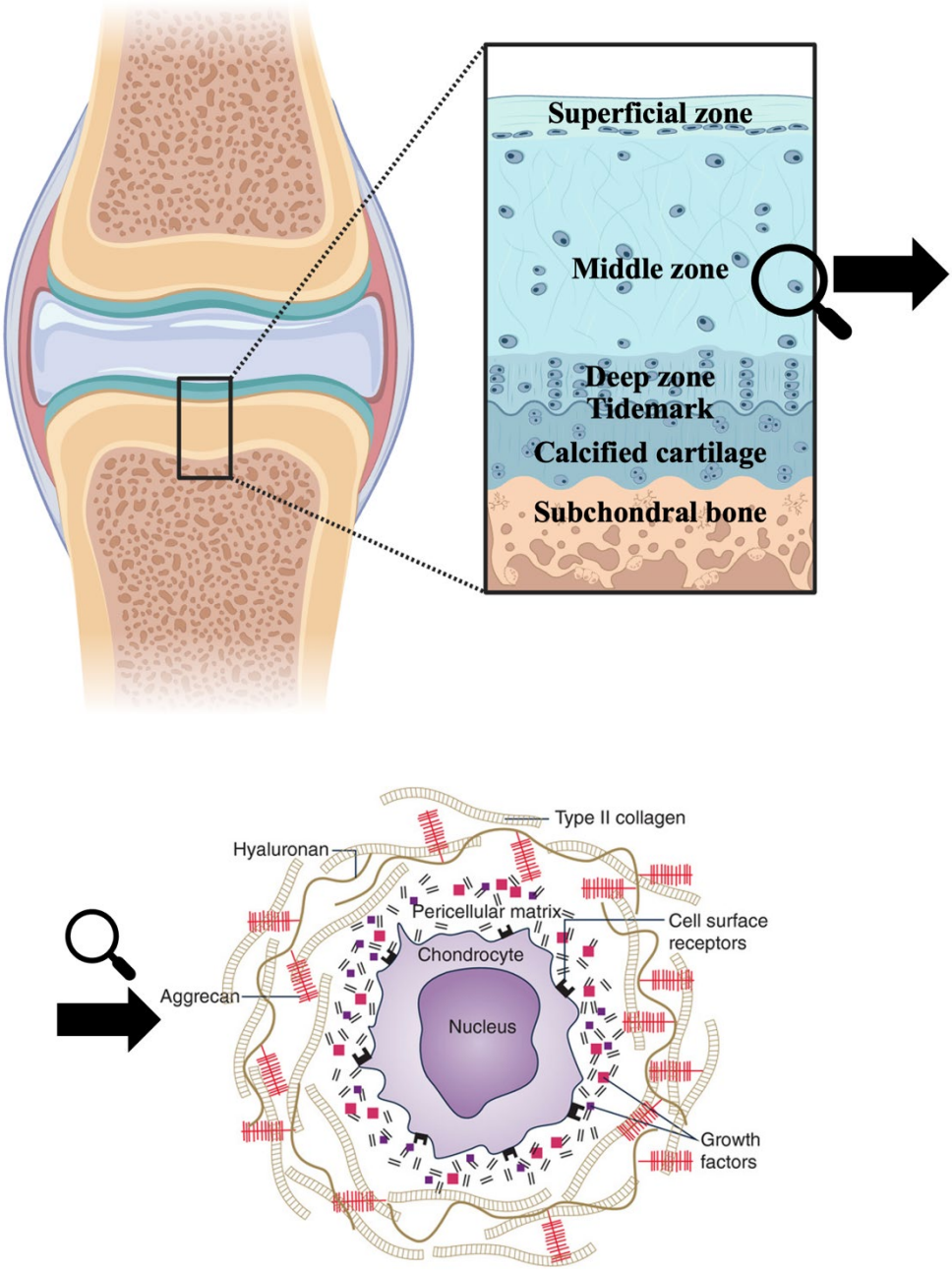

Figure 1.1. Microscopic structure of articular cartilage. Zones of articular cartilage are labelled and the magnified view of the chondrocyte with its surrounding matrix is shown. Image of the cartilage is created in BioRender. The image of the chondrocyte is taken from Vincent & Wann, *J Physiol*, 2019.[32]

1.3.2. Cartilage repair

For a long time, cartilage has been regarded as a tissue with limited capacity to repair. In 1743, William Hunter, a Scottish anatomist and physician, wrote: "from Hippocrates down to the present Age, we shall find, that an ulcerated Cartilage is universally allowed to be a very troublesome Disease; that it admits of a Cure with more Difficulty than a carious Bone; and that, when destroyed, it is never recovered."[33] This notion remained largely unchallenged until the mid-19th century when researchers and doctors began questioning its validity. Through a combination of clinical observations, animal studies, and *ex vivo* tissue models, scientists have since explored repair mechanisms of what was once thought to be an irreparable tissue.

Over a century after Hunter's statement about the lack of reparative capacity in cartilage, Redfern provided evidence to the contrary, demonstrating that cartilage responded to injury by forming fibrous tissue.[34] Haas further advanced this research through animal studies, demonstrating that costal cartilage was capable of regenerating from the perichondrium.[35] Shortly after, Shands proposed distinct stages of cartilage regeneration: 1) fibrin formation, 2) granulation tissue development, 3) connective tissue formation, 4) emergence of cartilage cells in connective tissue (connective tissue cartilage), 5) formation of fibrocartilage, and 6) its transformation into hyaline cartilage.[36] Bennett et al showed that, while cartilage exhibited a limited ability to heal superficial defects with better healing documented in weight-bearing regions, deeper defects were repaired with cartilaginous tissue originating from the bone marrow (BM), synovium, and cartilage itself.[37] Collectively, these studies shifted the perception of cartilage from a non-repairing tissue to one with regenerative potential.

1.3.3. Intrinsic versus extrinsic cartilage repair: the historical perspective

Buckwalter et al defined "repair" as "the restoration of a damaged articular surface with new tissue that resembles but does not duplicate the structure, composition, and function of articular cartilage", whereas the term "regeneration" referred to the "formation of new tissue indistinguishable from normal articular cartilage."[38] Broadly speaking, one can classify the process of intrinsic cartilage repair as one that relies on cells residing within the cartilage, whereas extrinsic cartilage repair is driven by cells originating outside of the cartilage.[39] Several mechanistic studies conducted in the 1960s greatly advanced the understanding of both intrinsic and extrinsic cartilage repair. These studies largely utilised two cartilage injury models: a superficial (or partial) thickness or a deep (or full) thickness scarification of the cartilage. Superficial defects were confined to the articular cartilage, whereas deep defects extended into the subchondral bone.

Research on superficial cartilage defects has generally demonstrated that such injuries stimulated chondrocytes in the vicinity of the injury site, prompting their activation, proliferation, and filling of the defect. However, this response tended to be short-lived, and the newly formed cartilage was not consistently hyaline in nature. Mankin examined cartilage of immature rabbits and its response to injury: he identified two distinct growth regions in the cartilaginous epiphysis - one beneath the articular cartilage, which contributed to articular surface formation, and another near the ossific nucleus of the epiphysis.[40] He suggested that the cartilage response to injury involved both necrosis and cellular proliferation observed on either side of the wound and likely originated from the superficial growth layer.[41] Similarly, Calandruccio & Gilman observed in immature dogs that partial-thickness defects initiated a reparative response arising from the superficial

cartilage layer. However, the production of hyaline cartilage was observed only in a limited number of cases.[42] Meachim et al reported that chondrocytes adjacent to an injury site in rabbit knees became activated, exhibiting migration and collagen degradation activity. Nevertheless, this response diminished over time, disappearing by six weeks.[43] Other studies have failed to show significant healing of superficial cartilage defects among adult animals,[44-47] even over extended periods, such as a two-year follow-up.[48] While some studies reported partial repair of superficial cartilage defects, this process was often incomplete and varied depending on the injury site.[49] [50] Notably, the only study that observed full spontaneous regeneration of superficial cartilage defects was conducted on foetal lambs. The study followed subjects for 28 days, potentially too short a timeframe to assess long-term outcomes, preceding the maturation of articular cartilage.[51] Another study examining age-related differences in superficial cartilage defect repair found no significant difference in cartilage repair between cartilage explants from immature and mature bovine articular cartilage.[52] It did, however, support earlier claims of the dual nature of the cartilage response to superficial injury with regards to proliferation and apoptosis: cells that did not die in response to injury were capable of proliferating, but no migration or healing was observed.[52] [53]

In contrast to superficial defects, research on deep cartilage defects has generally reported evidence of cartilage repair. However, the nature of this repair and whether it resulted in the formation of hyaline cartilage remains a topic of debate. Shands and Bennett et al first proposed that hyaline cartilage could emerge from the subchondral bone via a transitional granulation tissue and fibrocartilage.[36] [37] Building on this idea, Calandruccio & Gilman observed that in cases where fibrocartilage did not completely fill the deep defect, hyaline cartilage appeared to

form. This observation led them to speculate that granulation tissue originating from the subchondral bone might actually hinder hyaline cartilage development.[42]

Subsequent studies investigating deep cartilage defects suggested that hyaline cartilage formation could be originating from cells from the subchondral bone and/or bone marrow-derived mesenchymal stem cells (BM-derived MSCs). DePalma et al identified subchondral granulation tissue as a cartilage-producing source, irrespective of age.[44] Some studies, however, have reported accelerated healing and increased cell proliferation in younger animals.[46 54 55] Specifically, Wei et al demonstrated that deep cartilage defects in young animals could heal with hyaline cartilage from the granulation tissue originating from the BM.[54]

Cheung et al compared full thickness cartilage defects with and without subchondral bone drilling, finding that deeper drilling promoted hyaline cartilage formation.[47] This finding has been reinforced by multiple later studies.[45 56-59] This method, known as Pridie drilling, is commonly employed in orthopaedic surgery. While in humans this technique primarily results in fibrocartilage rather than hyaline cartilage formation, it has been shown to improve OA-associated pain.[60] Other invasive techniques tested in the context of cartilage included Milgram's study examining the response to cartilage injury in patients with chondromalacia who had undergone an elective cartilage shaving procedure. He concluded that the healing observed was fibrocartilaginous without evidence of involvement of local chondrocytes.[61] Fibrocartilage was also observed by Kaul et al after microfracture in patients with OA.[62]

Even in the early studies by Bennett and Calandruccio, the newly formed cartilage was often described as "imperfect," exhibiting discontinuities, fibrillations, and fibrous components.[37 42] Later research largely concluded that the

predominant resultant cartilage was fibrocartilage.[50 63 64] A study by Mitchell & Shepard demonstrated that, while hyaline cartilage initially developed from the subchondral bone within two months of an injury, it progressively lost its hyaline appearance at 8 months, transforming into a collagenous dense tissue by the 12-month mark.[65] A critical perspective on cartilage healing following deep defects was presented by Shapiro et al. Their findings indicated that, although new cartilage emerged from the BM, it failed to integrate seamlessly with the existing cartilage. Subjecting it to mechanical stress and micromotion led to widespread joint degeneration.[66] Overall, the findings of these studies indicate that while deep cartilage defects exhibit a greater capacity for repair, the resultant cartilage often differs from the original hyaline cartilage in both composition and mechanical properties.

1.3.4. Origin of cartilage repair cells

The source of intrinsic cartilage repair cells has been subject to debate over the years. A number of sources of repair cells have been proposed including BM MSCs, synovium-derived cells, and articular cartilage itself (Figure 1.2).[67] A population of putative progenitor cells which were termed chondrogenic progenitor cells (CPCs) was identified in immature bovine articular cartilage after multiple passaging of isolated cells.[68] A study of late-stage OA cartilage revealed the presence of CPCs in human cartilage and demonstrated migratory, clonogenic, and stem-like potential of these cells, suggesting their function as intrinsic cartilage repair cells.[69 70] In animal tissue, CPCs were also identified as a potential source of intrinsic cartilage repair in equine tissue. While similar in stemness characteristics to BM MSC, CPCs were able to generate cartilage that was closer in composition

to articular cartilage than the hypertrophic collagen X-rich cartilage produced by BM MCS.[71]

Collins & McElligott looked at the cellular changes accompanying OA progression in humans. They characterised sulphate incorporation by human chondrocytes, indicative of new proteoglycan synthesis, at different stages of OA and observed increased chondrocyte activity as patients aged and as OA progressed. These findings led the authors to conclude that OA was not a disease of declining function of chondrocytes, but rather the opposite - that the loss of matrix was associated with an increased synthesis of new matrix by chondrocytes.[72] A study by Mankin and colleagues found that, in human OA femoral heads, DNA synthesis was increased in early/moderate OA, but declined significantly as disease progressed.[73] More recent studies indicate that, in the OA joint, cell populations that have the ability to proliferate and undergo chondrogenesis can be found in the synovial fluid, synovium, and cartilage. Many of these studies have characterised the repair cell in question *in vitro* and the relative role of these *in vivo* is unanswered.[74-81] A recent study of deep cartilage defects in mice demonstrated that cartilage repair cells originated from growth and proliferation factor 5 (Gdf5)-lineage cells in a Yap-dependent manner. These cells may have arisen from the synovium as there was evidence of proliferation of Gdf5-lineage cells in the synovium.[82]

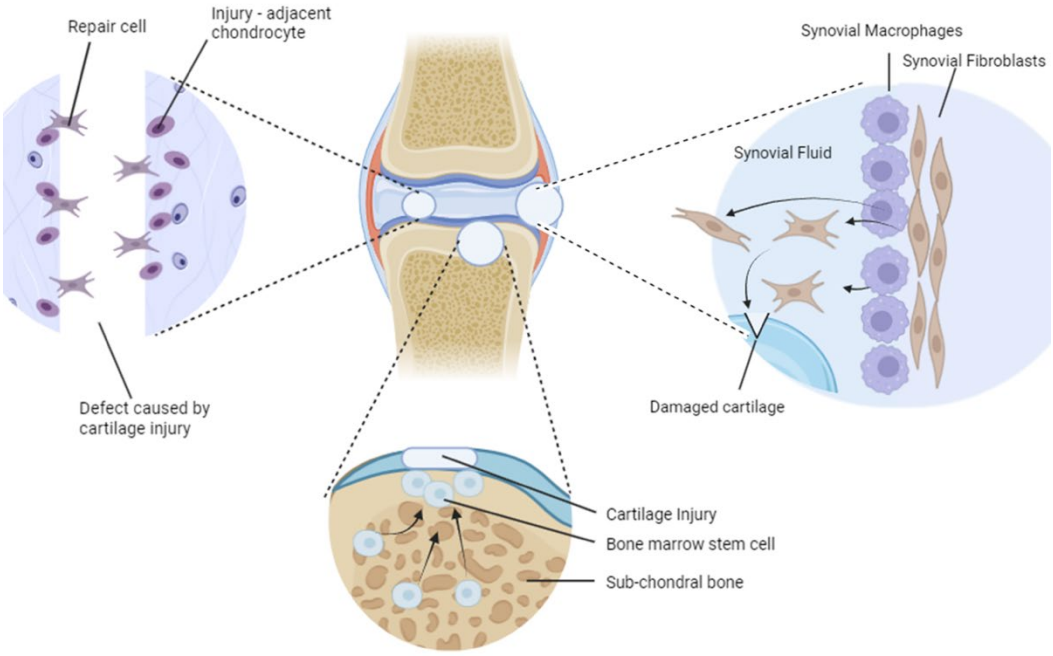

Figure 1.2. Summary of proposed sources of cartilage repair. Studies examining cartilage repair can be largely divided into three categories based on their proposed source of repair, with three main sources being: "repair" chondrocyte progenitor cells (derived from the cartilage), bone marrow-derived stem cells, and synovium-derived cells. Image created in BioRender by Harry Walton, a master's student in the Vincent group.

1.3.5. Evidence of intrinsic repair in human and murine cartilage

In the clinical setting, two procedures that improve cartilage repair are joint distraction and high tibial osteotomy. A knee joint distraction procedure involves placing an external frame consisting of two rods with internal springs around the joint, with each rod fixed to the bone with pins above and below the joint. The joint is then pulled for 5 millimetres (in the knee) in stages over a period of 6-12 weeks, causing mechanical offloading.[83] Both 1- and 2-year follow-up patients demonstrated increased cartilage thickness on MRI imaging following joint distraction. Additionally, at the 2-year follow-up, patients with end-stage knee OA that underwent joint distraction demonstrated improvement in their WOMAC pain score and increased ratio of collagen II synthesis over breakdown.[84] Positive effects of joint distraction (improved WOMAC score and increased cartilage thickness) were evident at longer 5- and 10-year follow-up.[85 86] Analysis of the synovial fluid of patients with joint distraction revealed consistent changes in levels of mechanosensitive inflammatory proteins, while some proteins showed clear directionality associated with distraction. This shows that joint distraction is accompanied by marked changes in the synovial fluid protein levels suggesting a change in joint biology.[87] Another procedure shown to improve cartilage repair, presumably through a similar mechanism, is high tibial osteotomy in individuals who have joint malalignment. This involves realigning the tibia in order to correct the weightbearing axis of the joint and to reduce the forces on the damaged side.[88] Patients who underwent high tibial osteotomy only showed some degree of cartilage regeneration, including by MRI imaging.[89] The quality of cartilage post-knee joint distraction was assessed in only one patient who underwent total knee replacement 6 years after joint distraction, and histological examination suggested that newly

formed cartilage was fibrocartilage, whereas proteomic analysis revealed no major differences in cartilage ECM protein abundance.[90]

A few attempts have been made to identify a disease-modifying drug for OA, and while no drug has been approved yet, a couple of potential candidates have been identified. A phase I clinical trial of the novel ANGPTL3-derived protein LNA043 by Novartis showed that it could induce human MSC chondrogenesis. Intraarticular injections of LNA043 in patients with knee OA showed increased hyaline cartilage markers including collagen II and decreased collagen X, a marker of hypertrophic cartilage. *In vitro* studies confirmed the chondrogenic effect of LNA043 on human MSCs.[91] Another potential disease-modifying drug is sprifermin - a truncated form of human fibroblast growth factor (FGF)-18. At 2-year follow-up, patients that received intraarticular injections of sprifermin showed increased cartilage thickness compared with the placebo group, but no significant difference in WOMAC pain scores.[92] Current Food and Drug Administration criteria require OA modifying drugs to improve OA or the symptoms.[93]

Intrinsic cartilage repair has been studied in multiple animal models. A study of murine full-thickness joint surface cartilage injury revealed that cartilage repair is age- and strain-dependent.[94] Young DBA, but not C57BL/6, mice showed good cartilage repair after full-thickness defect creation. Older mice failed to repair focal cartilage joint defects, regardless of their genetic background. Moreover, in C57BL/6 older mice, secondary OA developed adjacent to the defect site. This study, however, did not identify the source of the cells mediating the repair or the mechanism explaining the difference with strain and age.[94] Full- and partial-thickness cartilage defects, as well as other injury models, conducted in various murine strains led to identification of super healer (e.g. MRL/MpJ strain) and non-

healer murine strains.[95] This opened an avenue to explore molecular mechanisms underpinning regeneration by studying differentially expressed genes in various strains and identifying genes associated with regeneration.

One study conducted on murine and ovine cartilage concluded that GDF5-lineage progenitor cells from the synovial membrane may serve as a source of cartilage repair upon injury, and this response was increased by intraarticular agrin administration.[96] Another compound shown to promote cartilage regeneration in mice is kartogenin. In a murine OA model, intraarticular administration of kartogenin led to less severe OA and increased expression of collagen II. *In vitro*, kartogenin increased synthesis of collagen II and aggrecan and decreased synthesis of cartilage degrading proteins, MMP13 and ADAMTS5, in chondrocytes.[97 98]

1.3.6. Growth factors and molecular pathways implicated in cartilage response to injury

Cartilage is a mechanosensitive tissue and one important mechanism by which cartilage responds to mechanical stress is by release of proteins that are sequestered in the pericellular matrix (PCM). This is due to an increase in local sodium that occurs when pure water is squeezed out of the tissue upon compression. Sodium concentration is maintained by charged proteoglycans in the tissue, so loss of proteoglycan, which occurs in OA, reduces the ability to release PCM growth factors.[99] The growth factors are bound to the heparan sulfate chains of perlecan and include: fibroblast growth factor 2 (FGF2), connective tissue growth factor (CTGF) covalently bound to transforming growth factor β (TGFβ), hepatoma derived growth factor (HDGF), and midkine (MDK).[99] Some of these proteins have been characterised by our group before, as murine studies have uncovered a chondroprotective role for FGF2 and CTGF following destabilisation of the medial

meniscus (DMM) surgery.[100 101] While the exact role of other PCM-derived growth factors is yet to be discovered, it is apparent that they act collectively to change the phenotype of articular chondrocytes by turning them into migrating and proliferating cells, and this process can be reversed by mechanically offloading the joint.[102]

TGFβ's role in cartilage function and OA pathogenesis has been extensively studied over the years. TGFβ signalling is important for chondrogenic differentiation of bone-marrow derived MCSs.[103] Mechanical loading of chondrocytes was shown to activate TGFβ signalling, and CTGF covalently bound to TGFβ was released by the cartilage in response to mechanical stress.[101 104 105] TGFβ1 was enriched in OA in a genome-wide association study and its levels were increased in synovial fluid of patients who had undergone joint distraction, with greater increase associated with better clinical response.[87 106] TGFβ signalling pathway was found to be enriched in surgically-induced OA in mice 2 weeks after surgery.[107] Injecting TGFβ into murine knees led to moderate synovial fibrosis and extensive osteophyte formation, its overexpression led to profound synovial fibrosis, whereas inhibiting TGFβ in mice with surgically induced OA inhibited synovial fibrosis.[108-110] Inhibition of TGFβ in subchondral bone reduced articular cartilage degeneration in anterior cruciate ligament transection mouse model of OA, and knockout of TGFβ receptor 2 in nestin-positive MSCs led to reduced OA.[111] A murine study knocking out TGFβ receptor 2 in chondrocytes showed progressive OA development via upregulation of TGFβ downstream targets Adamts5 and Mmp3.[112] Knocking out Alk5, a TGFβ receptor 1, in lubricin-expressing articular cartilage stem cells led to decreased number of senescent cells and less lubricant

secretion accompanied by accelerated cartilage degeneration following surgical induction of OA in mice.[113]

Other molecular pathways important in cartilage injury include Wnt and bone morphogenic protein (BMP) signalling pathways. Mechanical injury of human and murine cartilage leads to upregulation of BMP-2 and activates recruitment of chondroprogenitors, synthesis of new matrix, and preservation of the phenotype of articular chondrocytes.[114] BMP-2 can drive canonical Wnt/β-catenin signalling in chondrocytes by increasing low-density lipoprotein receptor 5 (LRP5) expression, which has dual activity: it can increase chondrocyte proliferation and differentiation, whereas its excessive activity can lead to chondrocyte hypertrophy and increased MMP synthesis.[115] Thus, modulation of both BMP and Wnt pathways is required for efficient repair responses.[114]

Mechanically activated ion channels - Piezo1 and Piezo2 - are also critical mediators of chondrocyte mechanotransduction and, like with the Wnt signalling, their effect on cartilage is context-dependent. For instance, they have been shown to be important for articular cartilage development and ECM formation following their knockout in mice.[116] At the same time, Piezo1 upregulation has been shown to be associated with higher levels of inflammation in load-bearing parts of OA joints in humans and overexpression in mice has shown to exacerbate OA .[117] [118] Another important pathway for cartilage mechanotransduction is the Hippo signalling pathway, important for cartilage regeneration and homeostasis. Yes-associated protein (YAP) and transcriptional coactivator with PDZ-binding motif (TAZ) are negative transcriptional regulators downstream of the Hippo pathway. Overexpression of YAP has been shown to result in increased expression of catabolic genes in chondrocytes and suppressed chondrocyte proliferation and

differentiation. However, overexpression in mesenchymal stem cells led to increased chondrogenesis, highlighting its variable effects which are context dependent. Wnt and YAP are interlinked, as YAP overexpression has been shown to activate Wnt/β-catenin signalling.[119] How these pathways interact after injury remains largely unexplored.

1.4. The skin

1.4.1. Skin anatomy and function

The skin is the largest organ in the human body by surface area and has a remarkable potential for regeneration. It serves as a vital barrier against environmental damage, pathogens, and water loss and provides sensory input, thermoregulation, and immunological surveillance. Anatomically, the skin is divided into three layers: the epidermis, dermis, and hypodermis (Figure 1.3). In humans, the top layer, epidermis, is composed of several strata, each serving a specific function. The bottom layer of the epidermis that borders the dermis, stratum basale, contains stem cells that give rise to keratinocytes. It also contains melanocytes that are responsible for skin coloration.[120] Another important cell type found in stratum basale are Merkel cells. These cells are mechanoreceptors, as well as neuroendocrine cells, that are responsible for the sense of touch.[121] The two layers above it, stratum spinosum, containing polyhedral keratinocytes connected by desmosomes, and stratum granulosum, containing cross-linked keratinocytes, give the skin its structural integrity.[120] Langerhans cells, the immune cells capable of phagocytosis, are found in stratum spinosum and contribute to the defence function of the skin. They are capable of sensing the environment and responding to foreign particles, such as microbes, by activating resident T-regulatory cells and mounting an adaptive immune response.[122] The next layer, stratum lucidum, contains a water-resistant protein eleidin, which contributes to the barrier function of the skin, and this layer is thicker on the palms and soles of the feet. Finally, the outmost layer of the epidermis, stratum corneum, is largely comprised of keratin swirls and dead keratinocytes.

The middle layer of the skin, the dermis, is mainly comprised of collagen and elastin fibres and contains blood vessels, nerves, adipose tissue, as well as housing hair follicles, sweat glands, and sebaceous glands (Figure 1.3). It is important to note, however, that glands and hair follicles are epidermal protrusions and are lined with basal keratinocytes of the stratum basale. The dermis is largely comprised of extracellular matrix (ECM) fibres. These include collagen, laminin, elastin, fibrillin/fibronectin, proteoglycans, and glycoproteins.[123] The main types of collagen in the skin are type I (85-90%) and type III (8-11%), while other collagen types are present in smaller amounts. The ratio of collagens is different between adult and foetal skin, with the most striking difference being the higher ratio of collagen III to I.[124] Higher percentage of collagen type III in foetal skin has been linked to scarless regeneration, while a low ratio of type III to I is associated with keloid scar formation in humans.[125] [126] Laminins are connected by perlecan-containing aggregates to collagen type IV fibres to form the epidermal basement membrane (the junction between the epidermis and dermis) and are important for keratinocyte adhesion (desmosomes), hair development, and the pathogenesis of squamous cell carcinoma.[127] [128] Elastin provides elasticity and resilience to the dermis, enabling skin to stretch and recoil after deformation. Elastin has a very low turnover that makes it vulnerable to ageing and environmental damage, resulting in a loss of elasticity and skin sagging over time.[129] The bottom layer of the skin, the hypodermis, contains mainly adipose tissue, blood vessels, and nerves. Its functions include energy storage, thermal insulation, and shock absorption.[120]

Skin is affected by a wide range of conditions caused by immune-mediated, infectious, genetic, and/or environmental factors. Skin diseases affect approximately 40% of the global population, representing a major public health

burden.[130] Data from the Global Burden of Disease 2019 study revealed that nearly 4.9 billion new cases of skin and subcutaneous diseases were reported worldwide, with fungal infections accounting for 34% and bacterial diseases for 23% of these cases. Other common skin conditions include acne vulgaris, dermatitis, scabies, urticaria, psoriasis, and viral skin diseases.[131] In Europe, more than 94 million people are estimated to suffer from skin-related conditions causing itch, burn, or dryness, with fungal infections, acne and atopic dermatitis as most prevalent causes.[132] These statistics emphasise the need for better understanding of skin health and healing with the view to improve public health interventions that will reduce the growing impact of skin diseases worldwide.

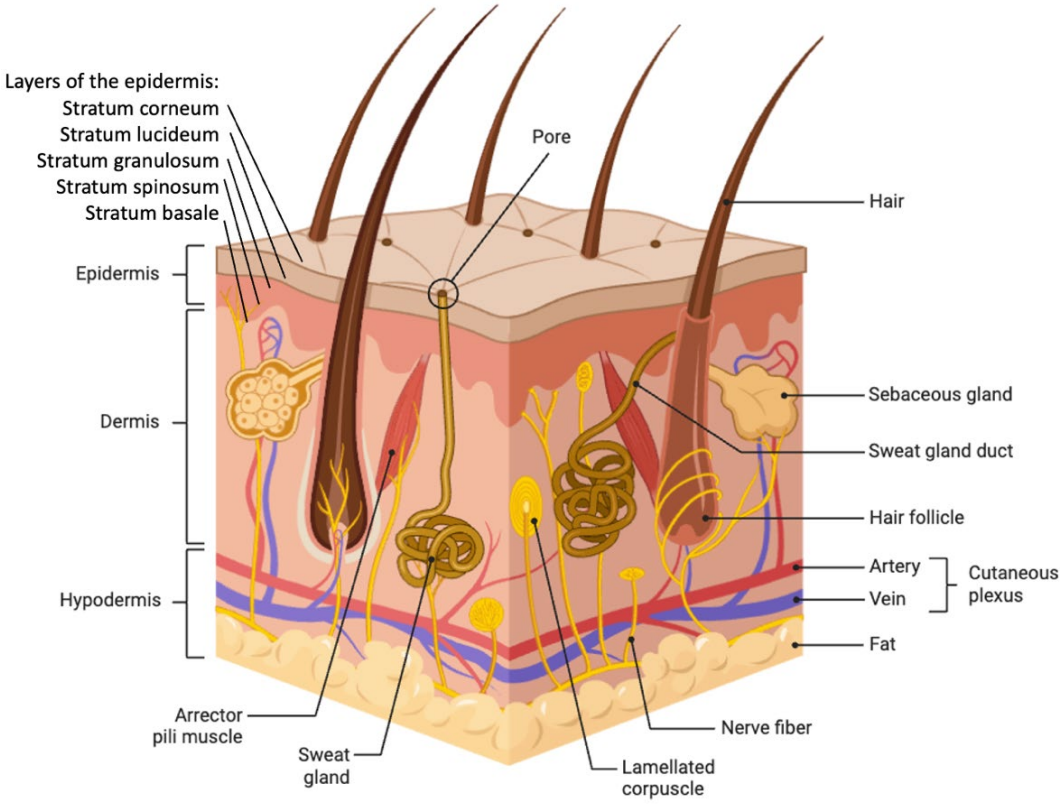

Figure 1.3. Microscopic structure of the skin. The skin is composed of three layers: the epidermis, dermis, and hypodermis. In humans, the epidermis is divided into several strata that each serve a specific function. The dermis contains ECM fibres, sweat and sebaceous glands, hair follicles, nerves, and blood vessels. The innermost layer, the hypodermis, contains fat and cutaneous plexuses. Image created in BioRender.

1.4.2. Skin wound healing: the history and current understanding

Skin wound healing is arguably one of the oldest medical problems that has been described by humans. Mesopotamian clay tablets dating back to 2200 BC provide one of the earliest records of therapeutic approach to wound care and described practices such as washing, making plasters from clay, herbs and oils, and bandaging.[133] Ancient Egyptians were the first people to apply adhesive bandages to wounds and used honey as an antiseptic, as well as applied absorbents and animal grease to wounds, as documented in the Edwin Smith Surgical Papyrus from 1650 BC. They also emphasised cleanliness and barrier protection as important factors for enhanced skin wound healing. Hippocrates also wrote about the importance of wound cleanliness, removal of pus and dead skin to facilitate healing, and of using wine and vinegar as topical antiseptics. Ancient Greeks were among the first to formally differentiate wounds into "fresh" (acute) and non-healing (chronic) wounds. Galen, a notable physician of Ancient Rome, expanded on wound dressings and documented the cardinal signs of inflammation: redness, swelling, heat, and pain.[134]

During the Middle Ages, wound management stagnated under humoral theory, but in 1500s a French surgeon Ambroise Paré demonstrated improved wound healing outcomes by introducing gentler wound dressings and avoiding the use of boiling oil, which was the standard of care at the time, for gunshot wounds. In the 19th century, Hungarian obstetrician Ignaz Semmelweis demonstrated the critical role of handwashing in infection control. Going off the work of Semmelweis, Louis Pasteur found that bacteria were responsible for turning wine into vinegar and soon discovered that same bacteria caused rotting of flesh, advancing the understanding of wound infections. A Scottish surgeon Joseph Lister

built on the work of Semmelweis and Pasteur and pioneered antiseptic surgery using carbolic acid, which drastically reduced surgical wound infections and mortality. Carl Reyher, a Russian military surgeon, expanded on Lister's work based on his experience serving in the Russo-Turkish War: he demonstrated that wound debridement (extensive mechanical wound cleansing) significantly reduced mortality.[135] In early 20th century, Alexis Carrel pioneered the use of Dakin's antiseptic solution in surgery due to its antibacterial effect, which was essential in the pre-antibiotic era, and its less irritating properties compared to other antiseptics available at the time. Further discovery of antibiotics slowly made Dakin's solution less necessary, but it is still used to date for treatment of chronic infected wounds and surgical site infections.[136] The 20th century saw many advances in wound dressings, with the concept of moist wound healing introduced in the 1960s by George Winter's research, showing that moist environments led to faster re-epithelialization compared to dry conditions.[137] This insight prompted the development of contemporary hydrocolloid, alginate, and other advanced synthetic dressings.

Modern science describes the process of skin wound healing as a sequence of four phases: haemostasis, inflammation, proliferation, and remodelling (Figure 1.4).[138] Immediately after injury, platelets adhere to exposed collagen and von Willebrand factor, forming a temporary fibrin clot. Platelet degranulation releases growth factors like platelet-derived growth factor (PDGF) and transforming growth factor β (TGFβ) that are crucial for subsequent healing.[139] The inflammatory phase is marked by recruitment of neutrophils and macrophages. Neutrophils clear the wound of pathogens and necrotic tissue via phagocytosis and deploying reactive oxygen species and neutrophil extracellular traps. It is during this stage that

macrophages shift from a pro-inflammatory M1 to a pro-reparative (or anti-inflammatory) M2 phenotype, marking the onset of a pro-repair state and initiating proliferation. Proliferation stage involves angiogenesis, re-epithelialization, and granulation tissue formation. M2 macrophages release a number of growth factors that promote angiogenesis, extracellular matrix (ECM) synthesis, and fibroblast proliferation. These include vascular endothelial growth factor (VEGF), fibroblast growth factor (FGF), PDGF, and TGFβ, as well as anti-inflammatory molecules such as IL-4 and IL-13.[140] M2 macrophages, together with epidermal growth factor, TGFβ, and keratinocyte growth factor, initiate migration of keratinocytes from wound edges across the wound bed to re-establish the epidermal barrier via re-epithelialization. Fibroblasts proliferate, produce matrix metalloproteinases (MMPs) that amplify the effect of plasmin on clot degradation, and synthesise ECM components such as collagen type III, glycosaminoglycans, and fibronectin, resulting in formation of granulation tissue.[138] Lastly, the remodelling phase is characterised by ECM reorganisation: collagen type III is replaced by stronger collagen I, improving tensile strength, while TGFβ transforms fibroblasts into myofibroblasts capable of contracting the wound. MMPs released by myofibroblasts degrade collagen type III and granulation tissue. Despite this, healed skin rarely regains its full properties, reaching about 80% of its original strength after 3 months.[141]

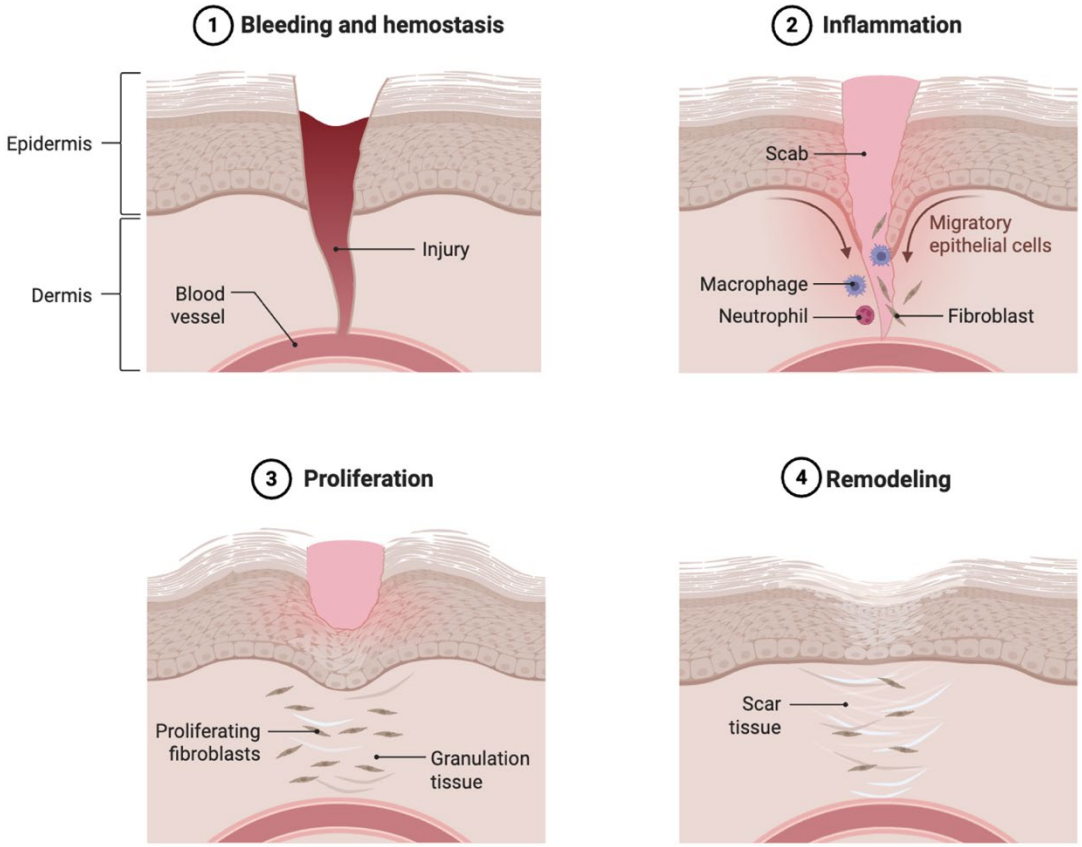

Figure 1.4. Schematic representation of skin wound healing stages. Skin healing consists of four stages: haemostasis, inflammation, proliferation, and remodelling. Each stage serves a specific function aimed at repairing the injury. Image created in BioRender.

1.4.3. Differences in human and mouse skin repair

Although mice are very popular as an animal model in translational research, their use in skin research poses some challenges. The structure of mouse skin is slightly different from human skin. Though the layers forming the skin in both species are the same, mouse skin is much thinner than human skin, with 5-10 layers present in human versus 2-5 layers in mouse skin.[142] One notable difference between human and murine hypodermis is a muscle layer called panniculus carnosus, which is virtually absent in human skin. This tissue is of particular importance in mice, as it contributes to contractile function of murine skin, which is especially important for skin healing in mice. Skin wound healing in mice and humans occurs through different mechanisms. In humans, it is mediated largely through granulation tissue formation and re-epithelization, whereas murine skin heals via dermal contraction driven by the panniculus carnosus muscle. Additionally, mouse skin possesses specialised γd dendritic epidermal T cells (DETCs) important for hair follicle regeneration.[142] Hair follicles are of special importance in both human and mouse skin because they contain stem cells. In mice, up to 25% of the epidermis is derived from hair follicle stem cells during cutaneous repair.[143] Compared to mouse skin, human skin has more sparsely distributed hair follicles and studies have shown that areas with higher hair follicle density heal faster.[144] Hair follicle stem cell niche is highly heterogenous and only a specific subpopulation of hair follicle stem cells play a role in wound healing.[145-147] Additionally, other stem cells niches in the skin, like the interfollicular basal epidermal layer and sweat glands (not present in murine skin) also have very complex response to wounding, with their environment largely dictating their fate.[148]

Transcriptomic analysis of human and mouse skin healing revealed many shared biological mechanisms.[149] For instance, both species showed upregulation of genes involved in ECM organisation and leukocyte migration after injury. Four genes - keratin 2 (KRT2), myristoylated alanine-rich C-kinase substrate-related protein (MARCKSL1), matrix metalloproteinase 1 (MMP1), and tenascin C (TNC) - displayed consistent expression trends in both humans and mice, providing evidence for conservation of skin wound healing mechanisms across species. Mice exhibited greater transcriptomic heterogeneity with more differentially expressed genes. Molecular network analysis identified subnetworks associated with collagen synthesis, immunity, cell-cell adhesion, and ECM as significantly changed after injury in both species.[149]

1.4.4. Growth factors and molecular pathways implicated in skin repair

Growth factors and molecular pathways play central roles in orchestrating skin repair, regulating cellular responses essential for skin wound healing. Some of the well-studied growth factors involved in skin repair include FGF2, TGFβ, and connective tissue growth factor (CTGF).

FGF2 (also known as basic FGF) is important for inducing keratinocyte migration during wound healing, as well as improving angiogenesis and stimulating collagen production in fibroblasts.[150 151] Murine studies identified a delay in healing of excisional scars in *Fgf2* knockout (*Fgf2*$^{-/-}$) mice, whereas topical application of FGF2 accelerated healing and increased expression of epithelial-mesenchymal transition (EMT)-associated markers.[152 153] Additionally, concurrent application of FGF2 and TGFβ amplified wound re-epithelialization by increasing expression of EMT markers.[153]

TGFβ is involved in the regulation of multiple processes during wound healing including inflammation, fibroblast proliferation, and ECM remodelling. The three isoforms (TGFβ1, TGFβ2, and TGFβ3) mediate healing through the SMAD signalling pathway, with differential expression influencing scar outcomes. Initially, excessive TGFβ1 and TGFβ2 were linked to hypertrophic scarring and fibrosis, whereas TGFβ3 was thought to be associated with scarless healing.[154] However, studies showed that each isoform serves a specific function during foetal and adult wound healing necessary for successful tissue healing and simply altering the ratios of isoforms did not lead to improved outcomes, reflecting the complexity of TGFβ signalling.[155]

CTGF, which is downstream of TGFβ1, regulates fibroblast proliferation and ECM synthesis. Prolonged CTGF exposure increased collagen deposition and fibroblast proliferation within granulation tissue leading to fibrosis.[156] Other growth factors involved in skin healing include VEGF that stimulates angiogenesis, as well as epidermal growth factor and keratinocyte growth factor (also known as FGF7) that are important for keratinocyte migration and proliferation.[138]

Molecular pathways implicated in skin wound healing include the Hippo pathway and Piezo channels. Yes-associated protein (YAP) and transcriptional co-activator with PDZ-binding motif (TAZ) are transcriptional co-activators negatively regulated by the Hippo pathway. YAP has shown to decrease fibrotic markers in human myofibroblasts *in vitro* in response to TGFβ1 treatment, illustrating YAP's ability to prevent fibrotic scarring.[157] Additionally, small-interfering RNA (siRNA)-mediated knockdown of YAP and TAZ in murine skin wounds led to delayed early wound closure marked by reduced cell proliferation and migration. Additionally, YAP/TAZ knockdown wounds showed decreased

expression of TGFβ1 and other components of its signalling such as Smad 2 and 7.[158]

Piezo1 and Piezo2 are ion channels that act as mechanosensors that are capable of converting mechanical forces such as shear stress, swelling, or tension into calcium-permeable cationic currents.[159] In skin wound healing, Piezo 1 promotes macrophage polarisation, supports angiogenesis and fibroblast-to-myofibroblast transition, as well as plays a role in hypertrophic scar formation due to its proliferative effects on fibroblasts.[160-162] Similarly, Piezo 2 has been shown to be important for generating scar tissue via activation of fibroblasts.[163] Together, these growth factors and molecular pathways establish a coordinated process that enables efficient skin wound healing. They also serve as potential targets for innovative therapies that can enhance skin healing outcomes while reducing, or potentially preventing, fibrotic scar formation.

1.5. Hepatoma derived growth factor

1.5.1. Identification and structure

Hepatoma derived growth factor (HDGF) was first purified from the conditioned medium of human hepatoma-derived cell line HuH-7.[164] HDGF is the founding member of a protein family sharing a highly conserved N-terminal PWWP domain (proline–tryptophan–tryptophan–proline motif) crucial for DNA binding, protein interactions, and heparin binding.[165] *Hdgf* gene is located on chromosome 3 in the murine genome and contains 6 exons, with exon 1 being separated from the rest of exons by a long (>6,000 base pairs) intron 1 (Figure 1.5).[166] Structurally, HDGF protein contains 240 amino acids and includes the PWWP domain, which forms a compact β-barrel fold essential for chromatin interactions and nuclear targeting, and two nuclear localization signals (NLS), one within the PWWP domain and another in the C-terminal (Figure 1.5).[167] PWWP domain is sometimes also called the HATH domain, which stands for homologous to the amino terminus of HDGF. The variable C-terminal domain provides diversity among family members and is also the reason why no full protein crystal structure exists for HDGF to date. High-resolution binding studies confirm that the PWWP domain, supported by adjacent regions, enables HDGF to specifically bind DNA sequences, and its NLSs are important for sustaining HDGF's mitogenic activity in the nucleus, namely stimulation of DNA synthesis and cellular proliferation.[168] [169] The receptor for HDGF has not yet been discovered and its mechanism of cellular signalling is not yet known.

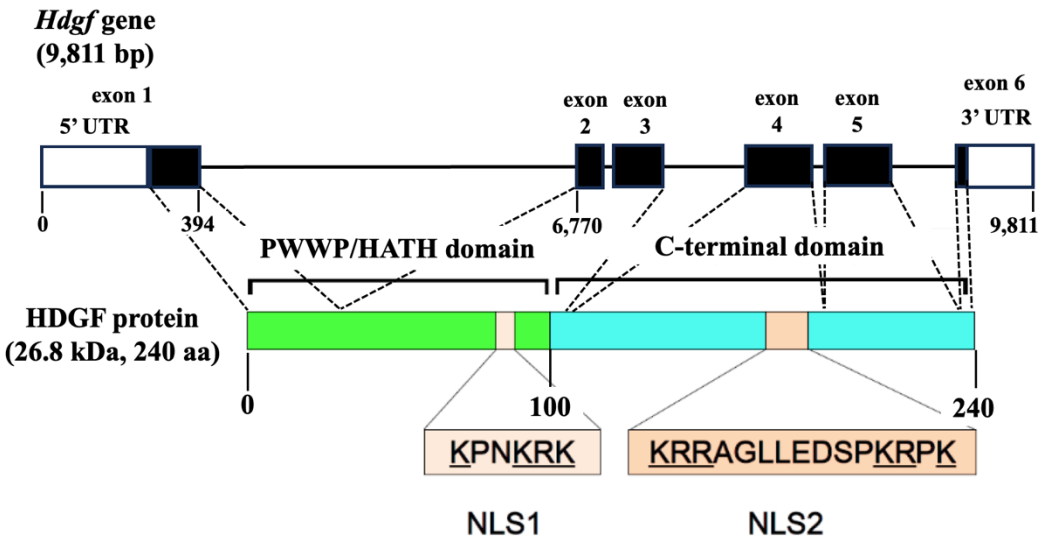

Figure 1.5. Schematic representation of HDGF's structure. Murine *Hdgf* gene consists of 6 exons, with exon 1 separated from other exons by a long intron.[166] Numbers indicate base pairs (bp), unfilled boxes represent untranslated regions of exons (UTR), filled boxes represent exons, and lines represent introns. HDGF protein is comprised of 240 amino acids containing the PWWP (or HATH) domain, two nuclear localization signals (NLS), and a variable C-terminal domain. Numbers indicate amino acid (aa) residues. Image of the protein structure modified from Enomoto et al, *Int J of Mol Sci*, 2015.[167]

Subsequent research uncovered a larger protein family - the HDGF-related proteins (HRPs) or HDGF-like proteins (HDGFLPs) - all defined by the presence of the PWWP domain. The HDGF protein family now includes HRP1 (also called HDGFL1), HRP2 (HDGFL2), HRP3 (HDGFRP3), HRP4 (HDGFRP4), and lens epithelium-derived growth factor (LEDGF). LEDGF is notable for promoting cell survival in stress, tethering proteins to chromatin, and is involved in HIV integration.[170-172] HRP2 (HDGFL2) has roles in chromatin binding and myogenic gene regulation, while other family members often show expression in various tissues but have more restricted or less-characterised functions. A summary table outlining known functions of HDGF protein family members is available in Table 1.1. Proposed role of HDGF in disease and tissue injury is discussed in detail in the next section.

Table 1.1. HDGF protein family members and their proposed functions.

Protein name	**Purified From**	**Function**
HDGF	HuH-7 human hepatoma cells	Mitogenic factor; nuclear localisation; DNA binding; chromatin targeting[164 169]
HRP1/HDGFL1	Murine cDNA library; identified via sequence homology	Presumed nuclear function[173]
HRP2/HDGFL2	Murine cDNA library; identified via sequence homology	Chromatin association; DNA repair; myogenic gene regulation; oncogenic activity[173-176]
HRP3/HDGFRP3	Deduced from murine and human cDNA	Predicted roles in neuronal development, microtubule binding activity[177]
HRP4/HDGFRP4	Deduced from bovine cDNA[178]	Unknown
LEDGF	Bovine lens epithelial cells	Transcriptional coactivation; chromatin tethering; stress survival; HIV integration[170-172]

1.5.2. Role of HDGF in disease and tissue injury

While HDGF got its name from hepatocellular carcinoma (HCC) cells it was derived from, it has been shown to be ubiquitously expressed across tissues.[179] HDGF has been largely implicated in carcinogenesis and was found to promote progression of multiple types of cancer. For instance, HDGF expression is markedly elevated in HCC tissues, where it is correlated with HCC cell proliferation and poorer disease-free and overall survival.[167 180 181] Additionally, HDGF was found to be increased in parenchymal hepatocytes following two types of liver injury (hepatectomy and drug-induced injury) before DNA synthesis peaked. This suggested that induction of HDGF was important for liver regeneration, and this effect was not limited to HCC cells only.[182] In pancreatic ductal carcinoma, HDGF was found to be an independent prognostic factor following resection, promoting tumour growth and fibrosis, and contributing to chemoresistance.[183-185] Higher expression levels of HDGF are associated with poorer survival and unfavourable prognosis in cholangiocarcinoma and gallbladder adenocarcinoma.[186 187] In oesophageal cancer, HDGF expression improved radiosensitivity but, paradoxically, was related to worse overall survival, likely due to its proliferative effects on irradiated fibroblasts.[188-190] HDGF is also implicated in gastric, colorectal, and gastrointestinal stromal tumours, where high HDGF expression was shown to promote proliferation of cancer cells and induction of vascular endothelial growth factor (VEGF) expression, which controls angiogenesis, tumour invasion, early recurrence, and is generally associated with poor prognosis.[191-196] In the gut, HDGF expression has been shown to be higher in foetal intestinal cells and its expression went down with age. Overexpression of HDGF inhibited maturation of foetal intestinal cells, possibly explaining HDGF's

contribution to colorectal cancer pathogenesis.[197] In melanoma, HDGF was found to promote tumour growth and metastasis by inducing epithelial-mesenchymal transition (EMT).[198] Overexpression of HDGF in murine hair follicle melanocytes did not lead to cancerous transformation of melanocytes, but HDGF deficiency led to an increased number of epidermoid cysts following ultraviolet exposure.[199] Upregulation of HDGF in breast cancer was found to be correlated with lymph node metastasis and EMT.[200] In non-small cell lung cancer, HDGF showed the ability to promote chemoresistance via activation of the PI3K/AKT and MEK/ERK pathways.[201]

HDGF plays a significant role in tissue injury responses, including vascular injury and tissue remodelling. HDGF is expressed in proliferating vascular smooth muscle cells (SMCs) and endothelial cells in the foetus, where exogenous treatment with HDGF promoted SMC expansion and DNA synthesis. HDGF also colocalised with the proliferating cell nuclear antigen in SMCs, suggesting importance of HDGF in SMCs growth and vascular injury repair.[202] A later study found that HDGF silencing led to reduced SMC proliferation and migration.[203] HDGF was found to induce expression of one of the key regulators of angiogenesis - VEGF.[204 205] In the lung tissue, HDGF expression was increased in foetal lungs following change in airway pressure, which is an important regulator of lung development, illustrating a potential role of HDGF in lung development.[206] Following lung injury, increased expression of HDGF was detected in bronchial and alveolar epithelial cells and HDGF was shown to induce their proliferation, suggesting HDGF's contribution to lung remodelling and repair.[207] In the heart, intramyocardial injection of recombinant HDGF reduced infarct size in wild-type, but not in protein-kinase C epsilon (PKCε)-negative mice, following myocardial

ischemia-reperfusion injury, demonstrating HDGF's protective role against reperfusion injury via PKCε activation.[208] In the cartilage, HDGF was shown to be one of the PCM-derived growth factors (together with FGF2 and CTGF) released immediately upon cartilage injury, although its role in mediating cartilage injury and mechanism of action are still unknown.[99] In the skin, HDGF was found to be increased in keloid scars, and exogenous treatment with HDGF induced proliferation of keloid fibroblasts via the activation of the extracellular signal-regulated kinase (ERK) pathway and upregulated the secretion of VEGF.[209]

1.5.3. Proposed mechanism of action

Despite HDGF's apparent importance in multiple malignancies and evidence of its involvement in responses of tissue to injury, the exact mechanism of action remains unknown. As discussed above, multiple studies showed HDGF's ability to activate the PI3K/AKT and ERK pathways, however, they did not manage to fully decipher the mechanism behind these observations.[167 201 209 210] The receptor for HDGF is unknown, but nucleolin (NCL) has been shown to operate as a functional receptor of HDGF, resulting in subsequent PI3K/AKT activation.[211] Formation of endogenous NCL-HDGF complexes had been demonstrated earlier, but its pattern of expression within the cell was very context-dependent. NCL is a nucleolar protein involved in ribosome biogenesis, RNA processing, and chromatin organisation, and is mainly expressed in the nucleus. However, in cells transfected with HDGF, NCL was found in the cytoplasm. Its interaction with HDGF required complex formation with specific mRNA, bcl-2 mRNA, rather than a direct and stable ligand-receptor binding that is typical for canonical growth factor receptors.[212] Thus, while surface NCL may facilitate HDGF internalisation

in cancer cells, its multifunctional nature and requirement for additional co-factors or RNAs suggest that NCL may not be a specific cell surface receptor for HDGF.

A liquid chromatography-tandem mass spectrometry (LC-MS/MS) interactome study performed on human HEK293T cells is arguably the only work that examined HDGF's interactome. It showed that HDGF is a multifunctional protein involved in processes that take place in the cytoplasm and in the nucleus, suggesting its wide-spread function within the cell. HDGF interacted with proteins involved in chromatin remodelling, DNA repair, transcriptional regulation, RNA processing and splicing, ribosomal assembly, and translation. The same work demonstrated the importance of the PWWP/HATH domain for HDGF's protein-protein and protein-RNA interactions, indicating that this domain might be essential for HDGF's function.[213] Together, these data demonstrate that, despite the lack of clear mechanism of action, HDGF is important for many cellular processes, including tumorigenesis and tissue repair, making it an attractive potential therapeutic target and an interesting molecule to study in the context of tissue injury.

1.6. Research aims

Part 1:

1) To investigate the nature of HDGF release upon injury using cartilage and skin as model tissues,
2) To examine the response of chondrocytes to medium conditioned by tissue injury (injury CM),
3) To investigate the role of HDGF and other PCM-derived growth factors of interest in this response *in vitro*.

Part 2:

1) To compare genotype-specific transcriptional differences between wild-type (WT) and HDGF-knockout (*Hdgf*$^{-/-}$) cartilage and skin,
2) To study injury-associated transcriptional changes in WT and *Hdgf*$^{-/-}$ cartilage,
3) To investigate proteomic differences between WT and *Hdgf*$^{-/-}$ skin following injury.

Part 3:

1) To investigate the contribution of HDGF to cartilage response to injury following OA induced by PMX surgery in WT and *Hdgf*$^{-/-}$ mice,
2) To examine the effect of HDGF deletion on skin repair following skin wounding of WT and *Hdgf*$^{-/-}$ mice.

Chapter 2: Materials and methods.

This chapter contains the list of materials and methods used throughout this thesis. Details of chapter-specific procedures are included in the methods section of each chapter.

2.1. Materials used for tissue dissection, *in vitro* chondrocyte experiments, and western blotting

Table 2.1.1. Materials used for injury CM generation and tissue culture.

Reagent	**Catalogue number**
DMEM	Gibco 41965-039
Penicillin-streptomycin	Sigma Aldrich P4333
Amphotericin B	Fischer Scientific BP264550
Foetal bovine serum	Sigma Aldrich F9665
Collagenase A	Roche Diagnostics 10103586001
2-well silicone insert	Ibidi 81176
24-well tissue culture plates	Falcon 353047
Rely+On Virkon tablets	LanXess D12555728
15- and 22-blade scalpels	Swann-Morton 0505 and 0508
0.2 μm filter	Corning 29822049
0.7 μm cell strainer	VWR 76327-100
Heparin column	Cytiva 17040601
4-chamber glass slides	Lab-Tek II 154917
Hyaluronidase	Sigma H3506-1G

Table 2.1.2. The list of antibodies and inhibitors used in *in vitro* chondrocyte assays.

Reagent	**Catalogue number**
FGF receptor inhibitor	SB402451
FGF2 neutralizing antibody (FGFRi)	Clone bFM-1 cat 05-117
TGFβ/activin A inhibitor	SB431542
Recombinant FGF2	100-18B
Recombinant HDGF	ab132259; LS-G12510 (for AKT phosphorylation only)
Recombinant MDK	258-MD
Ki67 antibody	Abcam ab92742
Donkey anti-rabbit antibody	Alexa fluor 647 ab2536183
Phalloidin antibody	CF594

Table 2.1.3. List of reagents used for western blotting.

Reagent	**Catalogue number**
4x laemmli sample buffer	Bio Rad 1610747
2-mercaptoethanol	Gibco 21985-023
Trans-Blot turbo transfer pack	Bio Rad 1704157
ECL	Bio Rad 1705061
X-ray films	Cytiva 28906836
PageRuler Plus Protein ladder	Thermo Scientific 26619

Table 2.1.4. List of antibodies used for western blotting.

Reagent	**Catalogue number**
Anti-HDGF antibody	Abcam ab128421 and Abcam ab131046
Phospho-AKT substrate antibody	9614S
Goat anti-rabbit	Thermo Fisher 31460

2.2. Generation of HDGF knockout mouse line

Whole-body knockout *Hdgf* mice were obtained from a research group at the University of Bremen.[214] They were crossed with C57BL/6 females at the Kennedy Institute of Rheumatology and rederived to obtain a homozygote breeding colony. Heterozygotes contained a null allele of the *Hdgf* gene generated by homologous recombination in embryonic stem (ES) cells. In this construct, exons 2–6 of the *Hdgf* gene were replaced with a fragment containing an enhanced green fluorescent protein (eGFP) with a *HindIII* digestion site and a *loxP*-flanked HPRT cassette (used for positive selection with HAT-containing medium).

Genotyping of offspring was performed using HDGF primers designed by Transnetyx. HDGF wild-type probes detected the WT allele by spanning intron 3, which is deleted by eGFP. The primers were as follows, with an amplicon size of 52 base pairs (bp): forward primer 5'-CAGCCTTCCAAGAGGAGGTT-3' and reverse primer 5'-GCCCTCCCGCCTTGTC-3'. eGFP probes were utilised to detect the mutant allele with an amplicon size of 82 bp: forward primer 5'-CGTCGTCCTTGAAGAAGATGGT-3' and reverse primer 5'-CACATGAAGCAGCACGACTT-3'.

2.3. Materials used for RNA extraction from cartilage and skin

Table 2.3.1. The list of reagents and equipment used for RNA extraction from murine cartilage and skin.

Reagent	**Catalogue number**
TRIzol reagent	Invitrogen 15596018
RNeasy Micro Kit	Qiagen 74104
RNA Clean and Concentrator-5 Kit	Zymo R1013
1-bromo-3-chloropropane	Sigma Aldrich B9673
gentleMACS M tubes	Miltenyi Biotec 130-093-236
100% ethanol BioUltra/Molecular Biology grade	Sigma Aldrich 51976-500ML-F
gentleMACS dissociator	Miltenyi Biotec 130-093-235
10-blade scalpels	Swann-Morton 0501

2.4. Materials used for proteomic labelling study of the skin

Table 2.4.1. Recipes of solutions used for sample preparation.

Solution name as it appears in Chapter 4	**Ingredients**
SILAC-supplemented culture medium	DMEM 100 mg/L L-lysine-$^{13}C_6$ hydrochloride 10% FBS 1% penicillin-streptomycin 1% amphotericin B
SDS lysis buffer	10% Sodium Dodecyl Sulfate 10mM Tris (2-carboxyethyl) phosphine (TCEP) 50mM Triethylammonium bicarbonate buffer (TEAB) Protease and phosphatase inhibitors

Table 2.4.2. The list of reagents used for proteomic labelling of murine skin.

Reagent	**Catalogue number**
DMEM	Gibco 41965-039
Penicillin-streptomycin	Sigma Aldrich P4333
Amphotericin B	Fischer Scientific BP264550
Foetal bovine serum, dialyzed	Gibco 15605639
L-lysine-$^{13}C_6$ hydrochloride	Sigma Aldrich 643459
15-blade scalpels	Swann-Morton 0505

2.5. Materials used for surgical procedures in mice

Table 2.5.1. Materials used in partial medial meniscectomy surgery.

Reagent/equipment
Isoflurane (IsoFlo) (Abbot 5260-04-05)
Buprenorphine Vetergesic Multidose (Ceva Animal Health)
Hair trimmer
Autoclaved Green Drapes
Autoclaved tweezer scissors and curved tissue tweezers
Swabs (small and large)
25G needles and 1mL syringe
3-mm 15-blade ophthalmic scalpel
6-0 Vicryl suture
5-0 Ethilon suture
Autoclaved surgical equipment
Cotton buds
Sterile gloves

Table 2.5.2. Materials used for skin wounding procedure.

Reagent/equipment
Isoflurane (IsoFlo) (Abbot 5260-04-05)
Buprenorphine Vetergesic Multidose (Alstoe Animal Health)
Hibiscrub (Mölnlycke 207110)
Autoclaved Green Drapes
Autoclaved tweezer scissors and curved tissue tweezers
Autoclaved 3-mm biopsy punch
Swabs (small and large)
25G needles and 1mL syringe
70% ethanol spray
Autoclaved surgical equipment
Cotton buds
Hot bead /microbead steriliser
Sterile gloves
Depilatory cream
Digital calliper

2.6. Histological staining of mouse knee joints and skin

Table 2.6.1. Materials used for histological staining of murine tissues.

Reagent/equipment
Paraffin (CellWax Plus (S), CellPath GCA-0400-00A)
Formic acid (Fisher Scientific F/1900/PB08)
Xylene (Fisher Scientific X/0250/21)
70% Ethanol (Sigma 458600-2.5L-M Ethanol denatured (UK IDA standard) diluted in dH_2O)
100% Ethanol (Sigma 32221-2.5L)
Haematoxylin Harris (Leica microsystems 3801560E)
Acid Alcohol (1400ml 100% Ethanol, dH_2O plus 600 ml and 20ml HCl 37% (VWR 20253.335)
Blueing Agent (ammoniated water, 600ml dH_2O plus 1.6ml ammonia (VWR 87766.20)
Fast Green (Sigma F7252-25g)
1% acetic acid (Millipore 8.187552500)
Eosin Y 1% aqueous (Cell Path RBC-0100-00A)
0.01% Crystal violet (Sigma C6158) in dH_2O
Di-n-butylphthalate (DPX) (Sigma 06522-100ml)
Masson- Light Green (Cell Path RBK-0601-00B)
Tissue TeK VIP 6 Processor Sakura
TEC 5 Embedding centre Sakura
DRS 2000 AutoStainer, Sakura

Chapter 3: HDGF is released from multiple connective tissues upon injury.

3.1. Introduction

As described in the introduction, one of the mechanisms by which cartilage responds to injury is through the release of growth factors from the pericellular matrix (PCM) of the chondrocyte. Some of these proteins have been characterised by our group before. For instance, murine studies have uncovered a chondroprotective role for FGF2 and CTGF following destabilisation of the medial meniscus (DMM) surgery.[100] [101] As discussed earlier, pro-regenerative effects of FGF2 and CTGF are not limited to cartilage, as both promote regeneration of the skin and facilitate skin repair following injury.[215] [216] However, little is known about HDGF in the context of tissue injury. A few published studies suggest its involvement in tissue response to injury through elevation of protein after vascular injury and transcriptional upregulation in retinal pigment epithelium wounding. [217] [218] The expression of HDGF by Cy3-labelled cDNA microarray was found to be increased (2.8-fold increase) in human dermal fibroblasts subjected to mechanical stimulation (grown in mechanically stressed lattices), suggesting possible involvement of HDGF in mechanosensation.[219] Overexpression of HDGF was observed in keloid scars and its exogenous application led to a stimulation of proliferation of keloid fibroblasts.[209]

As HDGF bears some similarities to FGF2 and CTGF in cartilage, such as its heparin-binding ability, location in the chondrocyte PCM, and its immediate release upon cartilage injury, we hypothesised that it could play a role in tissue repair.[99] We hypothesised that HDGF would be released upon tissue injury in multiple connective tissues and that it might be important for the injury response/repair. In this chapter, I validated the previous findings from our group of

HDGF release upon cartilage injury and explored its release upon ear and skin injury, which has not been done before. I have also explored the response of isolated chondrocytes to medium conditioned by injured tissue and attempted to decipher the role of HDGF and other PCM-derived growth factors, namely MDK and FGF2, in this response.

Chapter aims:

1) To investigate the nature of HDGF release upon injury using cartilage and skin as model tissues,
2) To examine the response of chondrocytes to medium conditioned by tissue injury (injury CM),
3) To investigate the role of HDGF and other PCM-derived growth factors of interest in this response *in vitro*.

3.2. Methods

3.2.1. Injury CM generation from porcine tissue

Porcine trotters from 4-7 months old male pigs were obtained weekly from a local abattoir. Trotters were disinfected in 2% Virkon/H_2O for 15 minutes. The dewclaws and the skin were removed using a 22-blade scalpel (Swann-Morton, Sheffield, England). The metacarpophalangeal joint was opened with a 15-blade scalpel under sterile conditions. Two methods were routinely used to generate injury CM. The first was by explanting cartilage from the metacarpophalangeal joint (approximately 1 g of cartilage) directly into 2 mL of Dulbecco's Modified Eagle Medium (DMEM) (Thermo Fisher Scientific, Waltham, MA, USA) supplemented with 1% penicillin-streptomycin (Sigma Aldrich, St Louis, MO, USA) and 1% amphotericin B (Thermo Fisher Scientific, Waltham, MA, USA), the mix later referred to as "medium", containing 1% foetal bovine serum (FBS) (Sigma Aldrich, St Louis, MO, USA). Cartilage was finely chopped with a 15-blade scalpel for 5 minutes and then medium was collected and spun at 1500 RPM for 10 minutes at 4°C. The obtained supernatant was collected and stored at -20°C for future use. This type of injury CM is later referred to as "explant" injury CM. The second method was by explanting cartilage into 20 mL of serum-free (SF) medium and leaving it on a shaker at 37°C for 48 hours. The cartilage was then placed in fresh 1% FBS medium (2 mL/trotter) and cut with a 15-blade scalpel for 45 minutes before spinning and storing, as described above. This type of injury CM is referred to as "recut" injury CM. The non-injury control, "rested" medium, was generated by resting explanted cartilage in SF medium for 48 hours on a shaker at 37°C, then replacing the media with a fresh 1% FBS medium (2 mL/trotter), and resting it for 45 minutes, spinning and storing.

3.2.2. Injury CM generation from murine tissues

Injury CM was also generated from wild-type (WT) (C57BL/6 strain) and HDGF knockout (*Hdgf*$^{-/-}$) mice following *ex vivo* hip avulsion. Mice were sacrificed at 4-6 weeks of age by CO_2 asphyxiation followed by confirmatory cervical dislocation. Hip joints were exposed by dissection, dislocated, and the femoral cap was then avulsed through the growth plate using sterile forceps. Hips were placed in 1% FBS medium (25 μL/hip), cut into 4 pieces with a 15-blade scalpel and conditioned for 5 minutes before spinning and storage. To generate injury CM from the ear, mouse ears of 4-6-week-old mice were sterilised topically with 70% ethanol/H_2O and dissected into 1% FBS medium (50 μL/ear), cut into small pieces (±2 mm^2) with a 15-blade scalpel and conditioned for 5 minutes before spinning and storage. To generate injury CM from the skin, 15-week-old mice were sacrificed by CO_2 asphyxiation confirmed by cervical dislocation, their backs shaved, shaving cream applied for 4 minutes, washed off with warm water followed by Hibiscrub to sterilise. A skin patch of approximately 2 cm by 4 cm was removed from the mouse, placed in 1 mL of SF medium, cut into small pieces (±5 mm^2) with a 15-blade scalpel and conditioned for 5 minutes. Medium was clarified by centrifugation (1500 RPM for 10 minutes at 4°C) and stored at -20°C for future use. A cartoon representing injury CM generation from porcine and murine tissues is shown below (Figure 3.1).

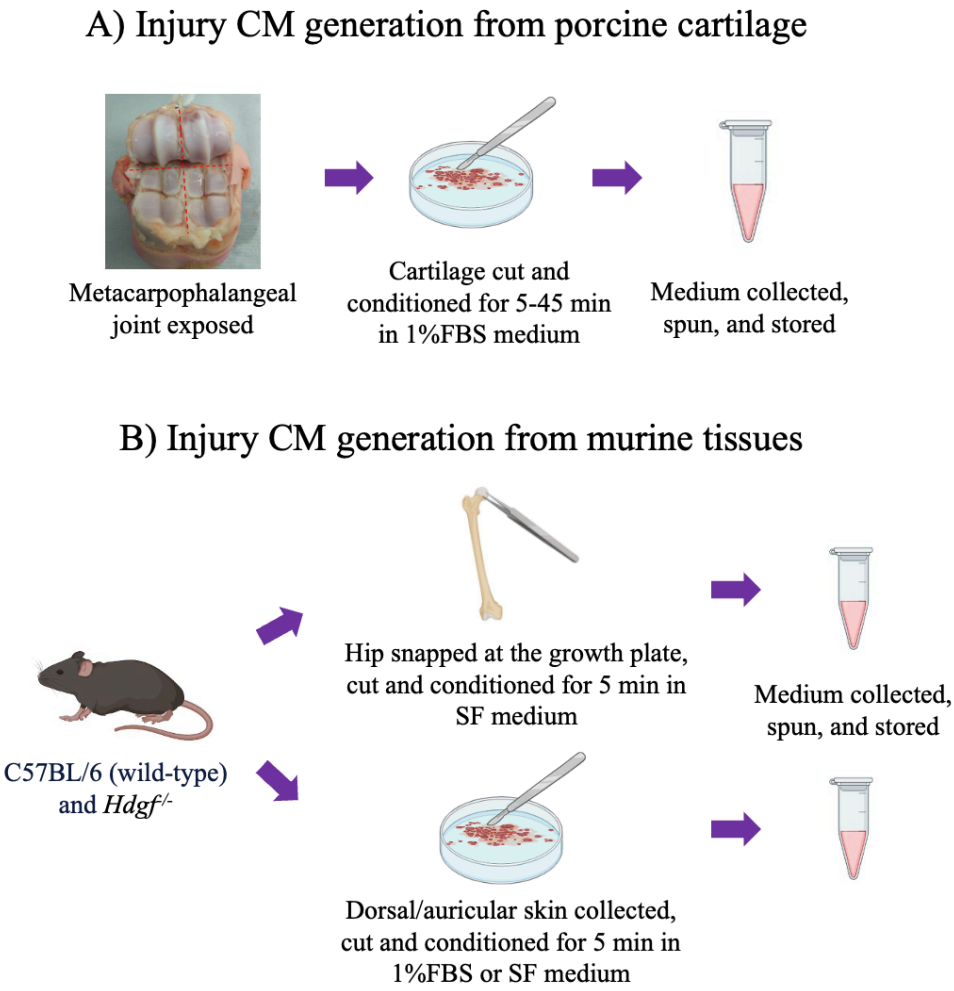

Figure 3.1. Generation of injury CM from porcine and murine tissues. A) Two kinds of injury CM (explant and recut) and one non-injury control (rested) were generated from porcine cartilage as described above. B) Injury CM was generated from wild-type (WT) C57BL/6 and *Hdgf* knockout (*Hdgf*$^{-/-}$) murine tissues following hip avulsion and ear and skin cutting. FBS - foetal bovine serum, SF - serum-free.

3.2.3. Western blotting of CM

Release of injury-associated growth factors in injury CM was characterised by western blot. Samples were mixed at a 1:4 ratio with 4x Laemmli blue buffer (BioRad, Hercules, CA, USA) containing 1:1000 β-mercaptoethanol (Sigma Aldrich, St Louis, MO, USA), denatured at 95°C, sonicated, and run on a 10% sodium dodecyl-sulfate polyacrylamide gel via electrophoresis (SDS/PAGE). Antibodies were dissolved to a desired concentration in 5% milk 1X TBST buffer. Primary antibody incubation was carried out overnight at 4°C and secondary antibody incubation was done at room temperature (RT) for 1 hour. Membranes were visualised via enhanced chemiluminescence (ECL) (BioRad, Hercules, CA, USA) and developed in a dark room onto an X-ray film (Cytiva, Marlborough, MA, USA). The antibodies and concentrations used were: 1:2000 anti-HDGF, 1:1000 phospho-AKT substrate, 1:2000 secondary anti-rabbit. Details for reagents used in this chapter are available in Chapter 2.

3.2.4. Chondrocyte culture

A 1 mg/mL collagenase A (Roche, Mannheim, Germany) solution was prepared in SF medium and filtered through a 0.2 μm filter (Corning, NY, USA). Using a 15-blade scalpel, the cartilage was explanted into the collagenase A-containing SF medium and placed on a shaker at 37°C overnight. Next day, the solution was poured through a 0.7 μm cell strainer (VWR, Radnor, PA, USA) to get rid of undigested pieces, spun at 1500 RPM for 5 minutes at 4°C, washed twice with SF medium, and resuspended in 10 mL 20% FBS medium. After counting, cells were made up to a $1x10^6$ cells/mL dilution and desired numbers were seeded

for treatment. Cells were cultured at 37°C and 5% CO_2, and all cell treatments were performed under sterile conditions in a class 2 biological safety cabinet.

3.2.5. Gap and low-density chondrocyte behaviour assays

To examine the effect of injury CM on behaviour of chondrocytes, two assays were deployed. The gap assay measured percent filling of a pre-determined space generated by a silicone insert. The low-density assay measured density over time by video after cells have been plated at low density. The gap assay was performed in 24-well tissue culture plates (Corning, NY, USA). Sterile forceps were used to place one 2-well silicon insert (Ibidi, Gräfelfing, Germany) per well, ensuring full adherence to the bottom of the well. Following chondrocyte isolation (described above), 100,000 cells, resuspended in 20% FBS medium, were plated in each chamber of the silicon insert. For the low-density assay, 50,000 cells/well were plated in a 24-well tissue culture plates. Cells were left overnight to attach.

The following day, media was removed, washed with 1% FBS medium and replaced with 500 μL/well of 1% FBS medium for 1 hour prior to applying treatments. This medium was then removed, and chondrocytes were treated with injury CM diluted 1:1 with 1% FBS medium. In both gap and low-density migration assays, various treatment conditions were added to the injury CM including: FGF receptor inhibitor (FGFRi) (final concentration of 250 nM), TGFβ/activin A inhibitor (final concentration of 500 nM), and FGF2 neutralizing antibody (concentration of 2-4 μg/mL). Optimisation of FGF2 neutralizing antibody addition included a pre-treatment of injury CM (diluted 1:1 with 1% FBS medium) with 15 units/mL of hyaluronidase (Sigma Aldrich, St Louis, MO, USA) on shaker at 37°C prior to adding the antibody to the mix. Further details on reagents are available in Chapter 2. The cells in the gap assay were visualised every 24 hours over 3-4 days

on Olympus CKX41 with the Q-Capture Pro 7 software (QImaging, Inc.), or every two hours for the period of 96 hours on the Incucyte (Sartorius, 2022B Rev2) for low-density assay.

Immunofluorescent staining to assess cell proliferation with antibody to Ki67 was performed on cells plated in the gap assay. Cells were grown on 4-chamber glass slides (Thermo Fisher Scientific, Waltham, MA, USA) and treated with injury CM diluted 1:1 with 1% FBS medium for 48 hours. Cells were fixed in 4% paraformaldehyde, permeabilised in 0.3% Triton X-100, incubated in cold room overnight with a primary antibody, for 1 hour at RT with a secondary antibody (1:500 donkey anti-rabbit), and 30 min with 1:200 Phalloidin antibody. Confocal imaging was performed on a Zeiss LSM880 microscope.

3.2.6. Injury CM heparin-binding growth factor depletion

To generate injury CM without heparin-binding factors, the explant CM was passed through a 1 mL heparin column (Cytiva, Marlborough, MA, USA) under sterile conditions. The flow-through was collected in a fresh tube and filtered through a 0.2 μm filter before being frozen at -20°C. To confirm depletion of heparin-binding growth factors, a western blot for HDGF was performed on the injury CM and its flow-through, as described earlier. Stimulation of chondrocytes with the injury CM flow-through was performed in the gap assay as described above.

3.2.7. Stimulation of primary chondrocytes with exogenous growth factors

To investigate the effect of selective individual injury-released growth factors on isolated chondrocytes, commercially available recombinant growth factors were added to chondrocytes cultured in 1% FBS medium. Recombinant

HDGF (rHDGF) (final concentration of 50 ng/mL) and rMDK (final concentration of 50 ng/mL) were added to chondrocytes in the gap assay. rFGF2 (final concentration of 20 ng/mL), rHDGF, and rMDK were added either in combination or alone to chondrocytes plated at low-density (100,000 cells/well in a 24-well plate). Cells were imaged every 24 hours over the course of 96 hours on Olympus CKX41 with the Q-Capture Pro 7 software (QImaging, Inc.). Details of the recombinant proteins used are provided in Chapter 2.

To test activity of recombinant proteins on chondrocytes, phosphorylation of AKT was also assessed after 1-hour treatment with recombinant proteins of chondrocytes plated in 12-well cell culture plates at the density of 1×10^6 cells/well, or 2.86×10^5 cells/cm^2. Cells were lysed with 400 μL/well Radioimmunoprecipitation Assay (RIPA) lysis buffer on ice for 45 minutes, spun down, and supernatants were run on a western blot as described earlier. Reagents used in this chapter can be found in Chapter 2.

3.2.8. Statistical analysis

Image analysis of the gap assay was performed in ImageJ (Fiji) (version 1.54f). In short, an image analysis pipeline was generated in Fiji that converted an image into an 8-bit format, the threshold was manually adjusted to achieve the best contrast between the background and cells, and a 3-pixel-radius filter was applied to mask the cells. The remaining area within the gap not occupied by cells was defined as the area of the gap remaining, and the area unoccupied by cells at each subsequent timepoint was divided by the area of the gap at 0 hours in that well to obtain the percent of the initial gap remaining at that specific timepoint. The low-density migration assay was analysed via the Incucyte software, using the standard settings of the Incucyte AI Confluence Analysis Workflow (Sartorius, 2022B

Rev2). Statistical analyses were performed using GraphPad Prism (version 10.4.1). For both gap- and low-density assays, a two-way ANOVA was performed (two factor variables included: condition and time) to compare the means between conditions at different timepoints; up to three replicates per condition, per timepoint. Standard settings (GraphPad Prism) for a two-way ANOVA were applied including: a full model was fitted, and no sphericity was assumed. Statistical significance was defined using the conventional threshold of $p \leq 0.05$, and Bonferroni multiple testing correction was applied.[220]

3.3. Results

3.3.1. HDGF is released upon cartilage and skin injury

In order to confirm the release of HDGF upon injury, I performed western blot on injury CM generated from either cartilage (porcine and murine), ear (murine) or skin (murine). HDGF was identified in explant and recut porcine cartilage injury CM, but not in the "non-injury" rested CM. Cartilage injury CM were conditioned over different time periods (between 5 and 45 minutes), and HDGF was released at both 5 minutes and 45 minutes, with a stronger signal in explant CM (5-minute conditioning) compared with recut CM (Figure 3.2).

In order to study whether injury-associated release of HDGF was conserved across species, I sought to investigate cartilage injury responses in mouse. Accordingly, I generated injury CM from *Hdgf* knockout (*Hdgf*$^{-/-}$) and wild-type (WT) C57BL/6 mice using hip avulsion as my cartilage injury model. HDGF was detected in the injury CM generated from avulsed WT hips by western blot and was absent in the *Hdgf*$^{-/-}$ injury CM (Figure 3.2). Similarly, HDGF was detected at the predicted molecular weight in the WT, but not *Hdgf*$^{-/-}$ ears. HDGF was also detected in WT skin, but not in *Hdgf*$^{-/-}$ skin (Figure 3.2).

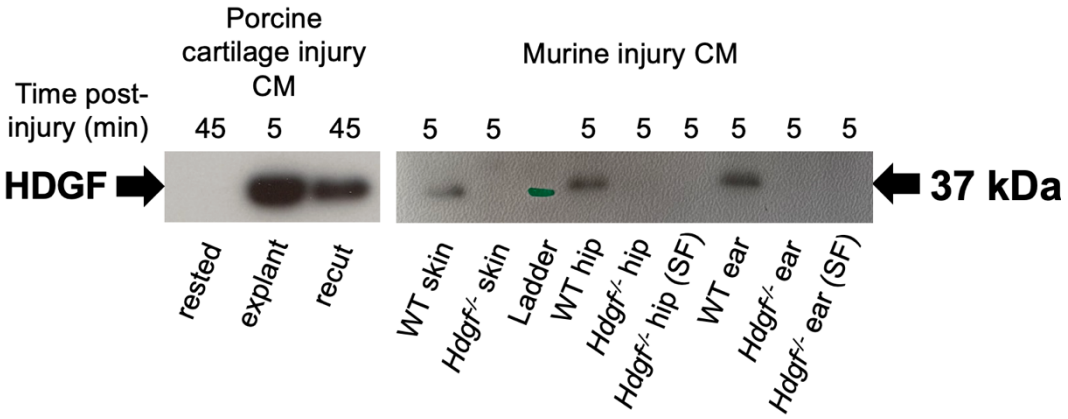

Figure 3.2. HDGF is released upon cartilage and skin injury in porcine and murine tissues. Following various periods (numbers in minutes) of conditioning, HDGF is detected in porcine cartilage injury CM and wild-type (WT) murine cartilage, ear, and skin injury CM, but not from *Hdgf* knockout ($Hdgf^{-/-}$) tissues. SF – injury CM made in serum-free medium; all other CM made in 1% FBS medium. Green marker on the protein ladder is a 35 kDa marker.

3.3.2. Injury CM changes the phenotype of primary chondrocytes

Following demonstration of HDGF release in response to cartilage injury, I set out to investigate the biological effect of the injury CM on chondrocytes. In order to assess this, I utilised two *in vitro* assays: the gap and the low-density assays. Chondrocytes at the gap edge stimulated with injury CM in the gap assay demonstrated a change in their rounded shape turning into fibroblast-like elongated cells by 24 hours following stimulation (Figure 3.3A). The gap was generally filled by 72-96 hours (Figure 3.3B, C). Staining of chondrocytes treated with injury CM for 48 hours with a marker of proliferation, Ki67, revealed that at least some of the cells in the gap were proliferating (Figure 3.3D), suggesting that filling of the gap is by a combination of migration and proliferation.

In the low-density assay, rounded chondrocytes stretched out and formed reticular networks in response to injury CM (Figure 3.4A). Chondrocytes proliferated along these reticular bridge-like projections and filled the spaces with cobble-stone shaped cells. Overall confluency in the chondrocytes treated with injury CM increased significantly from the mean ± standard deviation (SD) starting confluency of 9.96±6.13% to 78.62±18.09% by 96 hours (Figure 3.4B, C). A video recording the activity of injury CM-treated chondrocytes over 96 hours can be found here: link.

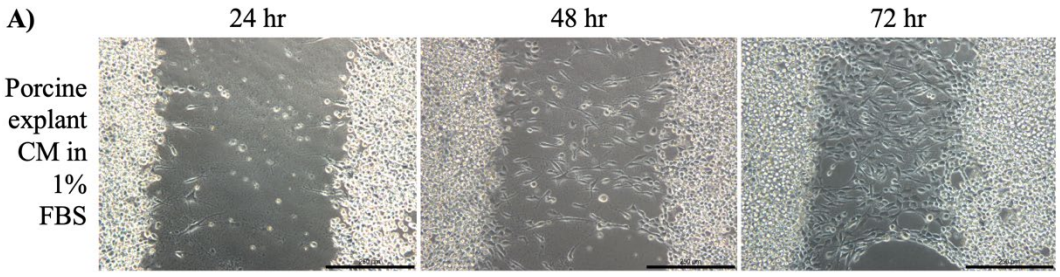

20X magnification, scale = 250 µm

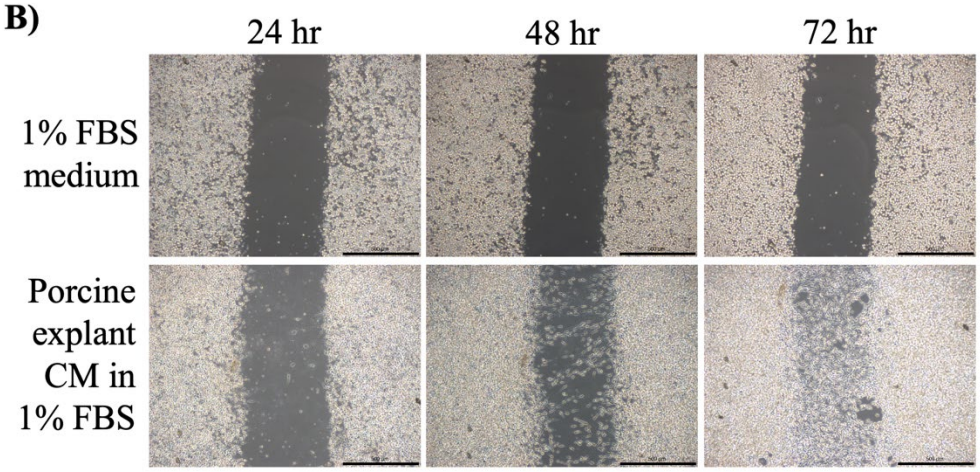

10X magnification, scale = 500 µm

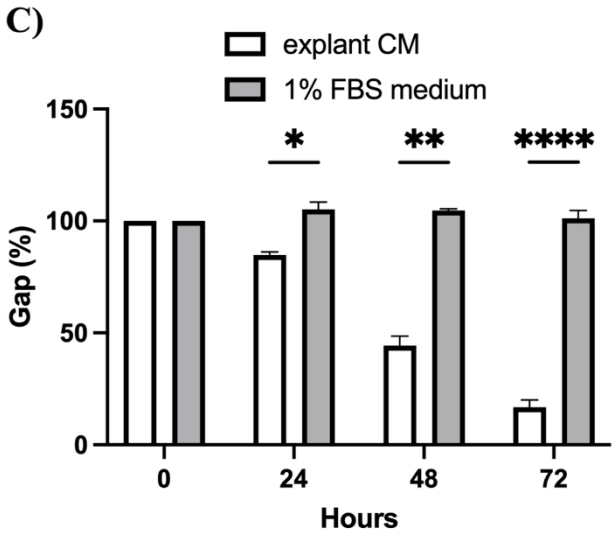

D)

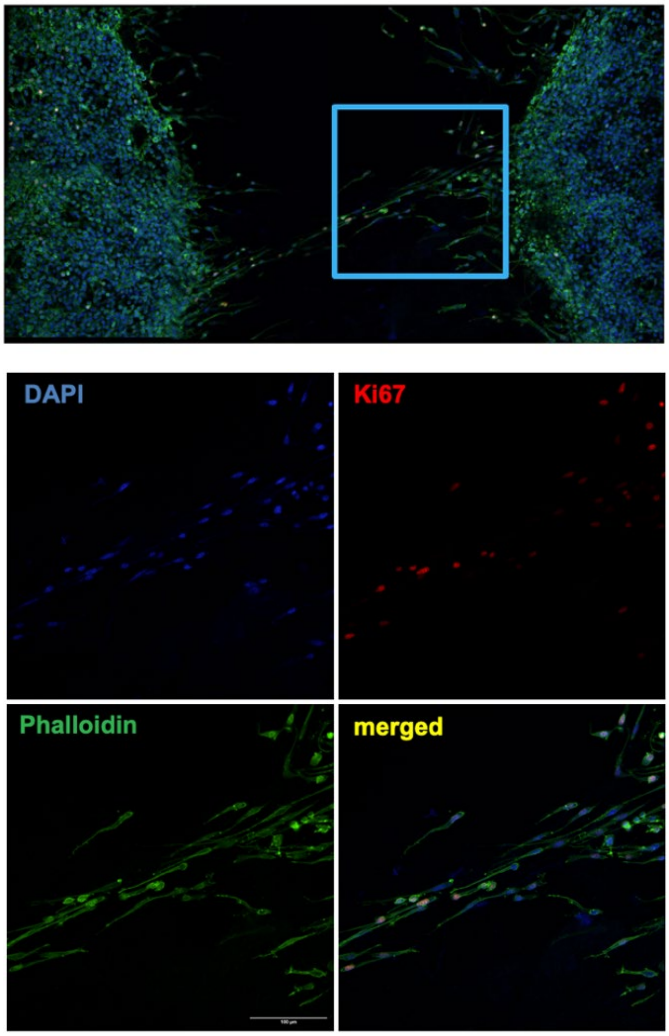

Figure 3.3. Injury CM changes the phenotype of articular chondrocytes in the gap assay, causing them to fill the gap by migration and proliferation. A) Chondrocytes changed their phenotype from rounded shape to elongated cells in response to injury CM. 20X magnification, scale bar = 250 μm. B) Chondrocytes plated in the gap assay respond to injury CM by filling the gap over time. 10X magnification, scale bar = 500 μm. C) Quantification of panel B. Mean ± standard deviation (SD) displayed, two-way ANOVA, Bonferroni's multiple comparisons test, n=3, *p<0.05, **p<0.01, **** p<0.0001. D) Ki76 staining revealed some proliferating cells in the gap. Blue square denotes the area of magnification represented below the stitched image. 10X magnification, scale bar = 100 μm.

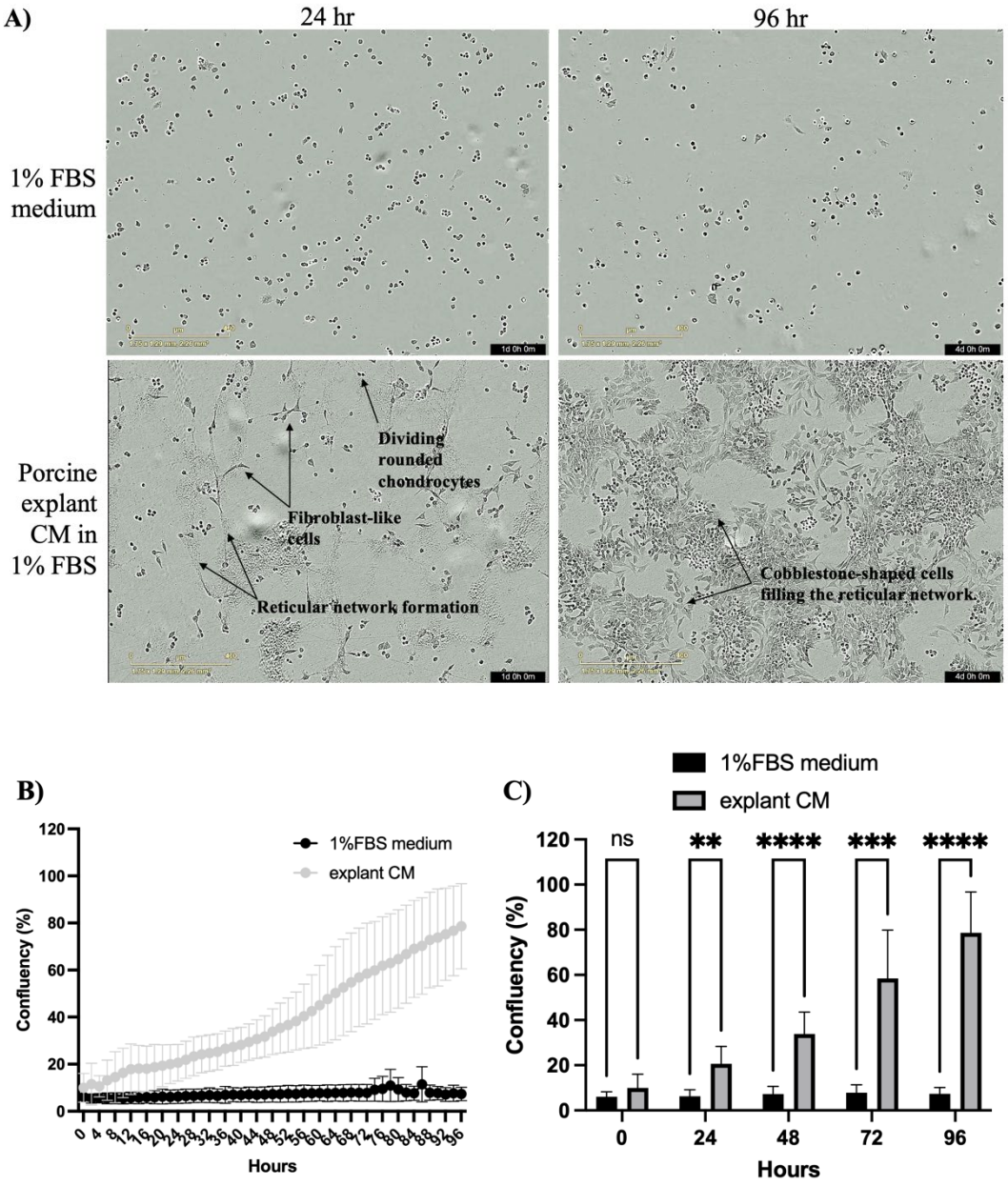

Figure 3.4. Injury CM changes the phenotype of chondrocytes in the low-density assay. A) Chondrocytes seeded at low density increased in confluency in response to injury CM. Time-lapse imaging revealed cells elongating and proliferating. 10X magnification, scale bar = 400 μm. B) Mean confluency ± SD performed over 3 separate days. C) Statistical significance displayed at 24-hour periods. Mean confluency ± SD, two-way ANOVA, Bonferroni's multiple comparisons test, n = 9 (injury CM), n = 7 (1% FBS medium), ns-not significant, **p<0.01, ***p<0.001, **** p<0.0001.

3.3.3. Injury CM elicits its effect through heparin-binding factors

In order to see whether heparin-binding proteins within injury CM were mediating the change of phenotype of chondrocytes, I depleted the injury CM of heparin-binding proteins by passing the material through a heparin column. Cells treated with the heparin column flow-through showed no response to injury CM and did not migrate or fill the gap (Figure 3.5A). Chondrocytes retained their rounded shape and did not turn into fibroblast-like cells. No statistically significant difference was observed between the injury CM flow-through-treated cells and the negative control (1% FBS medium) (Figure 3.5B).

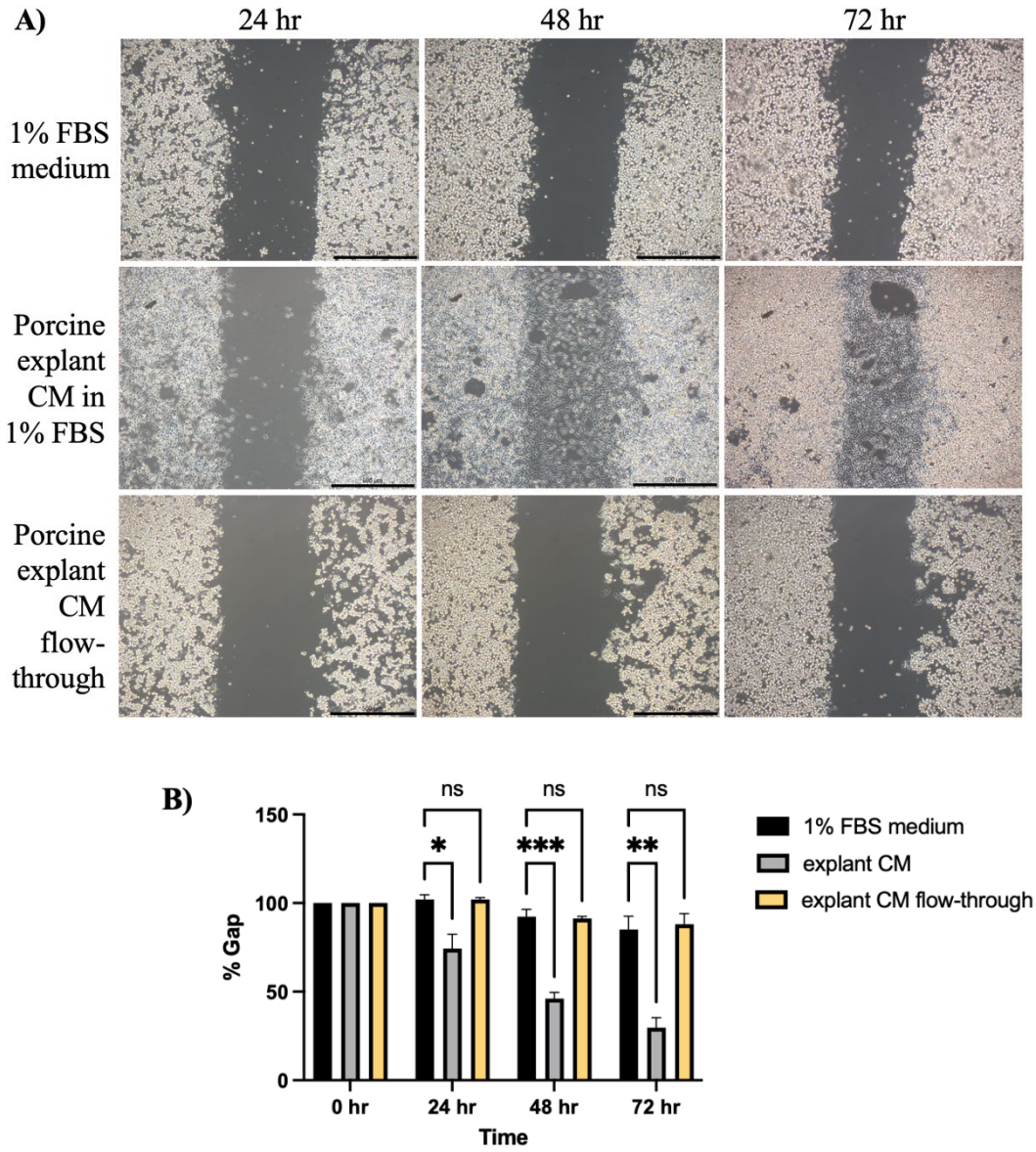

Figure 3.5. Heparin-binding proteins within injury CM drive the phenotype change of articular chondrocytes. A) Chondrocytes treated with injury CM depleted of heparin-binding factors (explant CM flow-through) did not change phenotype or migrate into the gap. 10X magnification, scale = 500 μm. B) Quantification of panel A. Mean ± SD, two-way ANOVA, Bonferroni's multiple comparisons test, n=3, ns-not significant, *p<0.05, **p<0.01, ***p<0.001.

3.3.4. Recombinant select growth factors do not change chondrocyte phenotype

To test whether known growth factors contained in injury CM have any direct effects on chondrocyte phenotype, I treated chondrocytes in the low-density and/or gap assays with recombinant HDGF, MDK, and FGF2, alone or in combination. In the low-density assay, addition of these growth factors to chondrocytes alone or in combination did not lead to a change in the chondrocyte phenotype (Figure 3.6).

Similarly, addition of rHDGF or rMDK to chondrocytes plated in the gap assay did not show any effect on chondrocyte phenotype (Figure 3.7A). To examine whether these proteins affected chondrocytes at the molecular level that may not be visible in the gap assay, I tested their effect on the PI3K/AKT pathway activation, a key pathway important for cell proliferation, growth, and repair.[221] Amongst other PCM-released growth factors, FGF2 is a known activator of this pathway, [222] [223] while HDGF has been reported to act as a PI3K activator.[224] [225] Stimulation with rHDGF and rMDK for 1 hour did not lead to phosphorylation of AKT, whereas rFGF2 showed some level of AKT phosphorylation, but was less than that in the positive control (20% FBS medium) (Figure 3.7B). I was unable to exclude the possibility that rHDGF and rMDK were not biologically active.

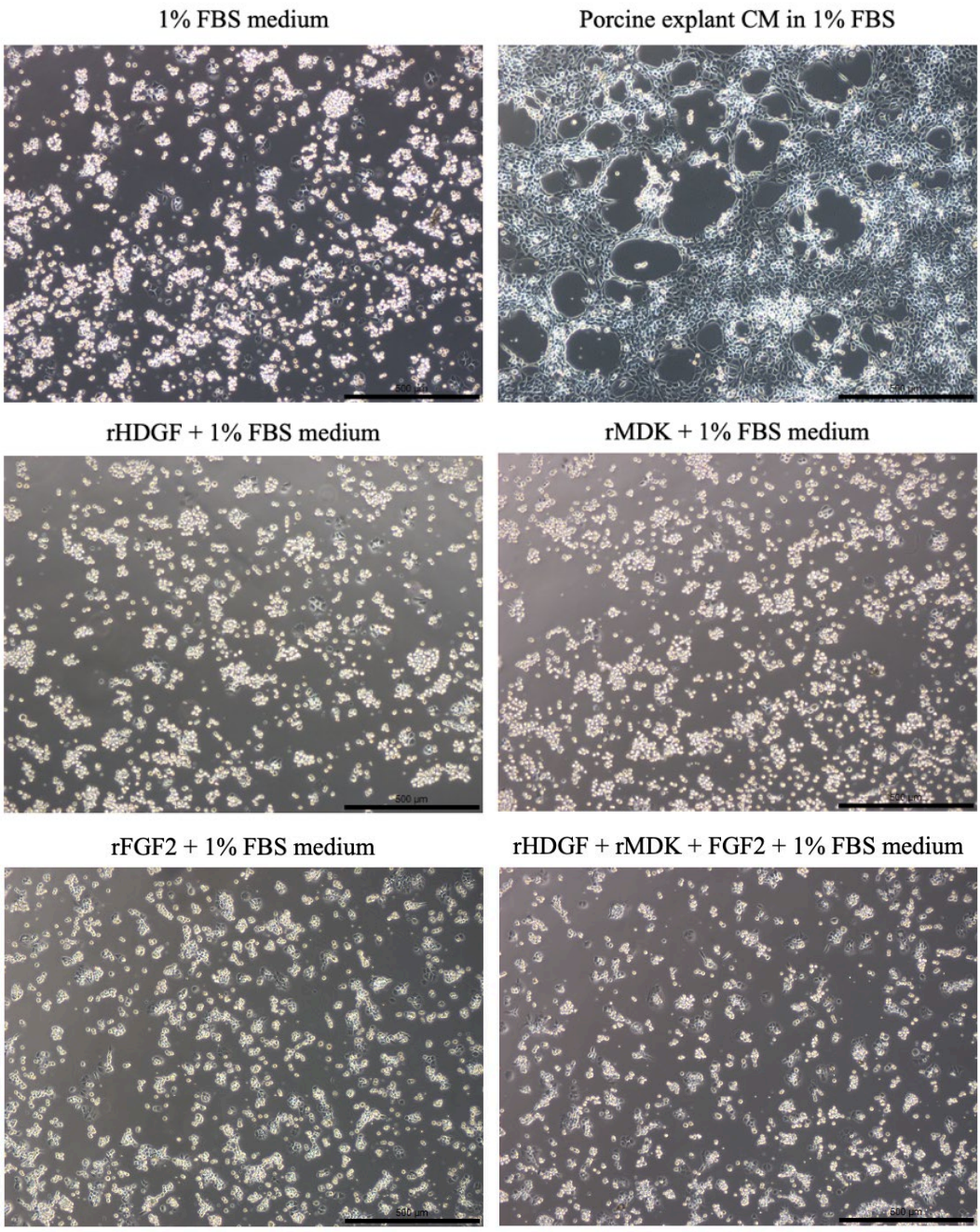

Figure 3.6. Recombinant HDGF, MDK, and FGF2 have no obvious effect on chondrocyte phenotype in the low-density assay. Porcine chondrocytes were seeded at 100,000 cells/well in a 24-well plate and stimulated for 48 hours with rHDGF (50 ng/mL), rMDK (50 ng/mL), and rFGF2 (20 ng/mL). Representative images of chondrocytes stimulated with recombinant growth factors for 48 hours. 10X magnification, scale = 500 μm.

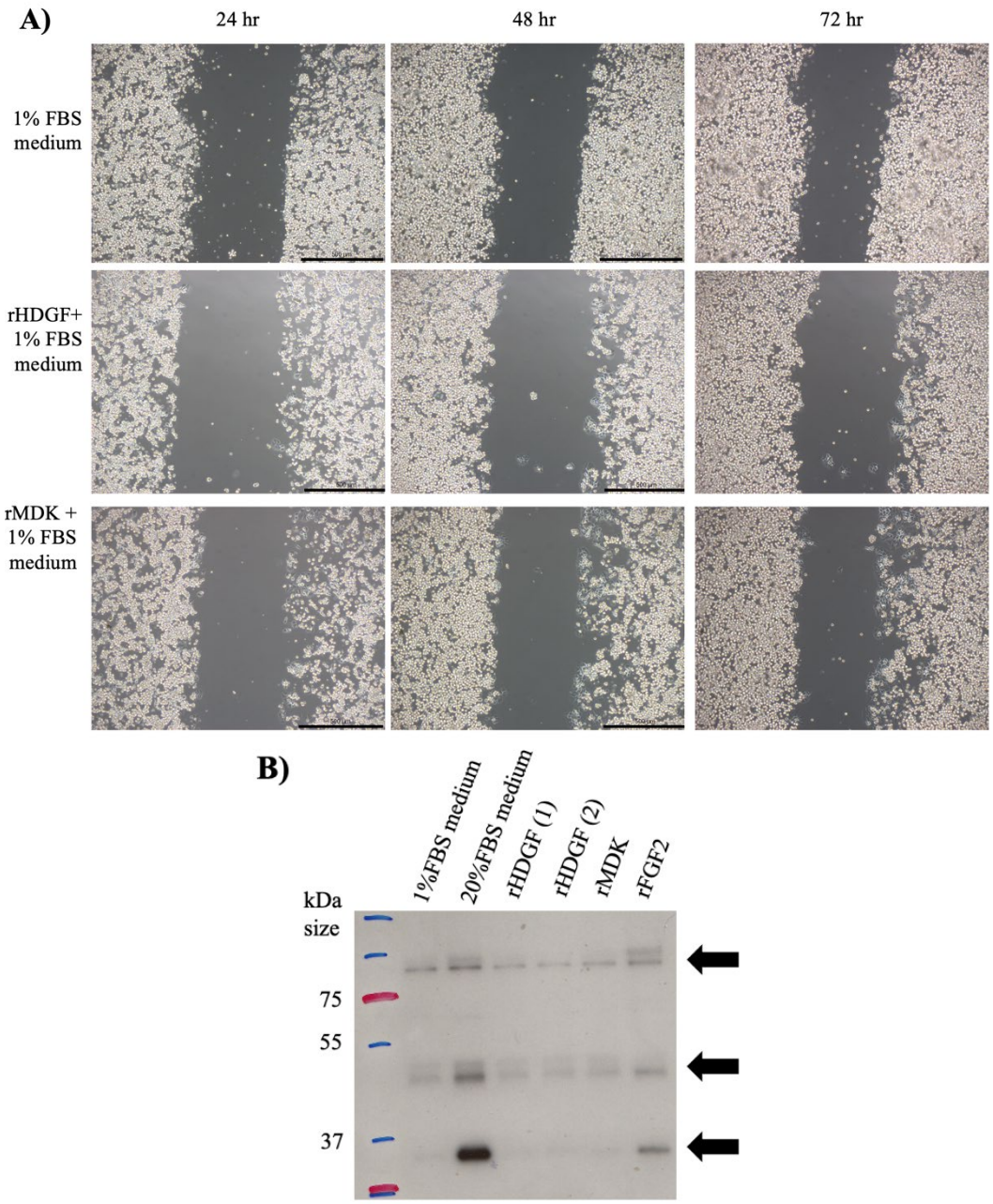

Figure 3.7. Recombinant HDGF and MDK applied in isolation have no effect on chondrocyte phenotype in the gap assay. A) Images of chondrocytes in the gap assay treated with rHDGF (50 ng/mL) (two recombinant proteins described in Chapter 2) or rMDK (50 ng/mL). 10X magnification, scale = 500 μm. B) Cell lysates immunoblotted for AKT substrates after treating chondrocytes for 1 hour with rHDGF (50 ng/mL), rMDK (50 ng/mL), or rFGF2 (20 ng/mL). 1% FBS medium used as a negative control and 20% FBS medium served as a positive control. Arrows show predicted weight of phosphorylated substrates.

Since recombinant growth factors did not mimic the chondrocyte phenotype change in response to injury CM, and limited reagents were available to inhibit HDGF and MDK, I chose to unpick the contribution of FGF2 to the injury CM response. FGF2 is released from the PCM upon cartilage injury and has a known chondroprotective effect *in vivo.*[100] Treatment of chondrocytes in the gap assay with 250 nM FGFRi added to the injury CM did not prevent chondrocytes from turning into elongated fibroblast-like cells and migrating (Figure 3.8A). It did, however, impede the overall gap filling, reaching statistical significance at the 96-hour timepoint (Figure 3.8B).

In the low-density assay, chondrocytes treated with injury CM containing 250 nM FGFRi showed stretching and proliferation along the newly formed reticular structures, similar to the response to injury CM alone (Figure 3.9A). There were, however, fewer cobblestone-shaped cells compared with that seen with injury CM alone (Figure 3.9A). The overall confluency after 96 hours was lower in the FGFRi group with (39.92±15.77% confluency) compared with injury CM-treated samples (78.62±18.09% confluency) (Figure 3.9B). Statistical significance between the two groups was evident by 48 hours (Figure 3.9C). The video showing the effect of FGFRi on the injury CM response can be found here: link.

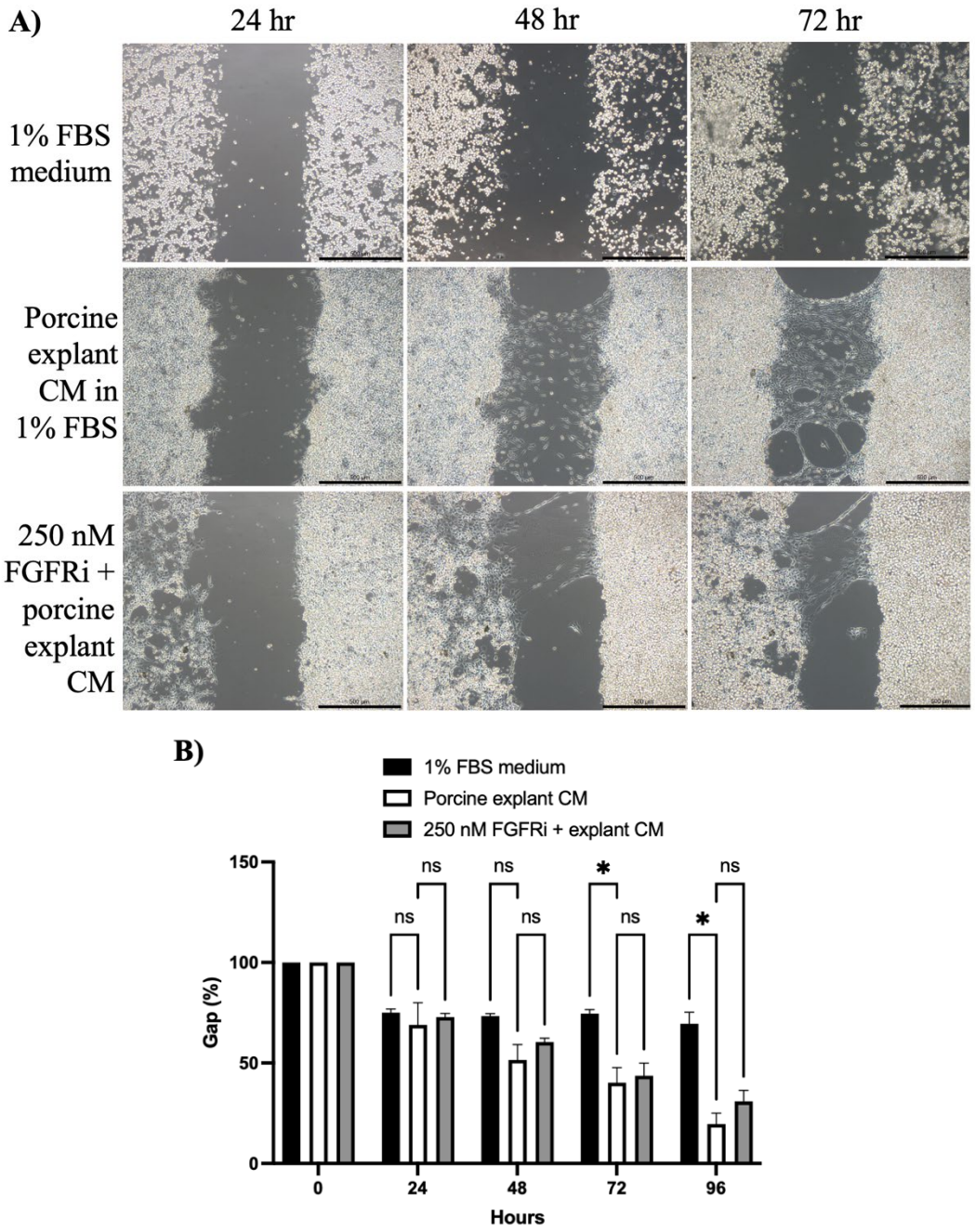

Figure 3.8. FGF receptor inhibition impedes overall filling of the gap. A) Chondrocytes treated with injury CM containing 250 nM FGFRi changed their phenotype and migrate into the gap. 10X magnification, scale = 500 μm. B) Quantification of gap filling over 96 hours. Mean ± SD, two-way ANOVA, Bonferroni's multiple comparisons test, n=3, ns-not significant, * $p<0.05$.

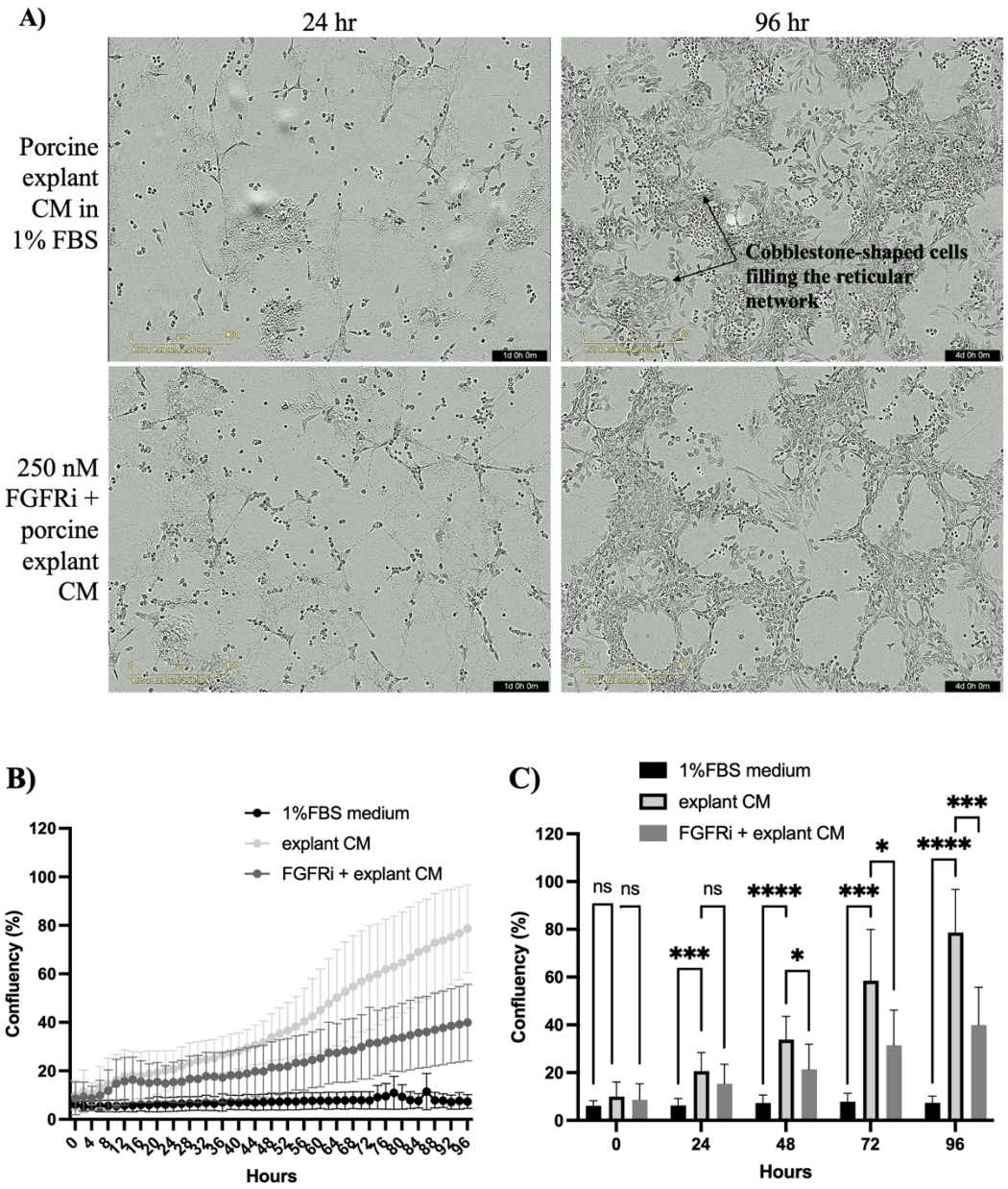

Figure 3.9. FGF receptor inhibition affects migration of chondrocytes in the low-density assay. A) Chondrocytes seeded at low density increased in confluency when treated with injury CM containing 250 nM FGFRi, but fewer cobblestone-shaped cells appeared than with injury CM alone. 10X magnification, scale bar = 400 μm. B) Mean percent confluency ± SD performed over 3 separate days. C) Statistical significance displayed at 24-hour periods. Mean percent confluency ± SD, two-ANOVA, Bonferroni's multiple comparisons test, n = 9, ns-not significant, * $p<0.05$, *** $p<0.001$, **** $p<0.0001$.

As FGFRi significantly blunted the injury CM response, I wanted to determine whether this was mediated specifically through FGF2. FGFRi targets the FGF receptor of multiple ligands of the FGF family, therefore, I used an FGF2-neutralizing antibody. In the gap assay, supplementing injury CM with 2 μg/mL of an FGF2-neutralizing antibody did not impede response of chondrocytes to injury CM (Figure 3.10A). To ensure that the lack of effect of the neutralizing antibody was not due to the antibody not being able to access its epitope in the hyaluronan-rich medium, I treated injury CM with hyaluronidase to get rid of hyaluronan that might have been interfering with antibody binding in injury CM-treated cells. Hyaluronan is known to be important for cell migration and proliferation, but hyaluronidase treatment did not affect chondrocyte phenotype change or response to an FGF2-neutralizing antibody (Figure 3.10B).[226] Neutralizing anti-FGF2 even at a higher dose (4 μg/mL), did not significantly change the chondrocyte response to injury CM in the low-density assay, though a trend towards lower density was observed in anti-FGF2 treated cells (Figure 3.10C).

Lastly, I tested whether the injury CM response was mediated by TGFβ/activin A. Latent TGFβ is also released upon cartilage injury from the PCM, covalently bound to another PCM-derived protein, CTGF.[101] Activin A is a TGFβ-family protein induced strongly by cartilage injury in an FGF2-dependent manner.[101] The inhibitor does not differentiate between receptor signalling through either ligand. No significant effect was seen when this inhibitor was added to injury CM in low-density chondrocytes (Figure 3.10D).

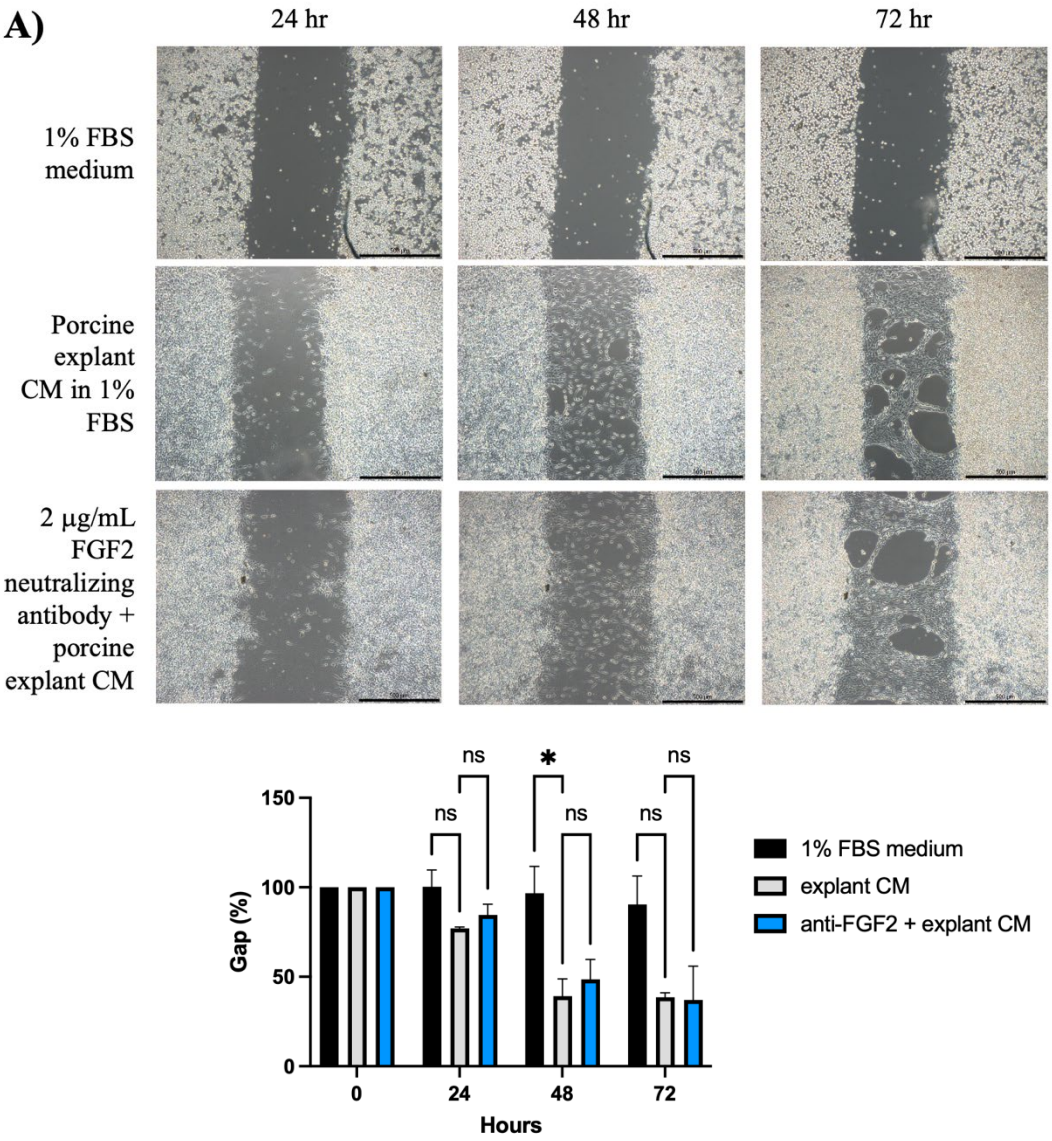
A)
24 hr
48 hr
72 hr
1% FBS medium
Porcine explant CM in 1% FBS
2 µg/mL FGF2 neutralizing antibody + porcine explant CM
ns
*
ns
ns
ns
ns
150
100
50
0
Gap (%)
0
24
48
72
Hours
1% FBS medium
explant CM
anti-FGF2 + explant CM

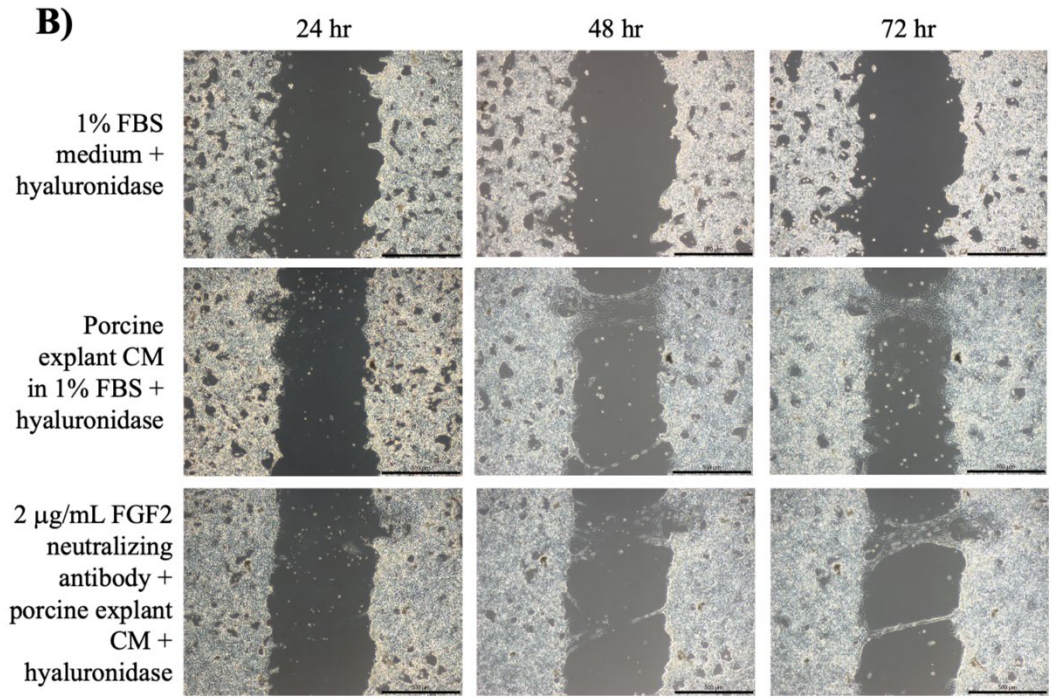
B)
24 hr
48 hr
72 hr
1% FBS medium + hyaluronidase
Porcine explant CM in 1% FBS + hyaluronidase
2 µg/mL FGF2 neutralizing antibody + porcine explant CM + hyaluronidase

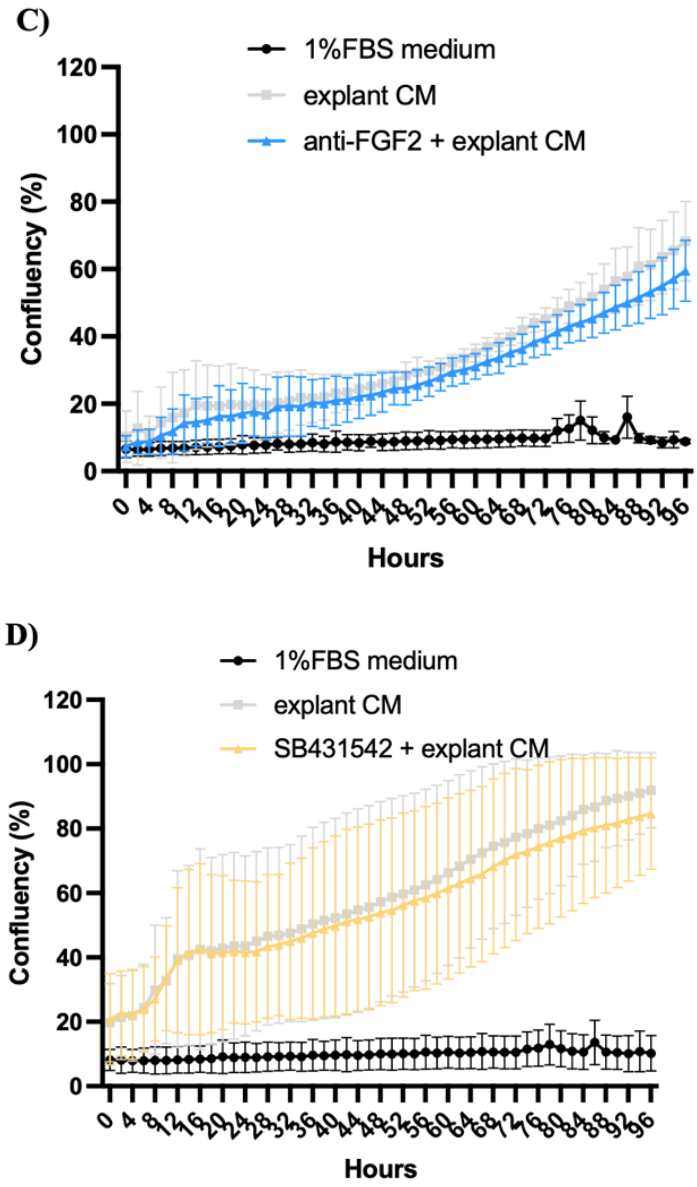

Figure 3.10. Injury CM effect on chondrocytes may not be mediated exclusively by FGF2 or TGFβ. A) There was no difference between chondrocytes treated with injury CM supplemented with FGF2 neutralizing antibody and injury CM alone. Mean ± SD, two-way ANOVA, Bonferroni's multiple comparisons test, n=3, ns-not significant, *p<0.05, 10X magnification, scale = 500 μm. B) Addition of hyaluronidase did not affect response to FGF2 neutralizing antibody, 10X magnification, scale = 500 μm. C) Supplementing injury CM with higher concentration of FGF2 neutralizing antibody (4 μg/mL) in the low-density assay did not impede chondrocyte response to injury CM. Mean ± SD, n = 6 (injury CM, anti-FGF2), n = 4 (1% FBS medium). D) Supplementing injury CM with 500 nM TGFβ/activin A inhibitor SB431542 did not affect chondrocyte response to injury CM. Mean ± SD, n = 9.

3.4. Discussion

While HDGF was previously reported to be released upon cartilage injury,[99] this work has demonstrated for the first time that HDGF is released immediately (within 5 minutes) upon injury of another connective tissue: the skin. HDGF was detected upon injury in ear tissue, which is a mix of cartilage and skin, suggesting that injury-associated release of HDGF happens across multiple tissues, though investigation of its release in more than three tissues is necessary to conclude whether it is released ubiquitously. Detection of HDGF immediately following injury from both porcine and murine tissues validated previously published results from our group,[99] and the absence of HDGF in *Hdgf*$^{-/-}$ tissues validated the specificity of the antibody for use in murine tissues. The predicted molecular weight of HDGF is 26.8 kDa (240 amino acids), but previously published results by others have reported it running at 37 kDa, sometimes with a presumed non-specific upper band, which has also been observed in murine tissues by others.[99 214 227] The discrepancy between the predicted molecular weight of HDGF and its appearance on SDS-PAGE gel can be affected by multiple factors including: post-translational modifications, incomplete protein denaturation, abnormal running on a gel, formation of protein complexes and/or protein shape.

The injury CM containing PCM-derived growth factors was able to change the appearance of chondrocytes into elongated fibroblast-like cells, capable of migration and proliferation. I was able to demonstrate that this response was independent of chondrocyte seeding density, as it was observed in both gap- and low-density assays. It is also important to mention that, in the gap assay, chondrocytes treated with injury CM assumed elongated fibroblast-like shape both at gap edges and also on the periphery (edges not facing the gap), indicating that

the observed change was not directional. Heparin-binding growth factors are essential for this phenotype change, as these cells did not appear in non-injury controls and in heparin-binding factor-depleted injury CM. Several works have reported the presence of CPCs within cartilage that have the ability to migrate in response to injury.[69 80] Our results suggest that chondrocytes can assume fibroblast-like migratory phenotype in response to injury-associated growth factors. These could represent the CPCs that others have described. In other words, this may suggest that chondrocytes turn into "CPC"-like cells, rather than CPCs being a separate cell population, as suggested before.[69] Also, our results highlight essential role that heparin-binding injury-associated growth factors play in this transition.

The process of deciphering the role of each growth factor in the injury response observed started with applying recombinant proteins onto isolated chondrocytes, as this could have provided an easy and fast read-out of their effect on chondrocyte phenotype. Recombinant HDGF and MDK did not show any effect on isolated chondrocytes applied in both gap- and low-density assays. One explanation could be that these recombinant proteins were not biologically active, as they failed to activate the PI3K/AKT pathway, in contrast to their reported effect in various types of cancer.[224 225 228] Alternatively, it may be that they do not have the same effect on isolated chondrocytes as on cancer cells, or that they need to act together with other PCM-derived growth factors to elicit an injury-associated response in chondrocytes. Additionally, the commercially available recombinant HDGF protein was derived from plant and did not have the same post-translational modifications as a mammalian protein, so the use of mammalian-derived HDGF could have yielded a different result. It is important to note that the biological effects of these cytokines are far from established as neither have been shown to bind to a

cell surface signalling receptor and their mechanism of activation remains unclear.[229] Thus, even with published evidence of their ability to activate the PI3K/AKT pathway, it is not possible to conclusively tell that recombinant HDGF and MDK I used were not biologically active. In the absence of validated neutralizing antibodies to HDGF and the lack of response to a commercially available protein, we were limited in ways we could explore the function of HDGF in the response of chondrocytes to injury CM. We attempted to apply hip- and ear-generated injury CM from WT and *Hdgf*$^{-/-}$ murine tissues onto isolated porcine chondrocytes, but this did not elicit any phenotype change in chondrocyte culture (data not shown). This might have been because the volume of injury CM generated from murine hips was very low, as it is desirable to keep the tissue-to-volume ratio close to that in porcine tissue (~1 gram of cartilage per 2 mL of medium). For instance, one murine hip produced just under 25 μL of injury CM. For the gap assay, the smallest size for fitting a silicone insert was a 24-well plate, which required a minimum culture volume of 500 μL per well. This would mean that to treat one well of chondrocytes plated in the gap assay, 250 μL murine hip injury CM would be necessary, requiring 10 hips or 5 mice to generate. In the view of this limitation, I decided to move on to *in vivo* experiments for any further work on HDGF, which will be described in the next two chapters. I did not apply skin-derived injury CM onto chondrocytes because I moved to working with the skin later in my project when most of my work was done in mice, and I did not have the opportunity to go back and repeat *in vitro* experiments due to time constraints. These experiments would be a nice addition to my data and should be done in the future to complete the characterisation of chondrocyte response to injury *in vitro.*

Contrary to HDGF and MDK, FGF2 is a much better characterised molecule, and it has a well-validated receptor inhibitor and a neutralizing antibody. This permitted me to study its function *in vitro* with a higher degree of confidence. Applying recombinant FGF2 onto chondrocytes did not elicit the same response as injury CM did, but I was also able to confirm the biological activity of the rFGF2 by demonstrating its ability to activate the PI3K/AKT pathway, which has been previously reported by others.[222 223] It is important to note, however, that to reliably demonstrate phosphorylation of AKT substrates experiments should have been repeated a few times more and quantified using densitometry. For my purposes, the goal was to compare the biological activity of rFGF2 to that of recombinant HDGF and MDK that I was using. The results of rFGF2 treatment of chondrocytes suggest that FGF2 may be important for maintaining the fibroblast-like phenotype of chondrocytes, but not for initiating a chondrocyte's transition into a fibroblast-like cell, illustrating the fact that it is not a sole mediator of this response. To take that experiment further, I could have added other PCM-derived injury-associated recombinant growth factors to isolated chondrocytes (e.g. CTGF, TGFβ) and tested what combinations would elicit chondrocyte phenotype change. I did not pursue that route because my goal was to decipher the role of HDGF specifically and I decided that moving to *in vivo* work on *Hdgf*$^{-/-}$ mice would provide the answer faster. If I had the opportunity to continue with *in vitro* experiments, I could have addressed this question by supplementing injury CM with recombinant HDGF, provided the recombinant protein was biologically active, as discussed above. This experiment would allow for over-expression of HDGF in injury and could have potentially shown how chondrocytes stimulated by injury CM would response to HDGF when it was present in higher-than-physiological concentration at the time

of injury. Another experiment could have been the supplementation of injury CM heparin column flow-through with rHDGF, which could have shown if rHDGF acted differently in injury CM compared to cell culture medium due to different chemical composition of the two (e.g. salt concentration, charge differences, other molecules present that were not heparin-binding).

Experiments with FGF-receptor inhibitor and an FGF2-neutralizing antibody allowed us to better understand its contribution to injury CM response. Various protocols for FGFRi were utilised: it was added either together with injury CM or cells were pre-incubated with FGFRi in 1% FBS medium for 1 hour prior to adding injury CM. This, however, did not make a difference to the observed cellular response. The FGF receptor inhibitor reduced confluency by about 30%, however, as it affects other FGF-family proteins, it cannot be concluded from the observed decrease in response to injury CM that this was specifically due to FGF2. The FGF2 neutralizing antibody demonstrated a slight decrease in injury CM response in both gap- and low-density assays, however, this response was not statistically different from the positive control (injury CM) in any of the experiments. Hyaluronidase treatment did not have any significant effect on the activity of an FGF2 neutralizing antibody in injury CM-treated chondrocytes.

TGFβ is also present in the injury CM, serves as a critical driver of chondrogenesis, and has well-validated tools.[99] [100] All known TGFβ receptor inhibitors also inhibit activin A signalling, another TGFβ family ligand.[230] We hypothesised that TGFβ and/or activin might be contributing to the injury CM response. The inability of the TGFβ/activin A inhibitor to interfere with the injury response suggests that TGFβ is not important for the initial transition of chondrocytes into fibroblast-like cells. It is important to remember that released

TGFβ in the injury CM is in its latent form.[101] It is possible that the biological contribution of TGFβ to the injury response is not immediate but delayed in some way.

Future work can explore in more detail the different stages of chondrocyte phenotype changes observed in response to injury CM. For instance, it would be interesting to investigate transcriptomic differences between the elongating fibroblast-like cells appearing by 24 hours with injury CM versus cobblestone-shaped cells that are more apparent by 96 hours of injury CM treatment in the low-density assay. It would also be worth examining if cobblestone-shaped cells appear in the gap assay, as there were not visible there, but this might have been due to high density of cells within the gap interfering with visualization on the microscope. One way to examine this would be to plate slightly less cells in the gap assay or to examine cells on the periphery of the seeding chamber (not facing the gap) to see if any of them assume cobblestone-shaped appearance by 96 hours. Additionally, it is possible that cobblestone-shaped cells and fibroblast-like elongated cells are different subtypes of cells that appear at different time points following injury, so it would be interesting to perform temporal characterisation of these cell types to understand better the mechanism of chondrocyte response to injury over time. Quantifying the amount of HDGF released from different tissues could provide an interesting insight into its relative abundance across tissues, as well as its potential role in tissue-specific response to injury. At present, it is not possible to say whether HDGF is more released from the skin, ear, or cartilage following injury. This is because, while I attempted to keep tissue size-to-volume of media ratio relatively similar across tissues, it is not exact and might not always be possible, given limitations of tissue size (e.g. murine hip). Additionally, tissues such as cartilage

have significantly less cells per unit area than skin, which would affect how much protein is present in the tissue at the baseline and might not necessarily translate into any functional significance.

Taken together, the results reported in this chapter demonstrate that HDGF is an injury-released growth factor in both cartilage and skin, as it is contained in injury CM generated from these tissues. I have also demonstrated that the generated porcine injury CM affects the ability of chondrocytes to respond to injury by changing them into fibroblast-like cells capable of migration and proliferation. This change is strongly dependent on heparin-binding growth factors, of which HDGF is part, and is partially mediated by FGF2, but other PCM-derived proteins are likely to be involved in this response also; however, from the data obtained, it was not possible to say what the role of HDGF in gap filling and proliferation was specifically. The tools to study this *in vitro* are limited. Therefore, to understand better the role of HDGF in tissue injury, I decided to take advantage of the *Hdgf*$^{-/-}$ mice available to us to investigate molecular differences that happen upon knocking out HDGF and to study how they may affect injury response in these animals using *in vivo* and *ex vivo* injury assays.

Chapter 4: Molecular changes in HDGF knockout tissues.

4.1. Introduction

As described in the previous chapter, investigating the role of HDGF *in vitro* came with its own challenges. Constitutive HDGF knockout mice (*Hdgf*$^{-/-}$) offered an opportunity for studying the effect of HDGF deficiency at the molecular and cellular level. The mechanism of HDGF activation and signalling is still unknown and there is limited understanding of what other proteins and/or pathways might be affected when HDGF is deleted, and whether they (or HDGF itself) have any effect on tissue response to injury. When *Hdgf*$^{-/-}$ mice were generated, they were initially used to study the role of HDGF in development. Results of this work concluded that HDGF was dispensable for development, as *Hdgf*$^{-/-}$ pups were not significantly different from WT pups phenotypically and/or behaviourally (comparison carried out at 2 weeks post-natally). Additionally, *in vitro* characterisation of *Hdgf*$^{-/-}$ dermal fibroblasts revealed that their proliferation and apoptosis rates were not different from that of WT cells.[214] This study, however, did not examine transcriptional differences associated with HDGF deletion, and the group had no further interest in keeping this mouse line, enabling our group to acquire it.

As this may be the only known *Hdgf*$^{-/-}$ mouse line, I had a unique opportunity to examine molecular differences between *Hdgf*$^{-/-}$ and WT animals. Additionally, as the first part of this work demonstrated the injury-induced nature of HDGF release across multiple connective tissues, I wanted to investigate the role of HDGF in tissue injury and/or repair. Identifying molecular differences associated with HDGF deletion in rested versus injured tissues could help answer this question. As mentioned previously, some studies suggested involvement of HDGF in injury and/or repair (e.g. increased expression in response to mechanical stress and in

keloid scars).[209 219] I thus hypothesised that HDGF deletion might lead to molecular changes that could affect the way tissues respond to injury.

As discussed in the introduction, most of the literature on presumed function of HDGF comes from cancer cell lines, where high expression of HDGF was correlated with various metrics, such as worse survival or poor response to chemotherapy.[231] None of these papers, however, were able to decipher the mechanism of action of HDGF. One clue about potential mechanism of action of HDGF comes from lens epithelium-derived growth factor (LEDGF), which is another member of the HDGF protein family structurally similar to HDGF.[232] LEDGF acts as a stress-mediating survival and transcription factor, as well as affects chromatin accessability.[170 233] Another insight into the mechanism of action of HDGF comes from an interactome study performed through streptavidin-binding peptide and Flag tag-based tandem affinity purification (SBP/Flag-TAP) coupled with liquid chromatography-tandem mass spectrometry (LC-MS/MS) of human HEK293T cells. This study identified that HDGF interacted with proteins involved in chromatin remodelling, DNA repair, transcription, splicing, ribosomal assembly, and translation.[213] These studies led us to hypothesise that potential effects of HDGF deletion might not be limited to transcription, prompting investigation of proteomic differences between WT and *Hdgf*$^{-/-}$ tissues, in addition to examining their gene expression profiles.

Chapter aims:

1) To compare genotype-specific transcriptional differences between WT and *Hdgf*$^{-/-}$ cartilage and skin,
2) To study injury-associated transcriptional changes in WT and *Hdgf*$^{-/-}$ cartilage,

3) To investigate proteomic differences between WT and *Hdgf*$^{-/-}$ skin following injury.

4.2. Methods

4.2.1. Cartilage and skin collection

Two tissues were used for studying molecular changes in *Hdgf*$^{-/-}$ mice. The first one was cartilage obtained via hip avulsion. Six-week-old female C57BL/6 (wild-type) and *Hdgf*$^{-/-}$ mice were sacrificed by CO_2 asphyxiation followed by confirmatory cervical dislocation. The mouse was topically sterilised with 70% ethanol and hip joints were exposed by dissection with autoclaved forceps and scissors pre-cleaned with RNAseZap (Thermo Fisher Scientific, Waltham, MA, USA). Hips were dislocated from the hip joint, and the femoral cap was avulsed through the growth plate using forceps. For 0-hour samples, hips were immediately transferred into a fresh 1.5 mL Eppendorf tube (2 hips per tube), placed on dry ice, and transferred into -80°C until RNA processing. For 4-hour samples, each hip was cut into 4 pieces, and 2 hips were pooled together and incubated in 500 μL of serum-free (SF) medium for 4 hours at 37°C (these are "cut"/"injured" samples). They were then placed into a 1.5 mL Eppendorf tube on dry ice and stored at -80°C. RNA was extracted from hips within 2 weeks of tissue collection.

The second tissue used for studying molecular changes associated with HDGF deletion was skin. For skin collection, full-thickness skin punch biopsies were made on the backs of 15-week-old male C57BL/6 (wild-type) and *Hdgf*$^{-/-}$ mice. Briefly, mice were anesthetised by inhalation of isoflurane (3% induction and 1.5-2% maintenance) in 1.5-2 L/min oxygen. All mice received a subcutaneous injection of buprenorphine (Vetergesic; Alstoe Animal Health) before skin biopsy was performed. The fur on the back was shaved with a trimmer, shaving cream was applied for 4 minutes and wiped with warm water followed by topical sterilisation with Hibiscrub (Mölnlycke Heath Care, Gothenburg, Sweden). Four 3-mm-

diameter biopsy punches were removed from the back of each mouse with an autoclaved leather biopsy puncher. Two biopsies were pooled together and immediately placed into a 1.5 mL Eppendorf tube on dry ice and stored at -80°C (0-hour sample). Two other biopsies were each cut into 4 pieces and incubated in 500 µL of SF medium for 4 hours at 37°C (4-hour sample). They were then transferred into Eppendorf tubes and stored at -80°C until further processing. RNA extraction was performed within 2 weeks of skin collection. Details of reagents and tools used for tissue collection are available in Chapter 2.

4.2.2. RNA extraction from cartilage and skin

RNA was extracted from avulsed hips of 6-week-old female C57BL/6 (wild-type) and *Hdgf*$^{-/-}$ mice. Two hips were pooled together per one RNA sample. Briefly, frozen hips were crushed and ground in liquid nitrogen with a cold mortar and pestle, and the powder was transferred into a freshly prepared RLT buffer (Qiagen, Hilden Germany) containing 2-mercaptoethanol (1:100 dilution) (Thermo Fisher Scientific, Waltham, MA, USA) (150 µL/sample). Samples were then digested with proteinase K (Qiagen, Hilden Germany) for 10 minutes at 55°C and processed according to the modified RNeasy Micro Kit extraction protocol (Qiagen, Hilden Germany). RNA was eluted with 14 µL of RNAse-free water and quantified using Nanodrop. The list of reagents used for RNA extraction from the cartilage is available in Chapter 2.

Skin RNA was extracted from 3-mm (in diameter) full-thickness punch biopsies of 15-week-old C57BL/6 (wild-type) and *Hdgf*$^{-/-}$ male mice. Two skin biopsies were pooled together per one RNA sample. Frozen biopsies were cut with pre-cooled 10-blade scalpel (Swann-Morton, Sheffield, England) on a Petri dish

placed on dry ice into smaller pieces (~1 mm). Smaller pieces were then transferred into gentleMACS M tubes (Miltenyi Biotec, Bergisch Gladbach, Germany) and 1 mL TRIzol reagent (Thermo Fisher Scientific, Waltham, MA, USA) was added to each sample. Biopsies immersed in TRIzol were homogenised using the GentleMACS tissue dissociator (Miltenyi Biotec, Bergisch Gladbach, Germany). Samples were then spun at 13,000 RPM at 4°C for 5 minutes, supernatant collected and mixed with 1-bromo-3-chloropropane (Sigma Aldrich, St Louis, MO, USA), followed by a 5-minute incubation at room temperature. The sample was spun again for 20 minutes, the aqueous phase containing RNA was collected and mixed 1:1 with 100% ethanol (BioUltra/Molecular Biology grade) (Sigma Aldrich, St Louis, MO, USA). The sample was then loaded onto Zymo-spin column and RNA was extracted using the Zymo RNA Clean and Concentrator-5 Kit (Zymo Research, Irvine, CA, USA). RNA was eluted with 14 μL of RNAse-free water and quantified using Nanodrop. Reagents used for RNA extraction from the skin are available in Chapter 2.

4.2.3. Bulk RNA sequencing and analysis

RNA quantity and integrity were assessed with Agilent 5400 Bioanalyzer. The minimum RNA integrity number (RIN) of samples sent for sequencing was 4.0 (Novogene Cambridge requirements). The range of RIN values for sequenced samples is shown in Supplementary Table 1. For cartilage RNA samples, four samples per genotype from two timepoints (0- and 4-hours post-hip avulsion) were sent to Novogene Cambridge for RNA library preparation and bulk sequencing. For skin RNA samples, only 0-hour timepoint samples (4 samples per genotype) were sent for bulk RNA sequencing, as RIN numbers of 4-hour (cut/injured) samples were too low.

Polyadenylation-selected sequencing libraries were prepared by Novogene Cambridge. Sequencing was performed using 150 paired-end Illumina's NovaSeq X Plus platform as part of Novogene's Whole-transcriptome One-Base Insertion (WOBI) RNA-seq package. RNA-seq analysis was performed using txseq pipelines (https://github.com/sansomlab/txseq). Sequence reads were aligned to the mouse genome with HISAT2 (version 2.1.0) using a "genome_trans" index built from the genome assembly Mus musculus GRCm39 version 110 annotations.[234] Data quality was assessed using pipeline_fastqc.py. The average alignment rate was 89.00%. Mapped reads were counted using featureCounts (GRCm39 version 110 annotations, with default parameters).[235] Salmon v0.9.1 was used to calculate transcript per million values using a quasi-index (built with GRCm39 version 110 annotations) and gc bias correction (parameter "--gcBias").[236] Differential expression (DE) analysis of cartilage at 0- (non-injured) versus 4-hours (injured) versus skin at 0 hours (non-injured) samples was performed in R (v4.4.0) using Bioconductor package DESeq2 (v1.44.0).[237] Prior to analysis, genes expressed at zero counts were filtered out to retain 33,985 protein-coding genes expressed at counts >0. For cartilage samples, gene set enrichment analysis with FGSEA[238] with Hallmark pathway annotations[239] was performed using the 18,070 genes for WT 4 vs 0 hours, 17,800 genes for *Hdgf*$^{-/-}$ 4 vs 0 hours, 15,704 genes for WT vs *Hdgf*$^{-/-}$ at 0 hours, 20,656 genes for WT vs *Hdgf*$^{-/-}$ at 4 hours, and 16,008 genes for comparing the magnitude of injury-associated change in WT vs *Hdgf*$^{-/-}$. A Pearson correlation was performed between gene expression of *Hdgf*$^{-/-}$ and WT genotypes following cartilage injury. Pearson correlation and p-value are reported. In skin samples, gene set enrichment analysis of Hallmark pathways was performed using 16,340 genes WT vs *Hdgf*$^{-/-}$ at 0 hours. One WT sample (WT_0h_1) was removed from analysis

due to low number of reads (Supplementary Figure 1). Statistical significance was defined by p-adjusted (padj) value of less than 0.05.

4.2.4. Proteomic labelling of the skin and proteomics analysis

For proteomic labelling of skin samples, a Stable Isotope Labelling by Amino Acids in Cell Culture (SILAC) technique was performed on skin biopsies *ex vivo*. Usually, SILAC is done on isolated cultured cells *in vitro*, and this may have been the first time SILAC labelling was done on full-thickness skin biopsies (based on published literature). The underlying principle of SILAC is incorporation of "heavy" lysine (L-lysine-$^{13}C_6$ hydrochloride) into newly synthesised proteins. Liquid chromatography-tandem mass spectrometry (LC–MS/MS) analysis of SILAC-labelled samples can detect "heavy"- and "light"-labelled protein abundances and heavy to light ratios for each detected protein can be calculated, with higher ratios reflecting increased new protein synthesis measured within the tissue.

Full-thickness skin biopsies were obtained from the backs of 15-week-old C57BL/6 (wild-type) and *Hdgf*$^{-/-}$ male mice as described above. Each biopsy was cut into four equal pieces with a 15-blade scalpel (Swann-Morton, Sheffield, England) on a Petri dish. One biopsy was immediately placed into an Eppendorf tube containing 400 μL SDS lysis buffer (recipe available in Chapter 2) and incubated on shaker at room temperature overnight. This was a 0-hour control sample biopsy. The following day, the sample was spun at 1500 RPM for 10 minutes at 4°C and supernatant was collected and stored at -20°C until further use. One biopsy was placed into 400 μL SILAC-supplemented culture medium (recipe available in Chapter 2) and incubated for 24 hours at 37°C before spinning and collection. This was a 24-hour SILAC-labelled skin biopsy. Finally, another biopsy

was placed into 400 μL SILAC-supplemented culture medium and incubated for 48 hours at 37°C before spinning and collection. This was a 48-hour SILAC-labelled skin biopsy. A cartoon summarising the workflow of sample preparation for the proteomic labelling study is shown in Figure 4.1. Two timepoints - 24 and 48 hours - were chosen to explore changes in the proteome during different phases (more and less acute) of the tissue injury response.

Sample preparation was done by Dr Anna Hoyle from the Kennedy Institute of Rheumatology. Briefly, the sample was reduced and alkylated in TCEP (10 mM) and Iodoacetamide (50 mM) respectively. This was then acidified using phosphoric acid (12%) followed by the addition of 7 volumes of S-trap binding buffer (90% methanol in 100 mM TEAB). Samples were loaded onto S-trap columns (ProtiFi, Fairport, NY, USA), which were then washed with S-trap binding buffer. This was then digested with Trypsin and incubated overnight. Samples were eluted with 50 mM TEAB, followed by 0.2% formic acid and finally with 0.2% formic acid in 50% acetonitrile. Elution's were pooled, dried down and resuspended in 0.1% formic acid.

LC–MS/MS was performed by Dr Iolanda Vendrell and Professor Roman Fischer at the Target Discovery Institute of Nuffield Department of Medicine, University of Oxford. LC–MS/MS was done using the Thermo Fisher Scientific Vanquish Neo UHPLC system connected to a Thermo Orbitrap Ascend (Thermo Fisher, Waltham, MA, USA) mass spectrometer. The Vanquish Neo was operated in the "Trap and Elute" mode where 1.5% of the tryptic peptides were trapped and separated using a 75-min linear gradient (from 2% to 20% B in 45 min, then to 35% in 15 min before rising to 99% in 1 min) at 300 nL/min flow, where solvent A was 0.1% formic acid and B was 0.1% formic acid in acetonitrile. MS data were

acquired in data-dependent mode (DDA) as previously described by Liang et al.[240] Survey scans (MS1) were acquired in the Orbitrap over the mass range of 380–1,500 m/z, with a 120 K resolution, maximum injection time of 251 milliseconds (ms), an AGC set to 100%, and an RF lens set at 30%. MS2 scans were then collected with a 15 K orbitrap resolution, normalised AGC target of 5,000%, maximum injection time set to 27 ms, and a 30% collision energy.

Proteomics data analysis was performed by Dr Anna Hoyle. Raw mass spectrometry files were quantified using a label-free approach with FragPipe software (version 23.0) against the UniProt/SwissProt mouse database (2024) with added decoys and known contaminants which contained a total of 43654 sequences (50% decoys). A maximum false discovery rate of 1% was used, with carbamidomethyl as a fixed modification to cysteine residues (57.021Da). The search was fully tryptic and 2 missed cleavages were allowed. Heavy arginine (6.0201 Daltons) labelling was included in the search for quantification of protein synthesis. Data was exported and onward analysis was conducted in Perseus (v2.0.11) and R (v4.3.2). Heavy to light ratios were calculated from heavy and light protein abundances.

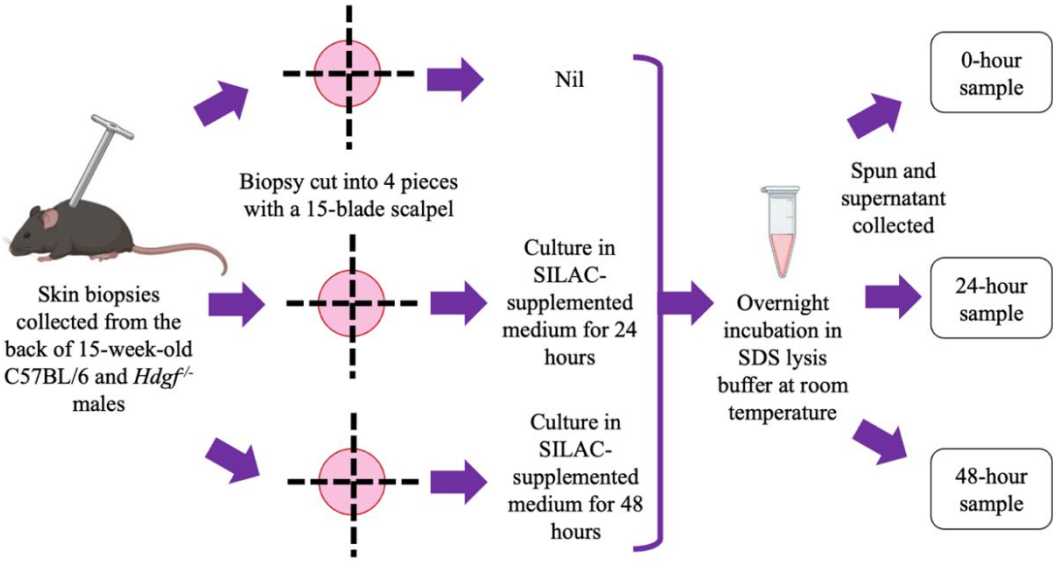

Figure 4.1. Workflow of sample preparation for the proteomic labelling study of WT and *Hdgf*$^{-/-}$ skin. Full-thickness skin biopsies were collected from the dorsum of mice and incubated with SILAC-containing medium for various periods of time before lysis and collection. Boxes indicate the names of respective samples as they will be referred to further. List of reagents is available in Chapter 2. SILAC – stable isotope labelling by amino acids in cell culture.

4.2. Results

4.2.1. Transcriptional changes between wild-type and *Hdgf*$^{-/-}$ tissues: cartilage and skin

To investigate if HDGF deletion affected the transcriptome, I first examined transcriptional differences between WT and *Hdgf*$^{-/-}$ animals in non-injured (0 hour) cartilage and skin. In cartilage, DESeq analysis detected a total of 79 genes differentially expressed at a statistically significant level (padj<0.05) between the genotypes at 0 hours. Encouragingly, *Hdgf* was one of the most differentially regulated genes when sorted by padj value; however, $\log_2$ fold-change of -2.42 in the cartilage and -3.5 in the skin suggested a knockout efficiency of 81.3% ($2^{-2.42}$=0.187, meaning gene expression of 18.7% in *Hdgf*$^{-/-}$ compared to WT) and 91.3% respectively. These values were lower than expected from an embryological knockout, where the values of expression for knocked out gene would be normally reach 97-100%. The volcano plot labelling the top 20 differentially expressed genes (sorted by padj) (Figure 4.2A) and the heatmap showing all 79 significantly expressed genes are shown (Figure 4.2B). In 0-hour skin samples, a total of 28 genes were differentially expressed between WT and *Hdgf*$^{-/-}$ animals at a statistically significant level (padj<0.05) (Figure 4.3A, B). Similarly to the results obtained from cartilage RNA, *Hdgf* was identified among the top differentially expressed genes (sorted by padj) in the skin. Next, I wanted to examine whether there was any overlap between differentially expressed genes detected in cartilage and skin. Comparison of statistically significant transcriptional differences identified in cartilage and skin revealed 5 genes that overlapped across the two tissues: *Hdgf*, ribosomal protein S3A1 (*Rps3a1*), ribosomal protein S3A2 (*Rps3a2*), ribosomal protein S3A3 (*Rps3a3*), and hypoxanthine phosphoribosyltransferase 1

(*Hprt1*). Further investigation showed that these overlapping genes were regulated in the same direction and to a similar extent in both tissues (Figure 4.4).

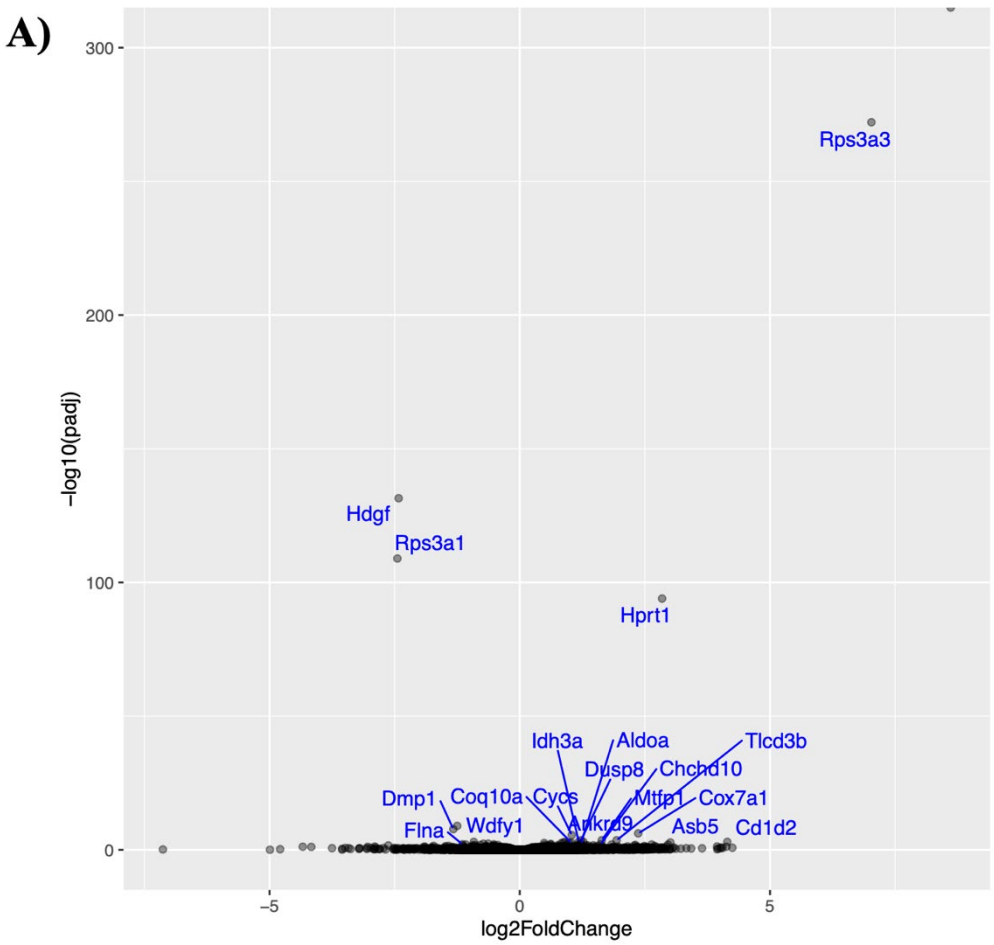

Figure 4.2. Differentially expressed genes between WT and *Hdgf*$^{-/-}$ (KO) cartilage at 0 hours (no injury). A) Volcano plot labelling top 20 differentially expressed genes (sorted by padj), padj<0.05.

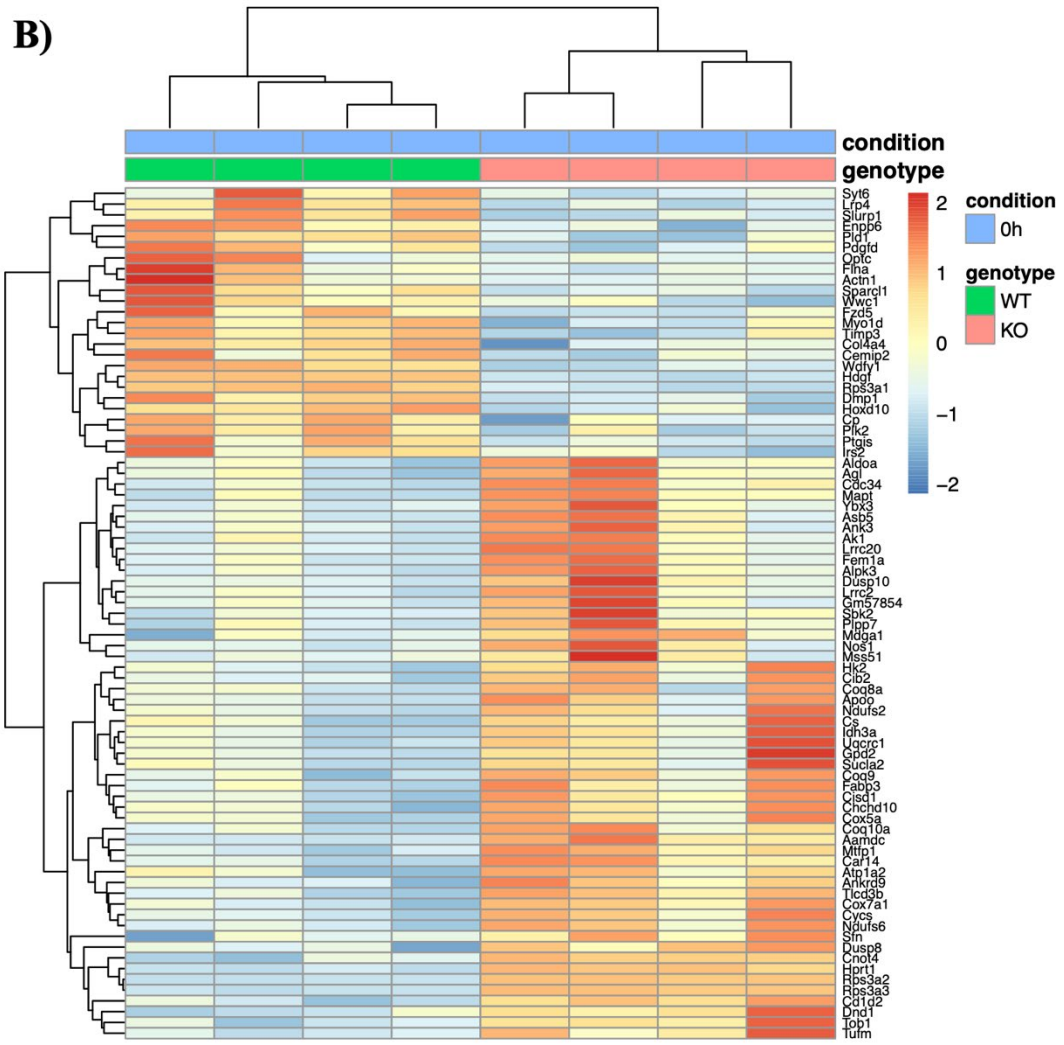

Figure 4.2 (continued). Differentially expressed genes between WT and *Hdgf*$^{-/-}$ (KO) cartilage at 0 hours (no injury). B) A heatmap representation of all significant 79 differentially regulated genes showing their relative expression in each individual sample, padj<0.05.

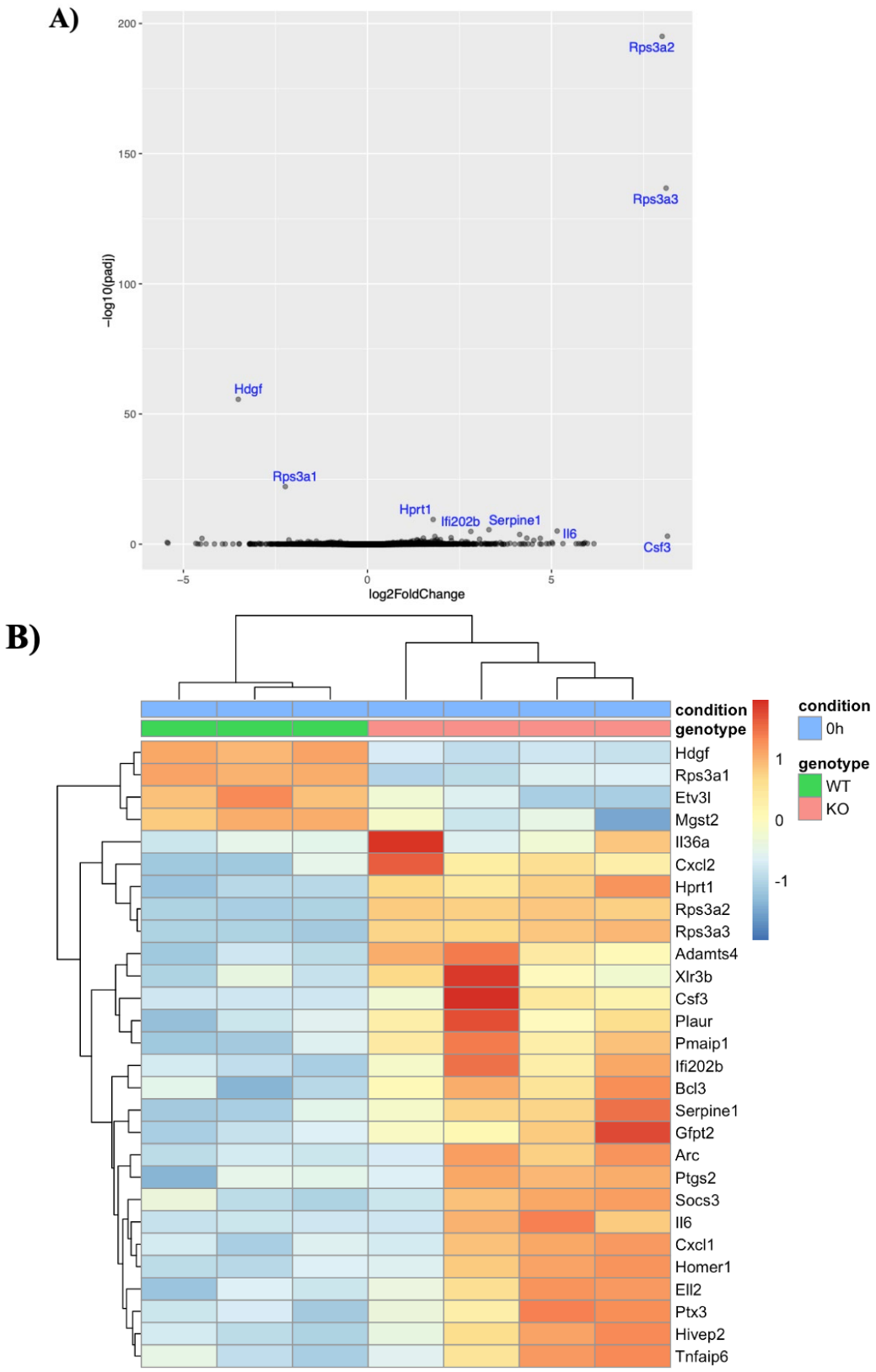

Figure 4.3. Differentially expressed genes between WT and *Hdgf*$^{-/-}$ (KO) skin at 0 hours (no injury). A) Volcano plot labelling top 10 differentially expressed genes (sorted by padj), padj<0.05. B) A heatmap representation of the 28 genes differentially expressed between WT and *Hdgf*$^{-/-}$ skin showing their relative expression in each individual sample, padj<0.05.

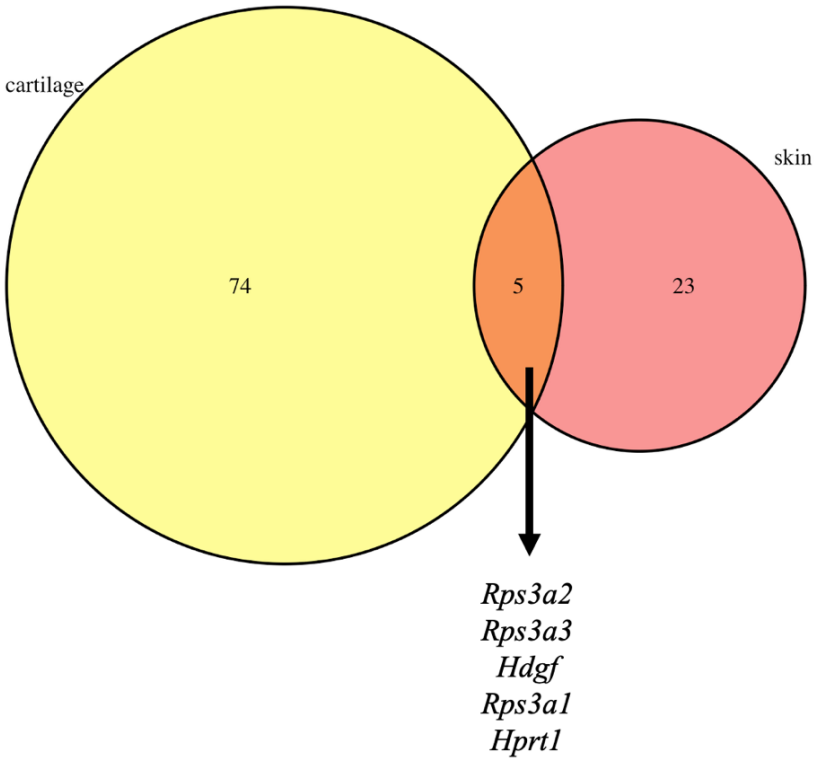

	Cartilage		Skin	
Gene	**log_2 fold-change**	**padj**	**log_2 fold-change**	**padj**
Rps3a2	8.612	0	8.005	9.17E-196
Rps3a3	7.026	7.778E-273	8.112	1.77E-137
Hdgf	-2.420	3.20E-132	-3.508	2.26E-56
Rps3a1	-2.445	1.10E-109	-2.231	7.50E-23
Hprt1	2.844	1.04E-94	1.785	3.29E-10

Figure 4.4. A Venn diagram comparing significant differentially expressed genes in WT and *Hdgf*$^{-/-}$ (KO) cartilage and skin at 0 hours. In cartilage, the total of 79 genes were significantly differentially expressed at 0 hours (padj<0.05). In skin, 28 genes were significantly differentially expressed at 0 hours (padj<0.05). The list of 5 overlapping genes is shown, alongside padj and log_2 fold-change values for each gene in each tissue.

To understand better the effect of observed transcriptional differences between genotypes at 0 hours, I performed gene-set enrichment analysis (GSEA) of Hallmark pathways in cartilage and skin. Twenty-one pathways (9 positive and 12 negative) were significantly enriched in *Hdgf*$^{-/-}$ cartilage compared to WT at 0 hours (padj<0.05) (Figure 4.5). Positively enriched pathways were largely pro-metabolic, including oxidative phosphorylation, mTORC1 signalling, peroxisome, fatty acid, bile acid, and heme metabolism. In skin, 24 significantly enriched pathways (20 positive and 4 negative) were identified (padj<0.05) in *Hdgf*$^{-/-}$ skin. Most of the positively enriched pathways could be described as pro-inflammatory (Figure 4.5). These inflammation-associated pathways included TNFα-signalling via NF-kappa B, inflammatory response, IL-2/STAT5, IL6/JAK/STAT3, and KRAS signalling, complement, hypoxia, apoptosis, and coagulation. Overlapping significantly enriched pathways from cartilage and skin identified 10 pathways shared between the two tissues. Out of these, only one pathway - mTORC1 signalling - was regulated in the same direction (positively enriched) and to a similar extent (NES of 1.66 and 1.65 in cartilage and skin, respectively). The other 9 overlapping pathways were regulated in opposite directions. Seven of them, mostly inflammation- and stress-associated pathways, were upregulated in the skin and the remaining 2 pathways (pro-metabolic) were upregulated in the cartilage (Figure 4.5).

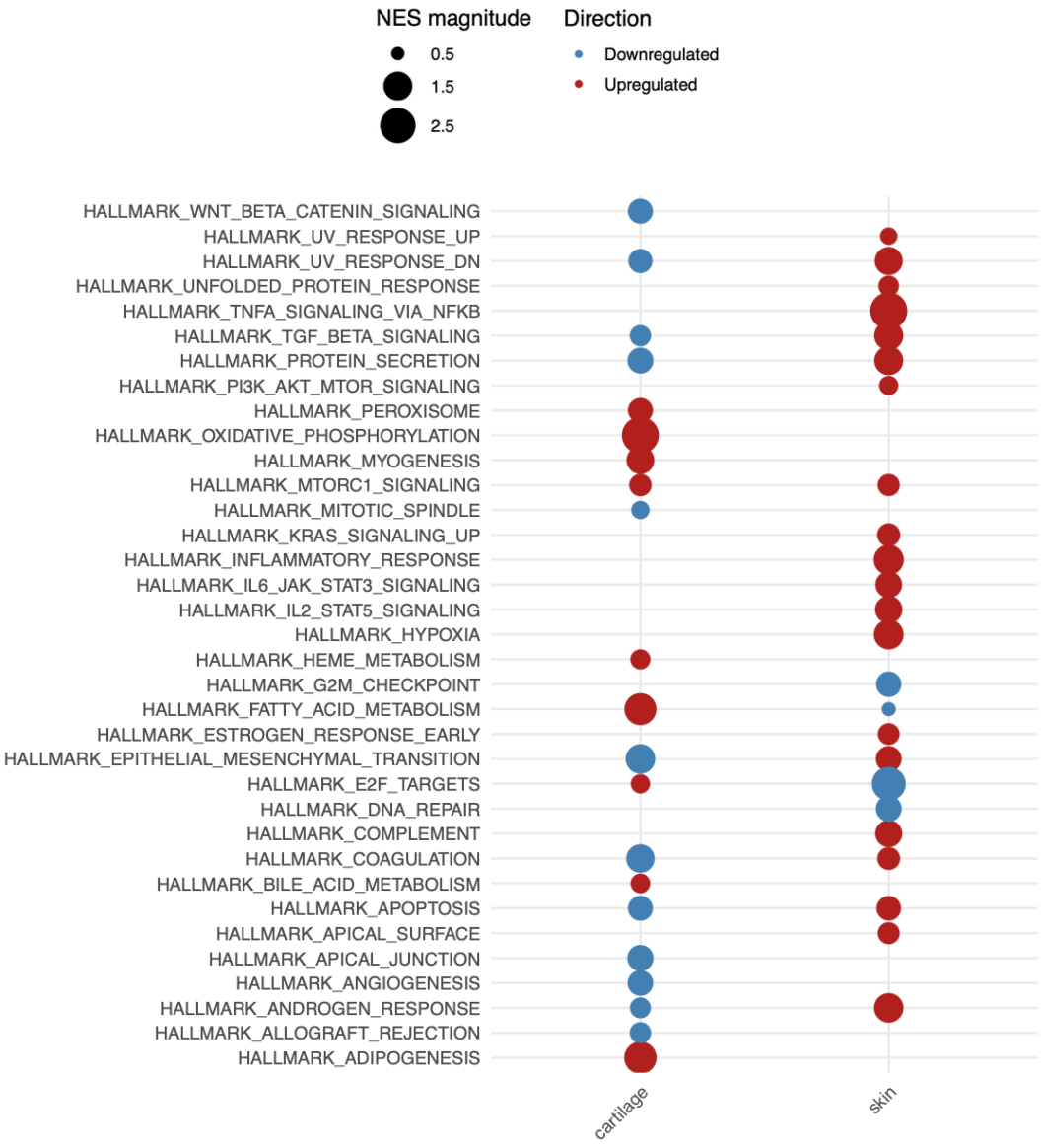

Figure 4.5. Gene set enrichment analysis (GSEA) of Hallmark pathways significantly enriched in *Hdgf*$^{-/-}$ (KO) cartilage and skin at 0 hours. A total of 21 significantly enriched (9 positive and 12 negative) pathways were identified in *Hdgf*$^{-/-}$ cartilage, padj<0.05. Pathways positively enriched in *Hdgf*$^{-/-}$ cartilage were largely pro-metabolic. A total of 24 significantly enriched (20 positive and 4 negative) pathways were identified in *Hdgf*$^{-/-}$ skin, padj<0.05. Pathways positively enriched in *Hdgf*$^{-/-}$ skin were largely pro-inflammatory. NES – normalised enrichment score.

4.2.2. Transcriptional response to cartilage injury was largely similar between the wild-type and *Hdgf*$^{-/-}$ animals

Following identification of transcriptional differences between WT and *Hdgf*$^{-/-}$ tissues at baseline (without injury), I moved on to answer the question of whether HDGF is important for tissue response to injury. Though I performed *ex vivo* injury in both cartilage and skin, I was unable to obtain good quality RNA from injured skin samples. Therefore, transcriptional differences associated with injury were investigated using RNA obtained from cartilage cultures in serum-free medium for 4 hours following hip avulsion injury.

DESeq analysis detected 18,070 genes regulated upon injury in WT cartilage. After applying the threshold of padj<0.05 and a $\log_2$ fold-change>1, the total of 4,632 genes were identified as statistically significant. In *Hdgf*$^{-/-}$ cartilage, the total of 17,800 genes were detected upon injury and, after applying the statistical threshold mentioned above, the total of 4,289 genes were statistically significant. Examining the top 20 (sorted by padj) differentially regulated genes upon cartilage injury revealed substantial overlap between the two genotypes. For instance, 16 out of top 20 differentially regulated injury-induced genes overlapped between WT and *Hdgf*$^{-/-}$ cartilage (Figure 4.6A). Comparing the top 100 injury-associated differentially regulated genes between genotypes revealed 83 overlapping genes that were all regulated in the same direction and to a similar extent in both genotypes (Figure 4.6B).

A)

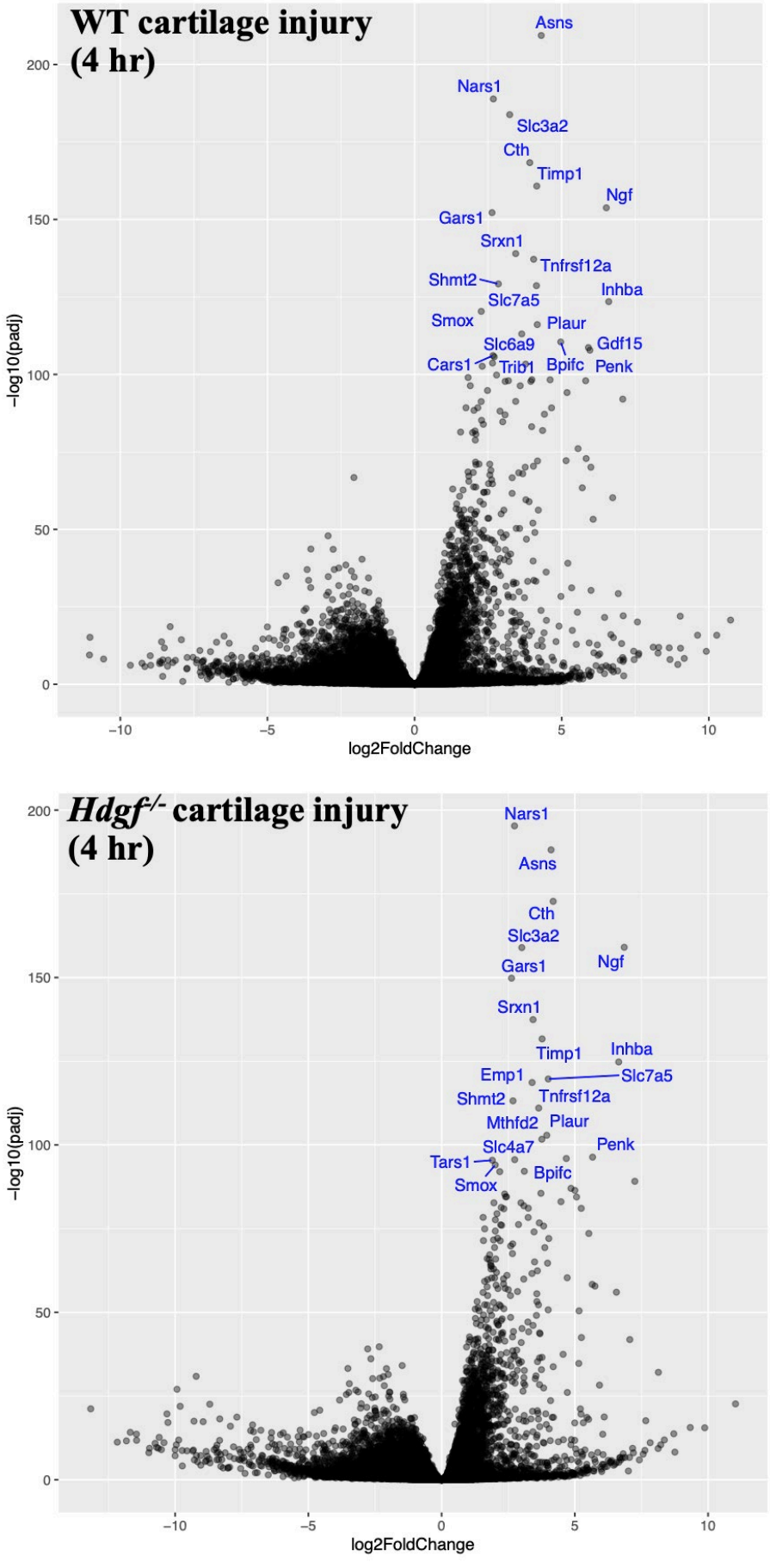
WT cartilage injury
(4 hr)
Asns
Nars1
Slc3a2
Cth
Timp1
Ngf
Gars1
Srxn1
Tnfrsf12a
Shmt2
Inhba
Slc7a5
Smox
Plaur
Slc6a9
Gdf15
Cars1
Trib1
Bpifc
Penk
−log10(padj)
log2FoldChange
Hdgf-/- cartilage injury
(4 hr)
Nars1
Asns
Cth
Slc3a2
Ngf
Gars1
Srxn1
Timp1
Inhba
Emp1
Slc7a5
Shmt2
Tnfrsf12a
Mthfd2
Plaur
Slc4a7
Penk
Tars1
Bpifc
Smox
−log10(padj)
log2FoldChange

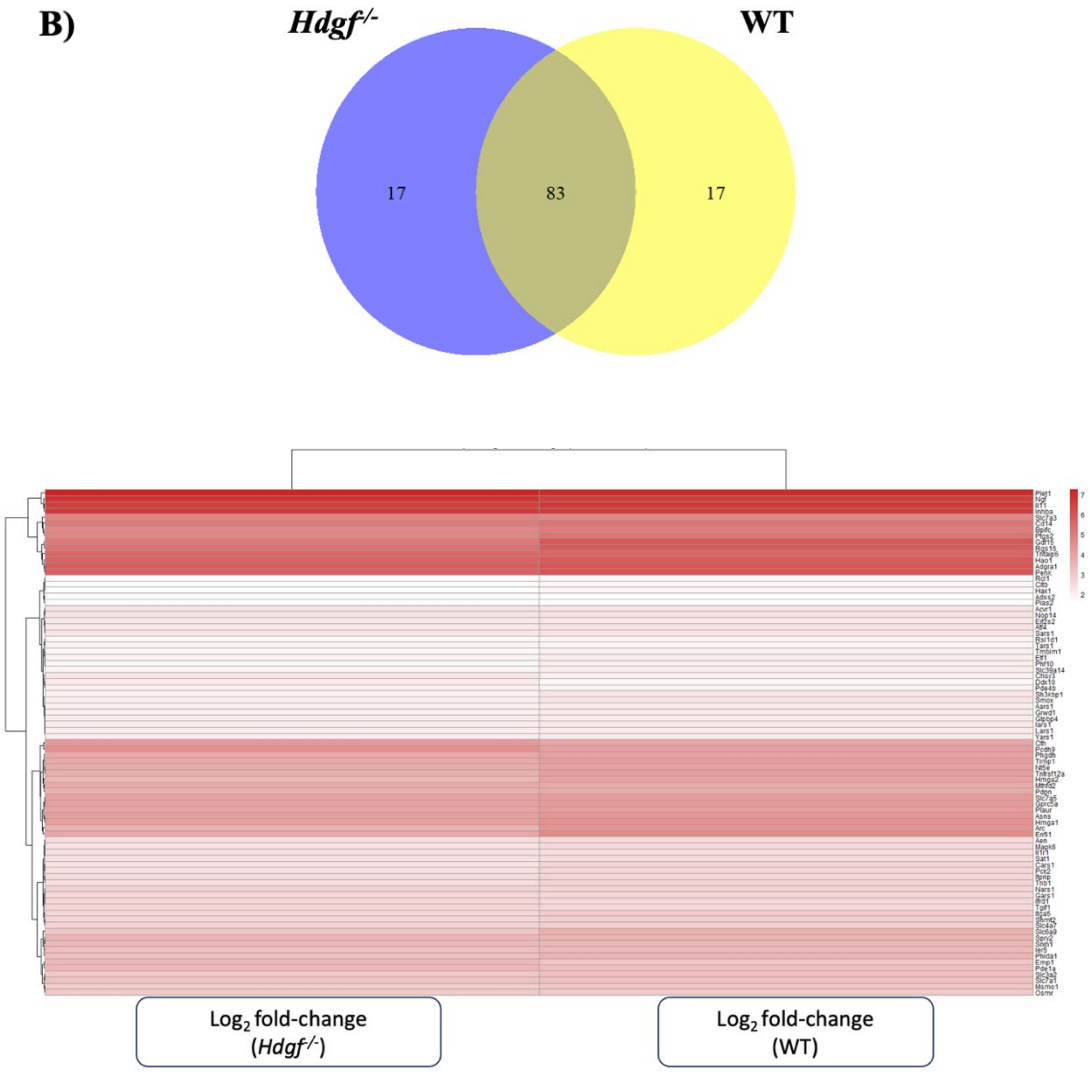

Figure 4.6. Transcriptional response to cartilage injury at 4 hours was similar between WT and *Hdgf*$^{-/-}$ (KO) mice. A) Volcano plots labelling top 20 genes (sorted by padj) differentially expressed with cartilage injury in both genotypes, padj<0.05, $\log_2$ fold-change>1. B) A Venn diagram of the top 100 genes (sorted by padj) differentially expressed with cartilage injury and a heatmap of 83 overlapping genes illustrating their regulation in the same direction in both genotypes. This graph was generated with the help of Dr Thomas Perry, a post-doc in the group.

To investigate further the degree of similarity between injury-induced differentially regulated genes, a Pearson correlation of all genes detected in both genotypes upon injury was performed. It revealed a significant correlation in transcriptional response to injury between the two genotypes ($r = 0.81$, $p<2.22e^{-16}$). Out of 17,800 genes shared across genotypes, 7,223 genes were significantly (padj<0.05) regulated in the same direction in both WT and *Hdgf*$^{-/-}$ cartilage. About 40% of detected genes (6,943 genes) were not statistically significant, whereas 1,996 genes were statistically significant only in WT cartilage and 1,636 genes in *Hdgf*$^{-/-}$ only (Figure 4.7). Two genes were regulated in opposite directions: zinc finger protein 119b (*Zfp119b*) and potassium inwardly-rectifying channel subfamily J member 15 (*Kcnj15*). Direction of regulation of these genes in each genotype and their respective padj and $\log_2$ fold-change values are reported (Figure 4.7).

Although over half of the genes regulated with injury in both genotypes were the same, I wanted to investigate whether detected differences altered molecular pathways that could affect injury response. To investigate this, I performed a gene-set enrichment analysis (GSEA) of Hallmark pathways in WT and *Hdgf*$^{-/-}$ injured cartilage. Among the top 20 statistically significant pathways (padj<0.05) detected in each genotype, 14 pathways overlapped and were regulated in the same direction and to a similar extent in both genotypes in response to injury (Figure 4.8). Many of the shared positively enriched pathways were associated with injury response (e.g. TNFα signalling via NF-kappa B, inflammatory response, interferon-α response, IL-2/STAT5, IL6/JAK/STAT3) and stress response (e.g. hypoxia, apoptosis, p53, unfolded protein response) (Figure 4.8).

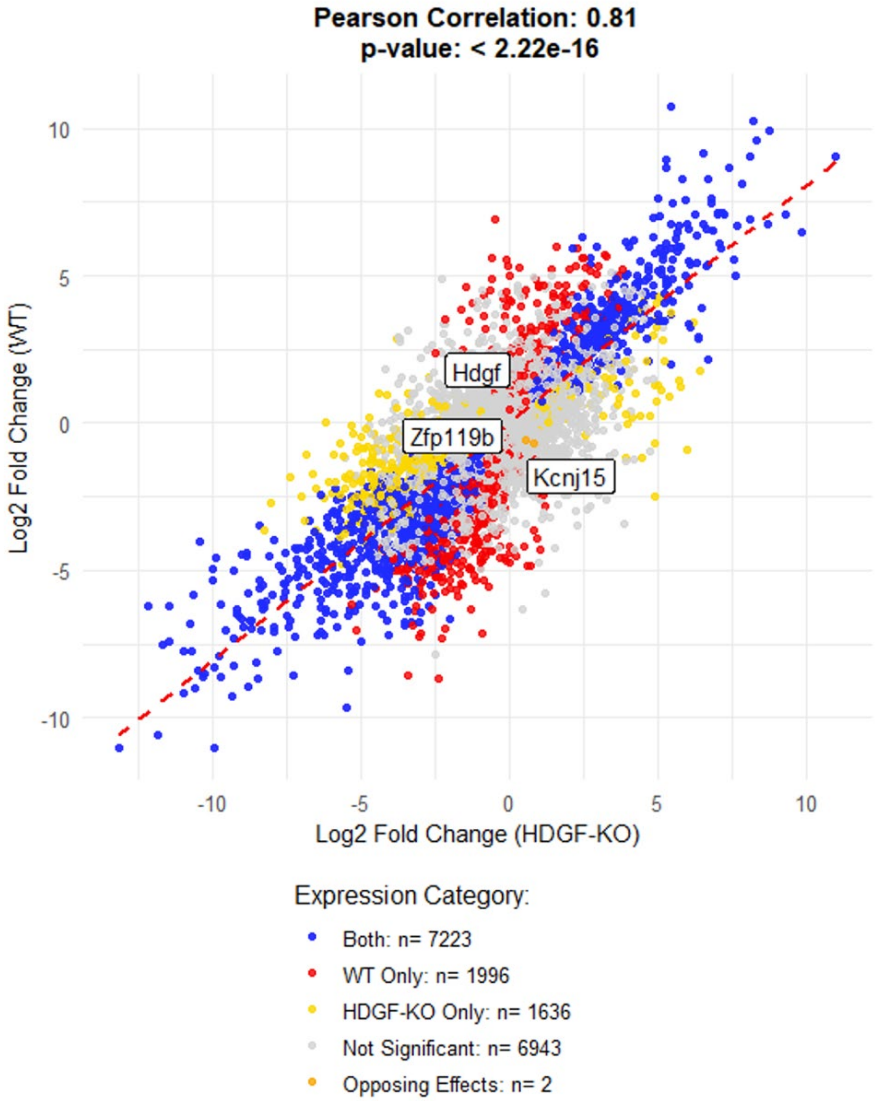

	WT		*Hdgf*$^{-/-}$	
Gene	**log_2 fold-change**	**padj**	**log_2 fold-change**	**padj**
Zfp119b	-0.603	0.015	0.562	0.027
Kcnj15	-0.687	0.036	0.832	0.009

Figure 4.7. Correlation between injury-induced gene expression in WT and *Hdgf*$^{-/-}$ (KO) cartilage. Each data point represents a gene (n = 17,800 genes), plotted by its log_2 fold-change in *Hdgf*$^{-/-}$ versus WT following hip avulsion injury. Only genes that were common to both WT and *Hdgf*$^{-/-}$ genotypes are represented. A dashed red line shows the linear correlation (Pearson correlation, r = 0.81, $p<2.2e^{-16}$). Genes are colour-coded by significance pattern: significant (padj<0.05) with effects in the same direction in both genotypes ("Both"), only significant (by padj) in WT or *Hdgf*$^{-/-}$, or showing opposing effects ("Opposing Effects"). Two genes were identified as having opposing effects (*Zfp119b* and *Kcnj15*), defined as padj<0.05 in both WT and *Hdgf*$^{-/-}$ but with effects in opposing directions. *Hdgf* is also labelled. Log_2 fold-change and padj values in WT and *Hdgf*$^{-/-}$ for the two genes having opposing effects are shown. This graph was generated with the help of Dr Thomas Perry, a post-doc in the group.

Figure 4.8. Gene set enrichment analysis (GSEA) of Hallmark pathways significantly enriched with injury in WT and *Hdgf*$^{-/-}$ (KO) cartilage. Top 20 significantly enriched (top 14 positive and 6 negative) pathways in WT cartilage and top 20 significantly enriched (top 13 positive and 7 negative) pathways in *Hdgf*$^{-/-}$ cartilage, padj<0.05. NES – normalised enrichment score.

Lastly, I wanted to compare differences in the magnitude of change of injury-associated genes between genotypes. For this, I performed a DESeq analysis examining the "difference of differences" in genes that change most differently with injury in each genotype. This analysis can be mathematically represented as:

"Difference of differences" = ($Hdgf^{-/-}{}_{4\ hours}$ - $Hdgf^{-/-}{}_{0\ hours}$) - ($WT_{4\ hours}$ - $WT_{0\ hours}$).

This analysis detected 16,008 genes that changed differently between the genotypes with injury, of which 16 genes were regulated at a statistically significant level (padj<0.05) (Figure 4.9A). Of these, half were positively changed in response to injury in the *Hdgf*$^{-/-}$ cartilage, while the other half were negatively changed (Figure 4.9B). Most genes that were positively changed in the WT were mitochondrial-related (*Cycs*, *Timm50*, *Mtfp1*, *Phb1*, *Cdc34*), whereas genes that were positively changed in the *Hdgf*$^{-/-}$ were related to cell surface, signalling, and differentiation (*Fzd5*, *Bambi*, *Mme*, *Enpp6*). GSEA Hallmark pathway analysis was performed on 16,008 genes and identified 19 statistically significant (padj<0.05) pathways that were differentially enriched (8 positive and 11 negative) (Figure 4.9C). Positively enriched pathways that changed in *Hdgf*$^{-/-}$ cartilage with injury included protein secretion, Wnt/β-catenin signalling, interferon-α response, and TGFβ signalling. Most of the negatively enriched pathways were metabolic (e.g. oxidative phosphorylation, mTORC1 signalling, fatty acid and heme metabolism, adipogenesis) and stress-related (e.g. reactive oxygen species, hypoxia) (Figure 4.9C).

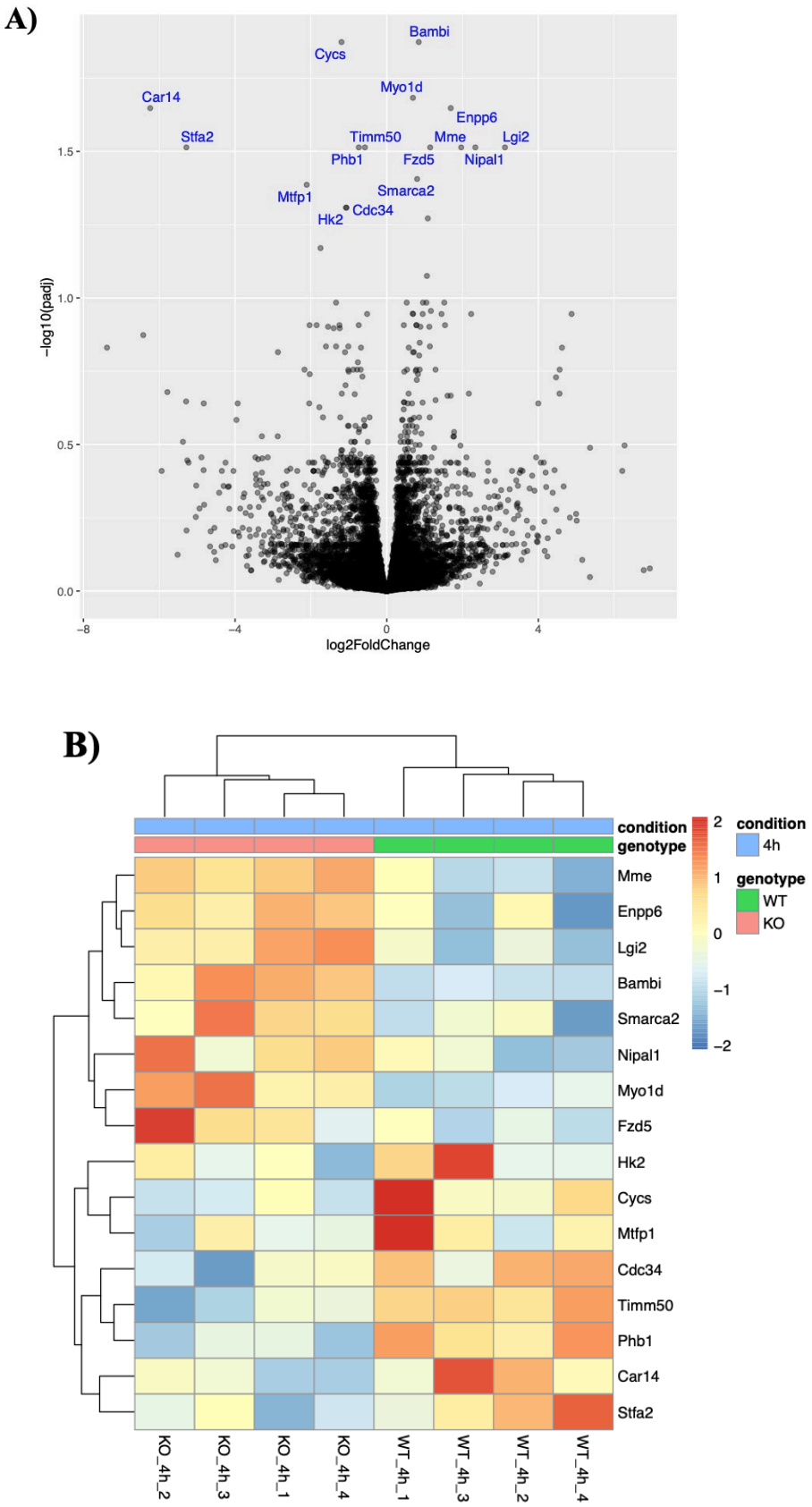
A)
Bambi
Cycs
Myo1d
Car14
Enpp6
Stfa2
Timm50
Mme
Lgi2
Phb1
Fzd5
Nipal1
Smarca2
Mtfp1
Cdc34
Hk2
−log10(padj)
log2FoldChange
B)
condition
genotype
Mme
Enpp6
Lgi2
Bambi
Smarca2
Nipal1
Myo1d
Fzd5
Hk2
Cycs
Mtfp1
Cdc34
Timm50
Phb1
Car14
Stfa2
KO_4h_2
KO_4h_3
KO_4h_1
KO_4h_4
WT_4h_1
WT_4h_3
WT_4h_2
WT_4h_4
condition
4h
genotype
WT
KO

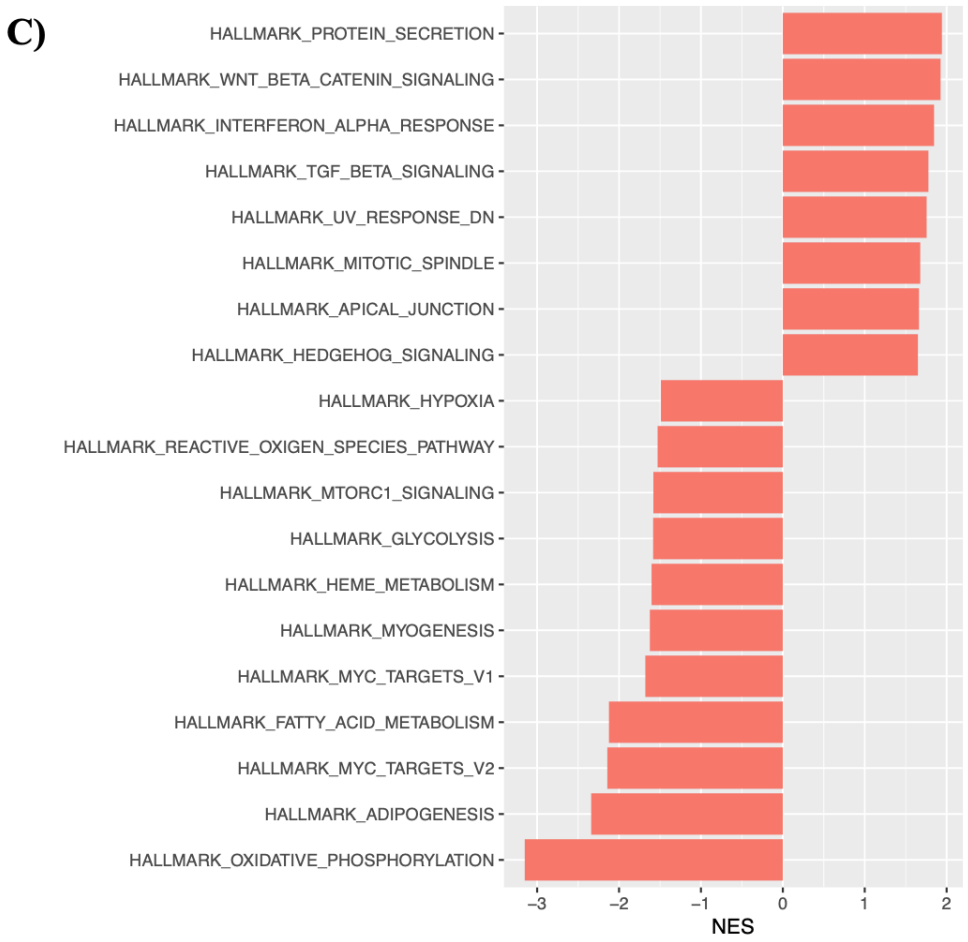

Figure 4.9. Comparison of the magnitude of injury-associated change between WT and *Hdgf*$^{-/-}$ cartilage. A) Volcano plot labelling 16 genes that were significantly differentially regulated in response between WT and *Hdgf*$^{-/-}$ cartilage, padj<0.05. B) A heatmap representation of these genes showing their relative expression in each individual sample, padj<0.05. C) Gene set enrichment analysis (GSEA) of Hallmark pathways. Nineteen (19) significantly enriched (8 positive and 11 negative) pathways are shown, padj<0.05. NES – normalised enrichment score.

4.2.3. Proteomic labelling of the skin after injury

Thus far, I had identified some modest changes in the time zero (0 hr) transcriptome that were partly conserved across skin and cartilage. I also was able to show a modest change in the 4-hour injury response. The lack of a strong transcriptional injury response prompted us to consider HDGF's role in translation. This was supported by several strands of evidence: striking regulation of the ribosomal protein *Rps3a* across skin and cartilage, literature showing direct interaction of HDGF with proteins involved in ribosomal assembly and translation, and pathway analysis showing that translation-related pathways were differentially regulated between WT and *Hdgf*$^{-/-}$ tissues upon injury. Thus, I hypothesised that HDGF could play an important role in translation. As one of the most differentially regulated genes in both cartilage and skin was *Rps3a1*, which encodes a component of 40S ribosomal subunit, I designed an experiment aimed at investigating proteomic differences between the WT and *Hdgf*$^{-/-}$ tissues. For this, I decided to use SILAC labelling of immediately explanted (*ex vivo*) skin to capture the change in newly synthesised proteins upon injury. The rationale behind the experiment was to incubate skin biopsies in SILAC-supplemented medium for 24 and 48 hours to measure changes in the proteome at different stages of the injury response. Analysis of the LC-MS/MS data generated the abundance of both "heavy" and "light" proteins where "heavy" indicated the protein that has incorporated the C^{13}-labelled lysine into newly synthesised protein within the tissue, and "light" largely reflected protein produced prior to the introduction of SILAC medium. These abundances were used to produce heavy to light ratios which reflect the degree of incorporation of heavy lysine into proteins, where higher ratios indicate higher protein synthesis and lower ratios indicate lower rates of protein synthesis.

In each genotype, heavy to light ratios were significantly higher at 48 hours compared to 24 hours following SILAC labelling, reflecting the higher incorporation of heavy label into protein over time from injury (Figure 4.10A). Heavy to light ratios were similar between the WT and *Hdgf*$^{-/-}$ skin at 24 hours, but significantly higher in WT skin at 48 hours ($p<0.0001$), indicating significantly increased protein synthesis in WT skin and a potential protein translation phenotype in the *Hdgf*$^{-/-}$ (Figure 4.10A). Examining proteins with differential rate of synthesis between WT and *Hdgf*$^{-/-}$ skin at 48 hours revealed that the 20 proteins with the most decreased synthesis in *Hdgf*$^{-/-}$ skin included matrix (e.g. Col6a3, Col1a2, Ogn, Dcn) and actin cytoskeleton-related proteins (e.g. Myh11, Ctnna1, Pfn1) (Figure 4.10B). Network analysis of *Hdgf*$^{-/-}$ skin at 48 hours revealed a large cluster of downregulated translational proteins, as well as proteins mentioned above involved in actin cytoskeleton, plasma membrane repair, and ECM (Figure 4.11A). A closer look at translational proteins revealed increased synthesis of several ribosomal proteins including RPL13A, RPS3A, RPS25, and others in the WT compared to *Hdgf*$^{-/-}$ skin (Figure 4.11B).

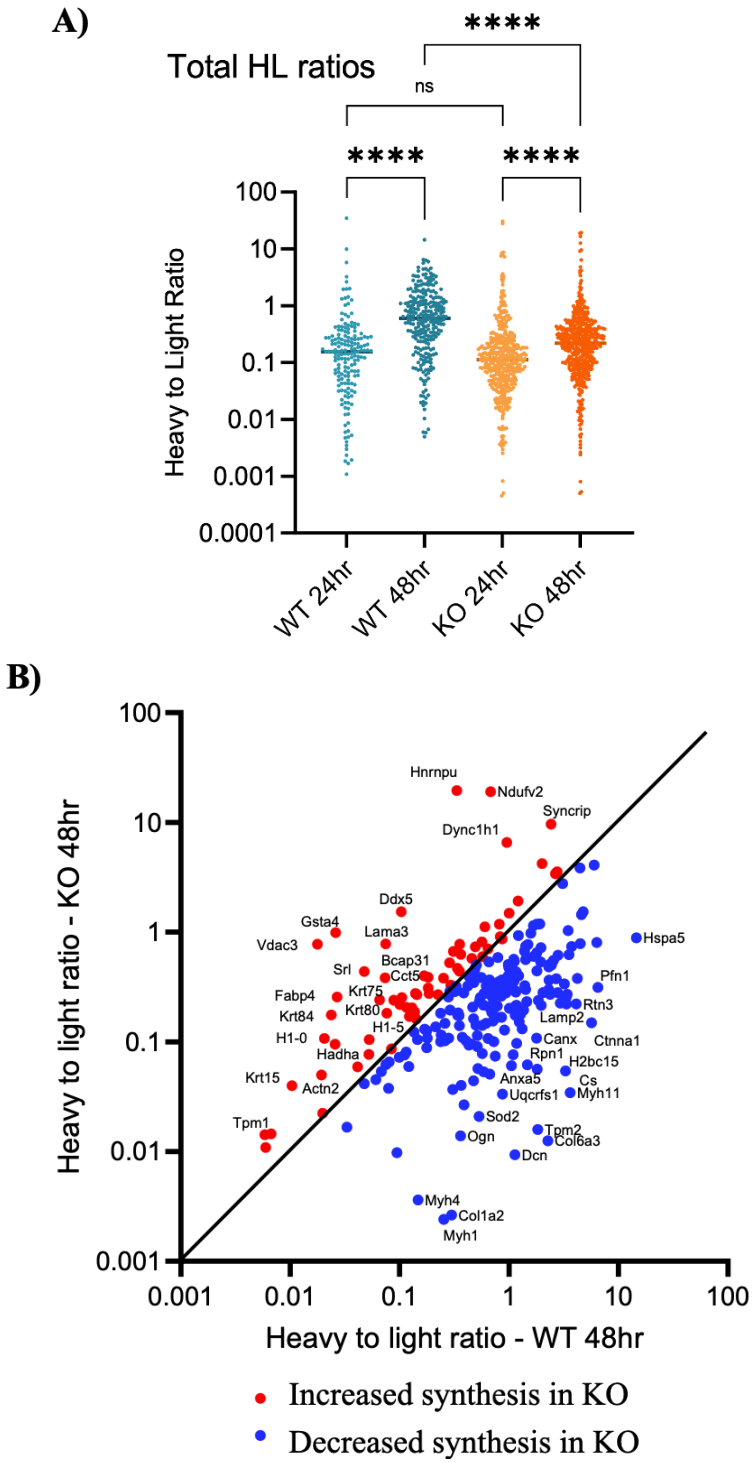

Figure 4.10. Proteomic analysis of SILAC-labelled WT and *Hdgf*$^{-/-}$ (KO) skin at 24 and 48 hours after injury. A) All heavy to light ratios calculated based on heavy and light protein abundances in WT and *Hdgf*$^{-/-}$ skin. Each dot represents a protein, data was compared using Kruskal-Wallis test with Dunn's multiple comparisons as the data was non-normal, ns-not significant, **** $p<0.0001$. B) A graph plotting correlation between heavy to light ratios of proteins in WT and *Hdgf*$^{-/-}$ skin after 48 hours of SILAC labelling. Blue dots represent proteins with decreased synthesis in *Hdgf*$^{-/-}$ skin, red dots represent proteins with increased synthesis in *Hdgf*$^{-/-}$ skin. Top 20 proteins in each group are labelled. These graphs were generated by Dr Anna Hoyle.

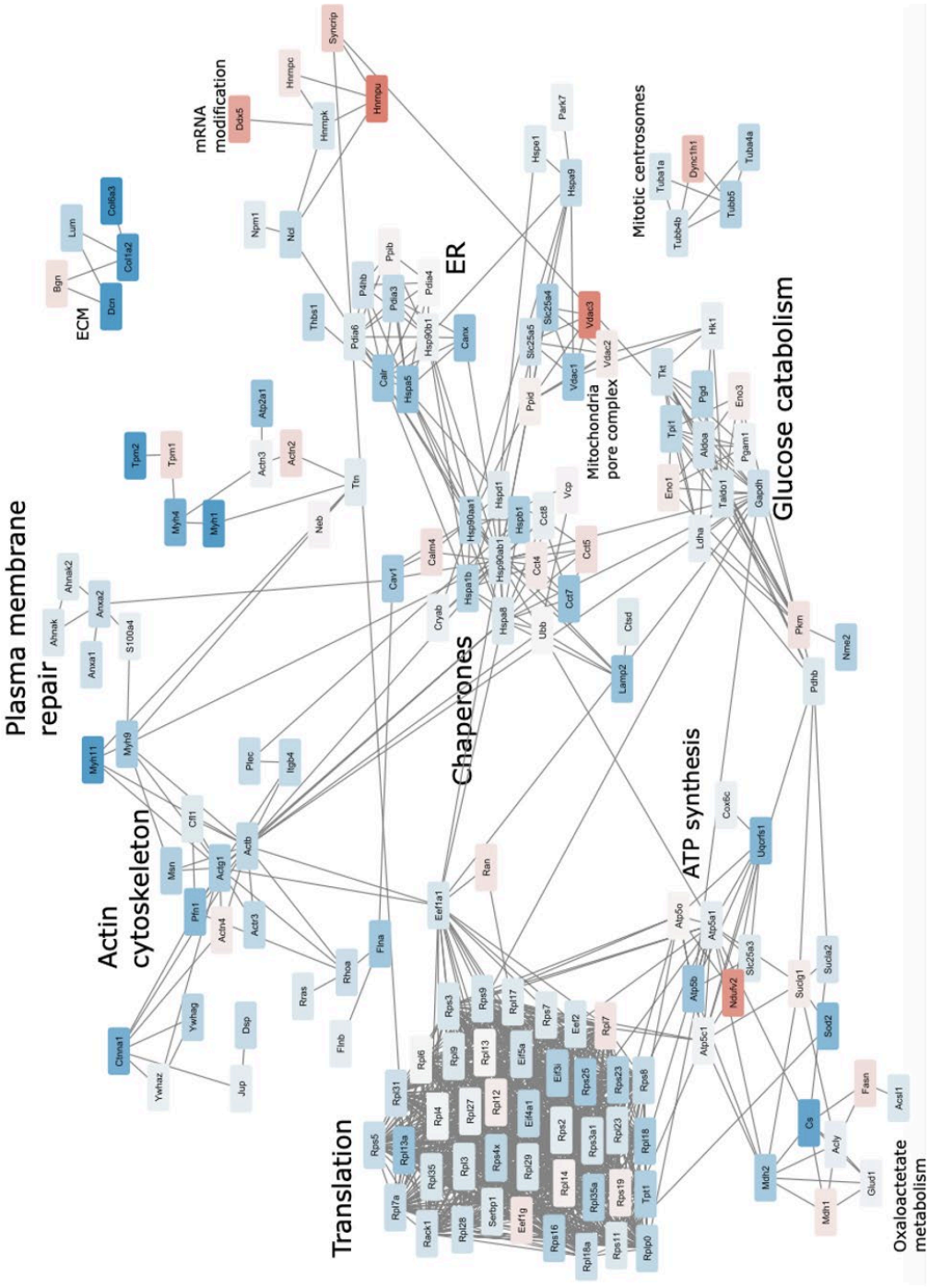
A)
Plasma membrane repair
Actin cytoskeleton
Translation
Chaperones
ER
mRNA modification
ECM
Mitochondria pore complex
Mitotic centrosomes
ATP synthesis
Glucose catabolism
Oxaloactetate metabolism

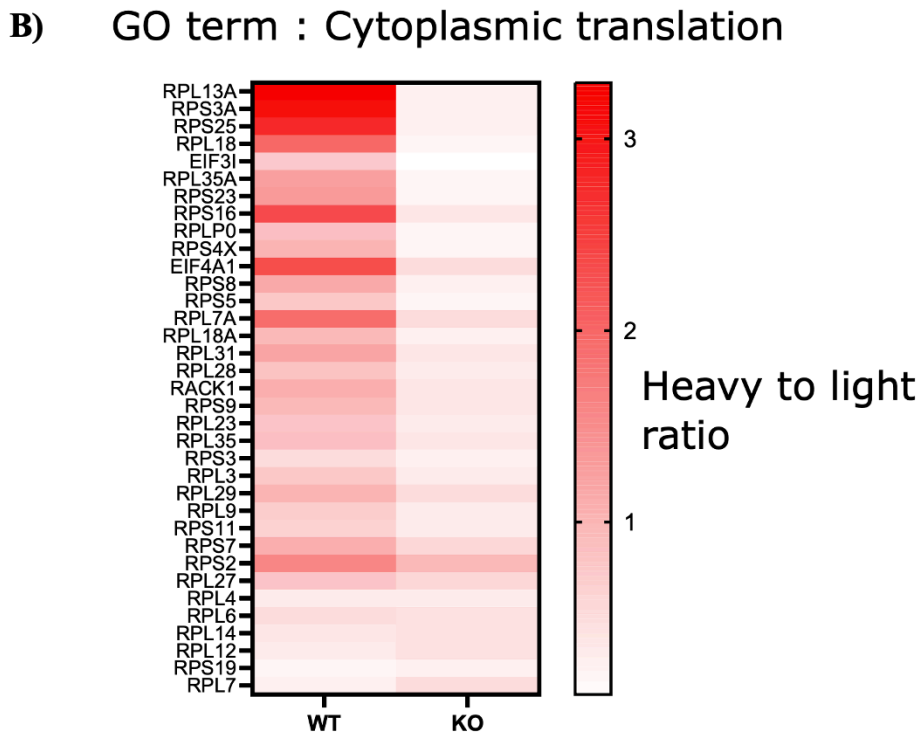

Figure 4.11. Translational proteins showed decreased synthesis in *Hdgf*$^{-/-}$ (KO) skin at 48 hours of SILAC labelling. A) Network analysis of proteins detected in WT and *Hdgf*$^{-/-}$ (KO) skin at 48 hours. Blue colour represents proteins with decreased synthesis in KO and red colour represents proteins with increased synthesis in KO when compared to the WT. Only including networks with >5 proteins. Proteins are represented as nodes and edges indicate known confident interactions according to STRING (v12). B) A heatmap of proteins involved in gene ontology (GO) term for cytoplasmic translation, showing largely increased synthesis (increased heavy to light ratios) of ribosomal proteins in WT skin compared with KO. These graphs were generated by Dr Anna Hoyle.

Next, pathway enrichment analysis was performed in order to see whether observed proteomic differences had wider biological significance. Pathway analysis of proteins with either increased or decreased synthesis in *Hdgf*$^{-/-}$ skin compared to WT at 48 hours identified differences in translation between the genotypes. Cytoplasmic translation and macromolecule biosynthesis were among the top gene ontology (GO) pathways enriched in proteins with decreased synthesis in *Hdgf*$^{-/-}$ skin (Figure 4.12A). Interestingly, these pathways were more significantly enriched ($-\log_{10}$(corrected p-value)>20) compared to all other identified pathways ($-\log_{10}$(corrected p-value)<8). Other pathways reduced in *Hdgf*$^{-/-}$ skin included regulation of apoptosis, protein stabilisation and a number of pathways related to ribosomal subunit biogenesis (Figure 4.12A). Hallmark pathway analysis identified Myc Targets V1 as the most significantly enriched pathway in proteins with decreased synthesis in *Hdgf*$^{-/-}$ skin at 48 hours (Figure 4.12B). This pathway includes many genes that encode proteins involved in translation, such as ribosomal proteins, translation initiation factors, and RNA processing proteins.[241] Other hallmark pathways significantly enriched in proteins with decreased synthesis in *Hdgf*$^{-/-}$ skin included oxidative phosphorylation, mTORC1 signalling, and myogenesis (Figure 4.12B).

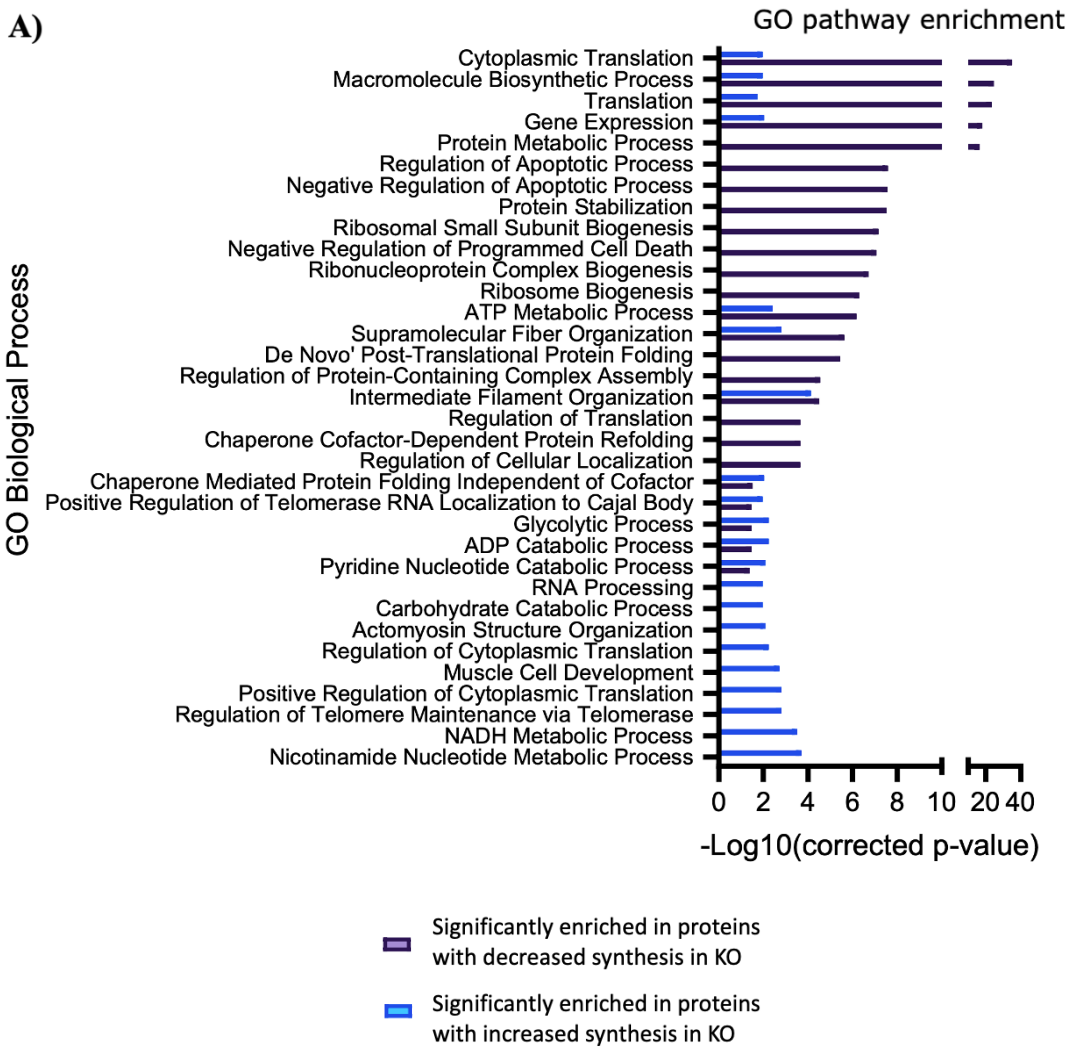
A)
GO pathway enrichment
GO Biological Process
Cytoplasmic Translation
Macromolecule Biosynthetic Process
Translation
Gene Expression
Protein Metabolic Process
Regulation of Apoptotic Process
Negative Regulation of Apoptotic Process
Protein Stabilization
Ribosomal Small Subunit Biogenesis
Negative Regulation of Programmed Cell Death
Ribonucleoprotein Complex Biogenesis
Ribosome Biogenesis
ATP Metabolic Process
Supramolecular Fiber Organization
De Novo' Post-Translational Protein Folding
Regulation of Protein-Containing Complex Assembly
Intermediate Filament Organization
Regulation of Translation
Chaperone Cofactor-Dependent Protein Refolding
Regulation of Cellular Localization
Chaperone Mediated Protein Folding Independent of Cofactor
Positive Regulation of Telomerase RNA Localization to Cajal Body
Glycolytic Process
ADP Catabolic Process
Pyridine Nucleotide Catabolic Process
RNA Processing
Carbohydrate Catabolic Process
Actomyosin Structure Organization
Regulation of Cytoplasmic Translation
Muscle Cell Development
Positive Regulation of Cytoplasmic Translation
Regulation of Telomere Maintenance via Telomerase
NADH Metabolic Process
Nicotinamide Nucleotide Metabolic Process
0 2 4 6 8 10 20 40
-Log10(corrected p-value)
Significantly enriched in proteins with decreased synthesis in KO
Significantly enriched in proteins with increased synthesis in KO

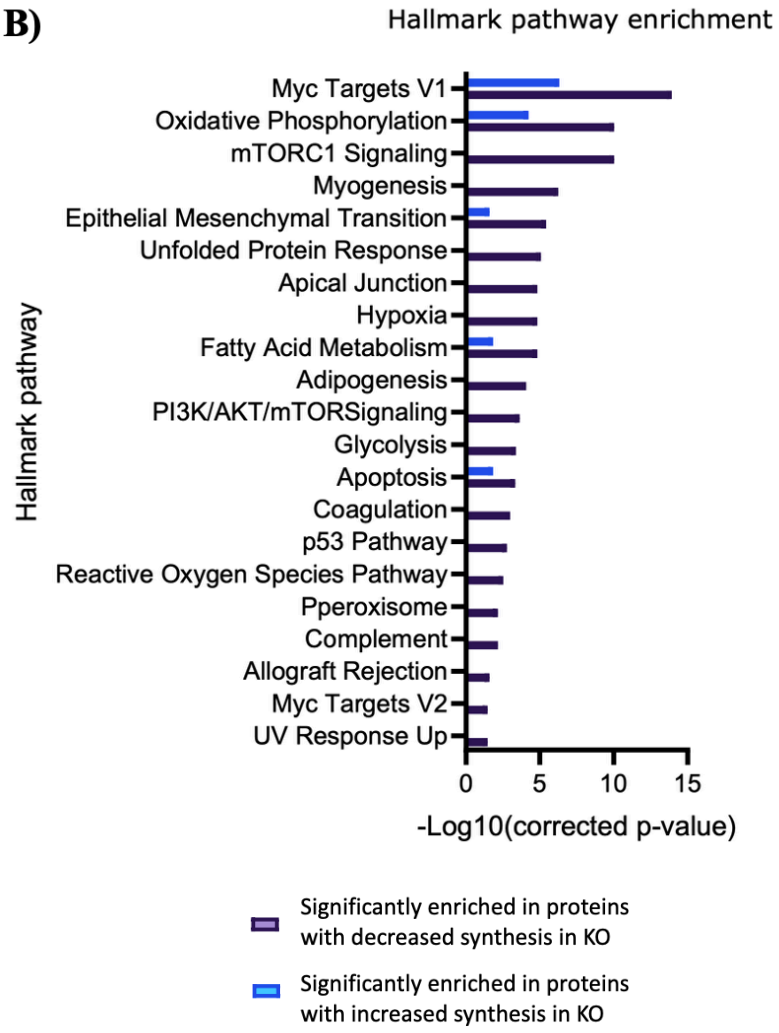

Figure 4.12. Pathway analysis of SILAC-labelled WT and *Hdgf*$^{-/-}$ (KO) skin at 48-hours after injury. A) Gene ontology (GO) pathways enriched in *Hdgf*$^{-/-}$ (KO) skin. B) Hallmark pathways enriched in *Hdgf*$^{-/-}$ (KO) skin. Purple colour indicates pathways significantly enriched in proteins with decreased synthesis in *Hdgf*$^{-/-}$ skin, light blue colour indicates pathways significantly enriched in proteins with increased synthesis in *Hdgf*$^{-/-}$ skin, $p<0.05$. Mouse proteome was used as a background for pathway enrichment. These graphs were generated by Dr Anna Hoyle.

4.3. Discussion

Transcriptomic analysis comparing WT and *Hdgf*$^{-/-}$ tissues identified molecular changes associated with HDGF deletion. Analysis of bulk RNA sequencing revealed that the HDGF knockout mouse model still had some *Hdgf* expression (18.7% in the cartilage and 9.7% in the skin). This was surprising given that the knockout mouse model is an embryological knockout, where the gene of interest would be expected to be undetectable. One possible explanation for this could be that part of Hdgf that was not deleted during the knockout line generating – exon 1 – was picked up during sequencing. RNA sequencing was performed using the 150 paired-end Illumina's NovaSeq X Plus platform, which does not use gene-specific sequencing primers or probes and generated libraries from randomly fragmented transcripts rather than targeted capture. Since exon 1 is 394 base pairs long, it is plausible that it was picked as part of 150 base pair sequencing fragments, generating a signal for *Hdgf*. Unfortunately, Novogene was not able to supply us with exact sequences of transcripts detected for *Hdgf* gene or BAM alignment files, as this type of analysis is outside the scope of the WOBI RNA sequencing service. To investigate this further, a new analysis should be ordered from Novogene that would enable them to perform an exon-level quantification and specifically examine whether exons 2-6 were reduced or fully absent compared to exon 1 in *Hdgf.* Thus, it might be that the knockout is inefficient due to a truncated version of *Hdgf* still present. RIN numbers are known to influence the quality of RNA sequencing data. While all samples sent for sequencing had RIN numbers of more than 4, which is the threshold for Novogene, cartilage samples on average had higher RIN numbers (~7) than skin samples (~5) (Supplementary Table 1). Lower RIN numbers can affect differential expression results by introducing false positives

that could be just artefacts or by increasing false negatives, especially if RNA quality differs between samples. In addition, DESeq2 has limited power and unstable fold-change estimates for low–copy number transcripts, increasing false positives and negatives unless such genes are carefully filtered or modelled. What is reassuring is that RIN numbers were similar for samples obtained from one tissue type (cartilage or skin), making it possible to compare samples from the same tissue type. Another possible reassurance for the knock-out mouse line comes from results of murine genotyping performed by Transnetyx. They confirmed that HDGF wild-type probes detected the WT allele by spanning intron 3, which was deleted by eGFP, and eGFP probes detected the mutant allele in tissues of *Hdgf*$^{-/-}$ mice. The absence of HDGF protein by western blot suggested that, even if the truncated version of the gene was present, it did not result in the production of protein. However, the only definitive answer explaining why *Hdgf* reads were present will come from exon-level analysis from Novogene. Another way to check it would be by designing primers spanning exon 1 and another region of the *Hdgf* gene and performing a quantitative PCR from isolated RNA to quantify levels of expression of exon 1 in *Hdgf*$^{-/-}$ tissues. Further to this, it would be helpful to perform this type of secondary confirmation of transcriptomics results for other differentially expressed genes either via quantitative PCR or immunohistochemistry staining.

RNA sequencing analysis identified four other genes (*Rps3a1*, *Rps3a2*, *Rps3a3*, and *Hprt1*) to be differentially expressed between the two genotypes in both cartilage and skin, showing that there is conserved regulation between tissues. The direction and magnitude of change in the expression of these genes was very similar in both cartilage and skin. These genes, regulated in a similar fashion in two different tissues of *Hdgf*$^{-/-}$ mice, may reflect a possible global function of HDGF.

Hprt1 encodes the hypoxanthine-guanine phosphoribosyltransferase (HPRT) enzyme that converts hypoxanthine to inosine monophosphate and guanine to guanine monophosphate; thus, it recycles purines from DNA and RNA. Loss-of-function mutations in *Hprt1* lead to reduced HPRT activity, resulting in overproduction of uric acid, which is the purine waste product. Uric acid can accumulate in the urinary system and joints, leading to nephrolithiasis and gouty arthritis. *HPRT1* disorders in humans fall into three phenotypes depending on severity of symptoms: Lesch-Nyhan disease, *HPRT1*-related neurologic dysfunction, and *HPRT1*-related hyperuricemia. All of these are X-linked and only manifest in males. They are characterised by motor dysfunction, self-injurious behaviour, and various degrees of neurologic deficit.[242] *Hprt1* is frequently used as a housekeeping gene, although there is some evidence of its differential expression in cancer cells. Overexpression of *Hprt1* has been reported in multiple cancers, including head and neck squamous cell carcinoma, colorectal cancer, and breast cancer.[243-245] Several of these studies correlated *Hprt1* overexpression with poor prognosis, most likely through its involvement in nucleotide synthesis that can fulfil needs of proliferating cancer cells.[243] [244] In *Hdgf*$^{-/-}$ tissues, *Hprt1* was overexpressed, however, purine metabolism did not come up in any of the pathway analyses. Thus, it is not yet clear what effect overexpression of *Hprt1* has in *Hdgf*$^{-/-}$ mice.

The remaining three differentially expressed genes conserved across WT and *Hdgf*$^{-/-}$ tissues were ribosomal: *Rps3a1*, *Rps3a2*, and *Rps3a3*. *Rps3a1* is a protein-coding gene located on chromosome 3 that encodes a component of the 40S ribosomal subunit. *Rps3a2* and *Rps3a3* are pseudogenes that are paralogues of *Rps3a1* and exist in mouse, but not human, genome. *Rps3a1* is orthologous to a

human RPS3A gene. Downregulation of *Rps3a1* in *Hdgf*$^{-/-}$ suggests a potential downstream effect on translation, as *Rps3a1* plays a role in translation. Although *Rps3a2* and *Rps3a3* are paralogues to *Rps3a1*, it is unclear whether their upregulation in the *Hdgf*$^{-/-}$ tissue has any compensatory effect on the downregulation of *Rps3a1.* Only one study found a similar pattern of dysregulation of *Rps3a1* and *Rps3a3*, where *Rps3a1* was downregulated and *Rps3a3* was upregulated in mice with a truncated version of adenosine deaminase acting on RNA 1 (*Adar1*) gene and a deletion of a gene encoding mitochondrial antiviral-signalling protein (*Mavs*). Polysome profiling of liver cells from these mice identified a distortion in 40S-to-60S ratio due to an increase in 60S ribosomal subunit.[246] This could potentially be explained by the role of *Rps3a1* in ribosome assembly, as it is essential for 18S rRNA processing.[247] Interestingly, *Rps3a3* demonstrated the ability to form ribosomal subunits, as free 40S and 60S subunits were detected in HEK293T cells transfected with a Flag-tagged Rps3a3 vector.[246] While this function of *Rps3a3* has never been demonstrated *in vivo*, it could be possible that downregulation of *Rps3a1* in *Hdgf*$^{-/-}$ mice could be compensated by upregulation of *Rps3a3*. Whether another paralogue of *Rps3a1* - *Rps3a2* - can produce protein products, is still unknown.

Rps3a1 plays an important role in translation, as polysome analysis revealed that it cross-links with 18S rRNA,[248] translation initiation factors eIF-2 and eIF-3,[249 250] initiator tRNA complex eIF-2β-Met-tRNA$_f$,[251] and mRNA.[252] Additionally, a study carried out in NIH 3T3-derived murine cell line found that increased expression of Rps3a was required to "prime" cells for apoptosis, whereas its suppression in cells overexpressing Rps3a, but not at physiological levels, led to induction of apoptosis.[253] Interestingly, downregulation of overexpressed RPS3a

led to apoptosis in undifferentiated, but not in retinoid-induced differentiated HL-60 cells.[254] This finding supports the observation from *Adar1*-truncated/*Mavs*-deficient mice that had reduced numbers of mature B cells, neutrophils, and monocytes, as well as increased B cell and neutrophil apoptosis.[246] Together, these studies suggest a potential role of *Rps3a1* in haematopoiesis and apoptosis.

RPS3A is also implicated in drug sensitivity, cell cycle, and cell growth. Human acute myeloid leukaemia (AML) cells overexpressing RPS3A protein *in vitro* demonstrated increased sensitivity to chemotherapy drugs cytosine arabinoside (ara-C) and doxorubicin, but not to paclitaxel. Tritiated-thymidine pulse labelling revealed that RPS3A-overexpressing AML cells had a higher proportion of cells in S phase, potentially explaining why they were sensitive to ara-C and doxorubicin, which act on DNA directly, and not to paclitaxel, which targets microtubules. Treatment of these cells with all-trans retinoic acid (ATRA) increased their sensitivity to ara-C and doxorubicin, while response to these drugs in cells with lower levels of RPS3A was either unaffected or decreased following ATRA administration. Higher RPS3A levels were correlated with increased cell growth *in vitro* and with better recovery of AML blasts following cryopreservation, suggesting a potential role of RPS3A in cell growth and survival.[255]

There is also some evidence of RPS3A being involved in adipogenesis and mitochondrial synthesis. One study found that expression of RPS3A protein was decreased in human epicardial adipose tissue in patients with coronary artery disease (CAD). In murine tissues, apolipoprotein E-deficient mice (a genotype used as an atherosclerosis disease model) demonstrated decreased expression of Rps3a in their perivascular adipose tissue (PVAT). Knocking down *RPS3A* with siRNA in brown preadipocytes *in vitro* resulted in decreased adipogenesis, decreased

expression of brown fat-specific markers, and decreased mitochondria biogenesis. Furthermore, they found that Rps3a knockdown in murine tissues resulted in decreased browning of PVAT and increased vascular inflammation.[256] Together, these findings suggest a role of RPS3A as a modulator of CAD.

Another study examining *Rps3a1* downregulation *in vivo* was done in zebrafish. It reported a shorter trunk and curved tail upon *Rps3a* knockdown in embryos at 25 hours post fertilisation, a timepoint when important organs start to develop.[257] These embryos died by 7-10 days post fertilisation. The *Adar1*-truncated/*Mavs*-deficient mice that showed a pattern of *Rps3a1* and *Rps3a3* dysregulation similar to that identified in *Hdgf*$^{-/-}$ mice, showed a 3.5-fold decrease in weight compared to those with the wild-type allele of *Adar1* at 15-days-old.[246] Whether these phenotypic changes observed upon *Rps3a1* downregulation reflect its role in regulating body size remains unknown. *Hdgf*$^{-/-}$ mice showed no significant difference in their body weight and other skeletal features when compared with WT mice.[214]

Interestingly, there is some evidence in the literature that might link *Rps3a1* and *Hdgf.* As mentioned earlier, HDGF was first isolated from human hepatoma cell line Huh-7.[164] One study found that RPS3A was expressed at high levels in hepatocellular carcinoma (HCC) cell lines and in patients with HCC. They also identified that high expression of RPS3A was correlated with worse prognosis (defined by shorter overall and recurrence-free survival) and with low immune cell infiltration, potentially accounting for poorer response to immune checkpoint blockade therapy.[258] Another study examined the function of RPS3A in survival of Hepatitis B virus X protein (HBx). HBx plays an important role in the development of HCC. This study detected RPS3A overexpression in Hepatitis B virus (HBV)-

associated HCC tissues. They have found that overexpressed RPS3A induced NF-kappa B signalling in HBV-infected cells via its chaperoning activity, leading to increased solubility of HBx protein. In line with this observation, knockdown of RPS3A led to decreased NF-kappa B activity in HBV-associated HCC cells.[259] The authors concluded that these findings suggested a role of RPS3A in amplifying HBx-related oncogenesis.

Bringing findings from the literature to molecular changes identified in *Hdgf*$^{-/-}$ mice at transcriptional and proteomic levels could help understand potential role of HDGF. Pathway analysis of cartilage and skin at 0 hours identified very different pathways enriched in each tissue. This suggests that HDGF might affect how specific cell types respond to their environment and potentially serves as a regulator of cellular activity, rather than a regulator of any specific pathway. It is important to note that one of the limitations was that sequencing was performed on whole tissues that housed various cell types. While our group has previously published that most (~90%) of the avulsed hip is cartilage, it also hosts a secondary ossification centre containing other cell types including hypertrophic chondrocytes, osteocytes, and osteoblasts, meaning that some gene reads picked up during sequencing could be coming from cells other than articular chondrocytes.[260]

Ribosomal proteins identified as highly regulated on a transcriptional level between WT and *Hdgf*$^{-/-}$ in both cartilage and skin suggest that this might be regulated through HDGF's impact on protein translation. A focus on translation might also explain why there were little transcriptional differences between the genotypes at 0 hours and why I saw a lack of transcriptional differences in response to cartilage injury (4 hours). Proteomic analysis did reveal profound differences between WT and *Hdgf*$^{-/-}$ at 48 hours after skin injury. Transcriptional study of

cartilage injury was performed 4 hours after injury, which might not be the timepoint when the effect of HDGF is most pronounced. Our previous work showed that acute injury response of chondrocytes is largely mediated by FGF2.[102] Thus, it is possible that HDGF does affect transcription but this happens a little later, e.g. 24 hours after injury as a late gene response. Analysis of genes most changed in response to injury in each genotype (the "difference of differences" analysis) identified many mitochondrial-related genes (e.g. *Cycs*, *Timm50*, *Mtfp1*, *Phb1*, *Cdc34*) as positively regulated in WT only. Meanwhile, genes that were positively regulated upon injury in the *Hdgf*$^{-/-}$ were mainly related to cell surface, signalling, and differentiation (e.g. *Fzd5*, *Bambi*, *Mme*, *Enpp6*). This type of regulation pattern may represent a functional adaptation of *Hdgf*$^{-/-}$ tissues to reduced mitochondrial activity in response to stress.

Together, results from this chapter demonstrated for the first time that there are some transcriptional and proteomic differences between WT and *Hdgf*$^{-/-}$ animals. I have demonstrated that differences in five genes (including *Hdgf* itself) were conserved across cartilage and skin. One of these genes, *Rps3a1*, is a key regulator of translation and it is downregulated in *Hdgf*$^{-/-}$ animals. Two of its paralogues, *Rps3a2* and *Rps3a3*, that exist only in mice, are upregulated in *Hdgf*$^{-/-}$ animals. There is no evidence from *in vivo* studies showing that paralogues of *Rps3a1* can compensate its function. As mentioned earlier, a secondary validation of transcriptomics results with quantitative PCR and/or immunostaining is warranted. Additionally, a close examination of why knock-out efficiency was less than 97% is also necessary to identify what region of *Hdgf* gene was picked up by sequencing.

Another significant contribution of this chapter is the proteomic labelling study of injured skin biopsies, which was, to our knowledge, the first time SILAC labelling has been performed on *ex vivo* tissue. Proteomic analysis detected significant decreased protein translation in *Hdgf*$^{-/-}$ skin following injury compared with WT injury. Many ribosomal proteins, including *Rps3a1*, showed decreased synthesis in *Hdgf*$^{-/-}$ animals. Taken together, these results suggest that ribosomal protein downregulation leads to a global downregulation of protein translation, which we presume is normally upregulated following injury. This is suggested by the enhanced protein synthesis observed in WT skin between 24 and 48 hours following injury, which is blunted in *Hdgf*$^{-/-}$ tissue. Based on published literature, it is possible to speculate that there might be a link between *Hdgf* and *Rps3a1*. As mentioned earlier, other proteins from HDGF family, like LEDGF, are able to regulate transcription by binding to chromatin directly via their HATH domain, which is also present in HDGF.[233] Additionally, ability of HDGF to interact with chromatin remodelling, transcription, and ribosomal proteins was demonstrated earlier.[213]

Finally, expression of HDGF and RPS3A proteins was reported to be elevated in patients with HCC, the disease in which HDGF has a well-established role as an oncogene and is associated with poorer prognosis.[181 261] There are far fewer studies about the role of RPS3A in HCC, but some suggested that higher expression of RPS3A was correlated with poorer survival outcomes in patients with HCC.[258] Putting all this information together with our findings, one might speculate that *Hdgf* could act as a regulator of ribosomal proteins, which, in turn, regulate translation. To prove this, one could consider performing chromatin immunoprecipitation sequencing (CHIP-seq) to identify where exactly HDGF

binds to DNA. If DNA binding is confirmed, this suggests that translational regulation is transcriptionally controlled, albeit not recognised at early points following injury (i.e. 4 hours). To address this, I have since sent cartilage RNA collected from hips incubated for 24 hours post-injury for bulk RNA sequencing, and results are awaited. Looking at transcriptional differences 24 hours following cartilage injury can help identify genes that are important for late injury response, and HDGF might be important for mediating them. As HDGF is released upon injury from both cartilage and skin suggesting a direct role in injury response, in the next chapter, I show *in vivo* injury studies that test the effects of HDGF deletion on tissue repair.

Chapter 5: HDGF role in tissue injury.

5.1. Introduction

Alongside studying molecular changes associated with HDGF deletion using transcriptomic and proteomic methods, I wanted to explore how HDGF might affect tissue response to injury *in vivo*. As previously demonstrated in this thesis, I used two tissues - cartilage and skin - to study this. The established procedure for studying cartilage injury *in vivo* used by our group is partial medial meniscectomy (PMX) surgery, which serves as an osteoarthritis model and enables one to assess the degree of cartilage degradation following joint destabilisation. In the skin, I performed full-thickness excisional wounding, which is a standard model for studying response of skin to injury and its repair over time. As mentioned in the earlier chapter, the transcriptional response to cartilage injury at 4 hours was very similar between WT and *Hdgf*$^{-/-}$ animals. This, however, did not come as a surprise, as work from our group has shown that acute cartilage injury is predominantly driven by release of FGF2, which is chondroprotective *in vivo*.[100] Given the important role of HDGF in protein translation following tissue injury *in vitro* I have demonstrated and the fact that other PCM-derived growth factors, like FGF2 and CTGF, are important in response of skin and cartilage to injury, I next explored HDGF's effects on the repair response in skin and disease severity in the joint.

Both FGF2 and CTGF have been implicated in skin injury response. For instance, *Fgf2*$^{-/-}$ mice aged between 2-3 months demonstrated a slight (3-day) delay in healing of excisional scars. In this study, the scar was defined as fully healed when the skin in the wounded area was smooth, fully restored, and no residual defects were visible. The endpoint of observation was day 16 post-wounding.[152] FGF2 was also shown to be important for diabetic wound healing through

improving angiogenesis and was found to have a concentration-dependent collagen-inducing effect in bovine luteal fibroblasts.[150] [151] Topical application of recombinant FGF2 in mice resulted in accelerated wound healing and increased expression of epithelial-mesenchymal transition (EMT)-associated markers by qPCR. Treatment of cultured keratinocytes with FGF2 did not have significant impact of their migration or morphology, however, when co-treated with TGFβ1, it increased expression of EMT-associated markers to a greater extent than in TGFβ1-only treatment group.[153] CTGF, which is downstream of TGFβ, has a well-established role in tissue fibrosis and activates tissue remodelling and matrix deposition that lead to fibrosis.[156] CTGF is important in early stages of wound repair, as it contributes to formation of stem cell-derived granulation tissue. The same study found that prolonged exposure (28 days) to CTGF resulted in more abundant collagen deposition and increased proliferation of fibroblasts within granulation tissue. Additionally, CTGF was detected at high levels in human burn wounds at days 5-6 post-injury and gradually decreased by day 20.[216] Together, these findings suggested that transient upregulation of CTGF in early stages of wound healing promoted repair, whereas its continuous upregulation led to fibrosis. These studies led us to hypothesise that HDGF might also have a function in skin wound healing, prompting us to carry out skin wounding experiments in WT and *Hdgf*$^{-/-}$ mice.

Chapter aims:

1) To investigate the contribution of HDGF to cartilage response to injury following OA induced by PMX surgery in WT and *Hdgf*$^{-/-}$ mice,
2) To examine the effect of HDGF deletion on skin repair following skin wounding of WT and *Hdgf*$^{-/-}$ mice.

5.2. Methods

5.2.1. Partial medial meniscectomy (PMX) osteoarthritis model and OARSI scoring of the knee joint cartilage

PMX surgery was performed by Dr Jadwiga Zarebska at the Kennedy Institute of Rheumatology. Briefly, male C57BL/6 (wild-type) and *Hdgf*$^{-/-}$ mice (aged 10 weeks) undergoing surgery were anesthetised by inhalation of isoflurane (3% induction and 1.5-2% maintenance) in 1.5-2 L/min oxygen. All mice received a subcutaneous injection of buprenorphine (Vetergesic; Alstoe Animal Health) before surgery. Induction of OA by PMX was performed: the right knee was opened using the medial parapatellar approach to identify the meniscus without releasing the meniscotibial ligament. The mice were fully mobile within 4-5 min after the withdrawal of isoflurane. List of reagents and equipment used for surgery is available in Chapter 2. Mice were sacrificed by CO_2 asphyxiation followed by confirmatory cervical dislocation 4- and 8-weeks following PMX surgery. Knee joints were collected, cleaned from muscle tissue with scissors, and placed in 10% neutral buffered formalin for 24-48 hours.

Histological processing was performed by Kennedy Institute of Rheumatology Histology Facility staff. Isolated knee joints were embedded in paraffin and tissue was processed with Tissue TeK VIP 6 Processor “Sakura” (Sakura, Alphen aan den Rijn, Netherlands). Following formalin fixation, knees were decalcified for one week in 20% formic acid solution (Thermo Fisher Scientific, Waltham, MA, USA). They were then placed in 70% ethanol diluted in dH_2O (Sigma Aldrich, St Louis, MO, USA) for 1 hour and 30 mins at 40 ^{0}C. They were then washed 5 times with 100% ethanol, 3 times with Xylene (Thermo Fisher Scientific, Waltham, MA, USA) for 1 hour and 30 mins at 40 ^{0}C, and 4 times with

paraffin (CellPath, Newtown, UK) for 1 hour and 30 mins at 63 ^{0}C, followed by overnight incubation in paraffin at 63 ^{0}C. The following day the samples were embedded using TEC 5 Embedding centre "Sakura" (Sakura, Alphen aan den Rijn, Netherlands) and sectioned with 5 μm intervals.

Safranin O (Saf O) staining was then performed. Briefly, slides were placed in water for 20 seconds, Harris haematoxylin (Leica Microsystems, Wetzlar, Germany) for 30 seconds, followed by 1 minute wash with water, 20 seconds in 70% ethanol in 10 mL/L hydrochloric acid (VWR, Randor, PA, USA), 1 minute wash with water, 1 minute in blueing water (600 mL water containing 1.6 mL ammonia) (VWR, Randor, PA, USA), 6 minutes in fast green (Sigma Aldrich, St Louis, MO, USA), 15 seconds in 1% acetic acid (Millipore, Burlington, MA, USA), 1 minute water wash, 2 minutes in Saf O (Electron Microscopy Sciences, Hatfield, PA, USA), 1 minute water wash, 3 washes with 100% ethanol (1 minute/each), and 3 washes with xylene (1 minute/each) and mounted in Di-n-butylphthalate (DPX) mounting media (Sigma Aldrich, St Louis, MO, USA) in the G2 Coverslipper Machine Sakura. Details of reagents are available in Chapter 2. OA severity was scored independently by two blinded reviewers based on the modified OA Research Society (OARSI) scoring system outlined below.

Table 5.2.1. Modified OARSI score description.

Score	**Description**
0	Normal cartilage
0.5	Loss of proteoglycan with no structural change
1	Superficial fibrillations with no cartilage loss
2	Superficial cartilage loss and vertical clefts
3	Cartilage delamination at the tidemark
5	Tissue loss extending into the calcified cartilage past the tidemark
6	Tissue loss extending into subchondral bone

5.2.2. Skin wounding model in mice

The skin wounding procedure was performed on male C57BL/6 (wild-type) and *Hdgf*$^{-/-}$ mice at the age of 10, 15, and 26 weeks. Mice were anesthetised by inhalation of isoflurane (3% induction and 1.5-2% maintenance) in 1.5-2 L/min oxygen and all mice received a subcutaneous injection of buprenorphine (Vetergesic; Alstoe Animal Health) before surgery. The fur on the back was shaved with a trimmer, shaving cream was applied for 4 minutes and wiped with warm water followed by topical sterilisation with Hibiscrub (Mölnlycke Heath Care, Gothenburg, Sweden). Four 3-mm-diameter biopsy punches were removed from the back of each mouse with an autoclaved leather biopsy puncher. The diameter in the x- and y-direction was measured with a digital calliper.

Measurements were repeated on day 1-7 under general anaesthesia with inhaled isoflurane (3% induction and 1.5-2% maintenance) and calculations were performed according to Rowland et al.[262] Briefly, the x- and y-axis measurements were each dived in half to obtain a semiminor and a semimajor axes. These were averaged between 4 wounds for each mouse to obtain one value for each day. The averaged semiminor and semimajor axes were multiplied by π to obtain the wound area. Subsequent measurements were divided by the wound area on day zero to obtain the percent wound area closure value for each day.

5.2.3. Histological analysis of skin wound healing

Fifteen-week-old male C57BL/6 (wild-type) and *Hdgf*$^{-/-}$ mice were sacrificed by CO_2 asphyxiation followed by confirmatory cervical dislocation on days 3, 5, 7, and 10 post-wounding. The whole back skin was removed with scissors, and thin strips of skin, each containing two wounds, were cut out in such a way that edges of each wound were on the edge of the skin strip. Unwounded skin

(control samples) was collected from 15-week-old animals that were sacrificed by CO_2 asphyxiation and confirmatory cervical dislocation. Their backs were shaved, shaving cream was applied for 4 minutes and wiped with warm water followed by topical sterilisation with Hibiscrub (Mölnlycke Heath Care, Gothenburg, Sweden). Two skin strips of approximately 0.5 cm by 2 cm were collected from each mouse. Skin strips were fixed in 10% Neutral Buffered Formalin for 24-48 hours and processed on Tissue TeK VIP 6 Processor Sakura (Sakura, Alphen aan den Rijn, Netherlands), as described above. In order to consistently collect comparable 5 μm-thick tissue sections from the middle of the wounds in all the specimens, the distance from the edge of the skin strip to the centre of the wounds was measured prior to the embedding in paraffin blocks.

Following sectioning, slides were stained with Haematoxylin& Eosin (H&E), Masson's trichrome (MT), and Gram stain. Slides were processed in the DRS 2000 AutoStainer Sakura (Sakura, Alphen aan den Rijn, Netherlands). For H&E stain, slides were washed with xylene twice for 3 minutes and twice with ethanol for 1 minute. Slides were placed in water for 1 minute, Harris haematoxylin for 6.5 minutes, followed by 2 minute wash with water, 40 seconds in 70% ethanol in 10 mL/L hydrochloric acid, 1 minute wash with water, 1 minute in blueing agent (600 mL water containing 1.6 mL ammonia), 1 minute wash with water, 1.45 min in Eosin Y 1% aqueous (Cell Path, Newtown, UK), 3 minute wash with water, 3 washes with 100% ethanol (1 minute/each) and 2 washes with xylene (1 minute/each), and mounted in DPX mounting media (Sigma Aldrich, St Louis, MO, USA) in the G2 Coverslipper Machine Sakura. For MT stain (Cell Path, Newtown, UK), slides were washed with xylene twice for 5 minutes and twice with ethanol for 1 minute. Slides were placed in water for 1 minute, filtered Harris

haematoxylin for 5 minutes, washed for 5 minutes with water, followed by 5 minute stain with Trichrome stain A, 30 seconds in phosphotungstic/phosphomolybdic acid solution, rinsed with water, stained in light green counterstain for 5 minutes, rinsed with water, incubated in 1% acetic acid for 1.5 min, dehydrated, and mounted in DPX mounting media (Sigma Aldrich, St Louis, MO, USA) in the G2 Coverslipper Machine Sakura. For Gram stain, slides were washed with xylene twice for 5 minutes and twice with ethanol for 1 minute. Slides were placed in water for 1 minute, filtered Crystal violet (Sigma Aldrich, St Louis, MO, USA) for 1 minute, washed with water, followed by 1 minute stain with iodine, rinsed with water, incubated in 1% acetic acid (Millipore, Burlington, MA, USA) for 10 seconds, rinsed with water, counterstained in Saf O (Electron Microscopy Sciences, Hatfield, PA, USA) for 1 minute, rinsed with water, dehydrated, and mounted in DPX mounting media (Sigma Aldrich, St Louis, MO, USA) in the G2 Coverslipper Machine Sakura. Details of reagents are available in Chapter 2.

The following characteristics of skin wound healing were measured: percent wound re-epithelialization, thickness of epidermis in the wound (for fully re-epithelialized wounds), epidermal thickness in non-wounded regions, dermal thickness (for wounds with regenerated panniculus carnosus muscle), and granulation tissue (GT) width in the wound area. Definitions of each histology metric were derived from van de Vyver et al[263] and modified as described further. Measurements of histological features of skin wound healing (e.g. percent re-epithelialization, thickness of epidermis, dermis, and GT width) were done in QuPath software[264] (v0.5.0). Percent re-epithelialization was defined as the ratio of the distance inside the wound covered by new epithelium over the distance between original wound edges (measured by tracking the shape of the wound in QuPath).

Epidermal thickness was measured in three places inside the wound, and this was only done in wounds that were fully re-epithelialized. Dermal thickness was defined as a vertical distance from the epidermal-dermal junction to the top of panniculus carnosus muscle. It was only measured in wounds with restored panniculus carnosus. GT width was measured in a straight line for a shortest distance between the remodelled dermis on both sides of the wound. Slides with wounds that were torn during histological processing were not included in final analysis.

5.2.4. Statistical analysis

Imaging of histology slides was performed using Zeiss AxioScan Digital Slide Scanner (10X objective) (Zeiss, Oberkochen, Germany) and Olympus BX51 (Olympus Corporation, Tokyo, Japan) at the Kennedy Institute of Rheumatology. Statistical analyses were performed using GraphPad Prism (version 10.4.1). For OARSI scores, an unpaired two-tailed t-test with Mann-Whitney correction was performed to compare the means between WT and *Hdgf*$^{-/-}$ OARSI scores at each timepoint (4- and 8-weeks post-PMX surgery). For percent wound area closure, an unpaired two-tailed t-test with Mann-Whitney correction was performed to compare means of wound area between WT and *Hdgf*$^{-/-}$ mice on each day. For assessment of histological features of wound healing, such as re-epithelialization and granulation tissue, an unpaired two-tailed t-test with Mann-Whitney correction was performed to compare the means of selected histological features between WT and *Hdgf*$^{-/-}$ mice at each day when the measurements were performed. Statistical significance was defined using the conventional threshold of $p \leq 0.05$, and significance levels are noted in figure legends.

5.3. Results

5.3.1. The degree of cartilage degradation post-PMX was similar in young wild-type and *Hdgf*$^{-/-}$ animals

In order to see whether there was a phenotype in OA, WT and *Hdgf*$^{-/-}$ male mice underwent a PMX surgery at 10 weeks of age, and their knees were assessed 4- and 8-weeks post-surgery. Ten weeks was chosen as the age for surgery because it is the earliest timepoint when animals reach skeletal maturity. A minimum of four animals were housed in one cage to maintain social behaviour and welfare of animals, and a minimum of three cages per genotype were used for assessing OA severity at each timepoint to account for any cage-related variability. The modified OARSI scores were similar between WT and *Hdgf*$^{-/-}$ mice at the assessed timepoints, although there was a trend towards more severe OA in *Hdgf*$^{-/-}$ mice at 8 weeks post-PMX, reflected by higher OARSI scores in that group (Figure 5.1A). This difference, however, was not statistically significant. Representative images of Saf O histology staining, which were not markedly different between the genotypes, are included (Figure 5.1B). Cartilage is stained red, and, in both genotypes, cartilage was degraded to a relatively similar degree.

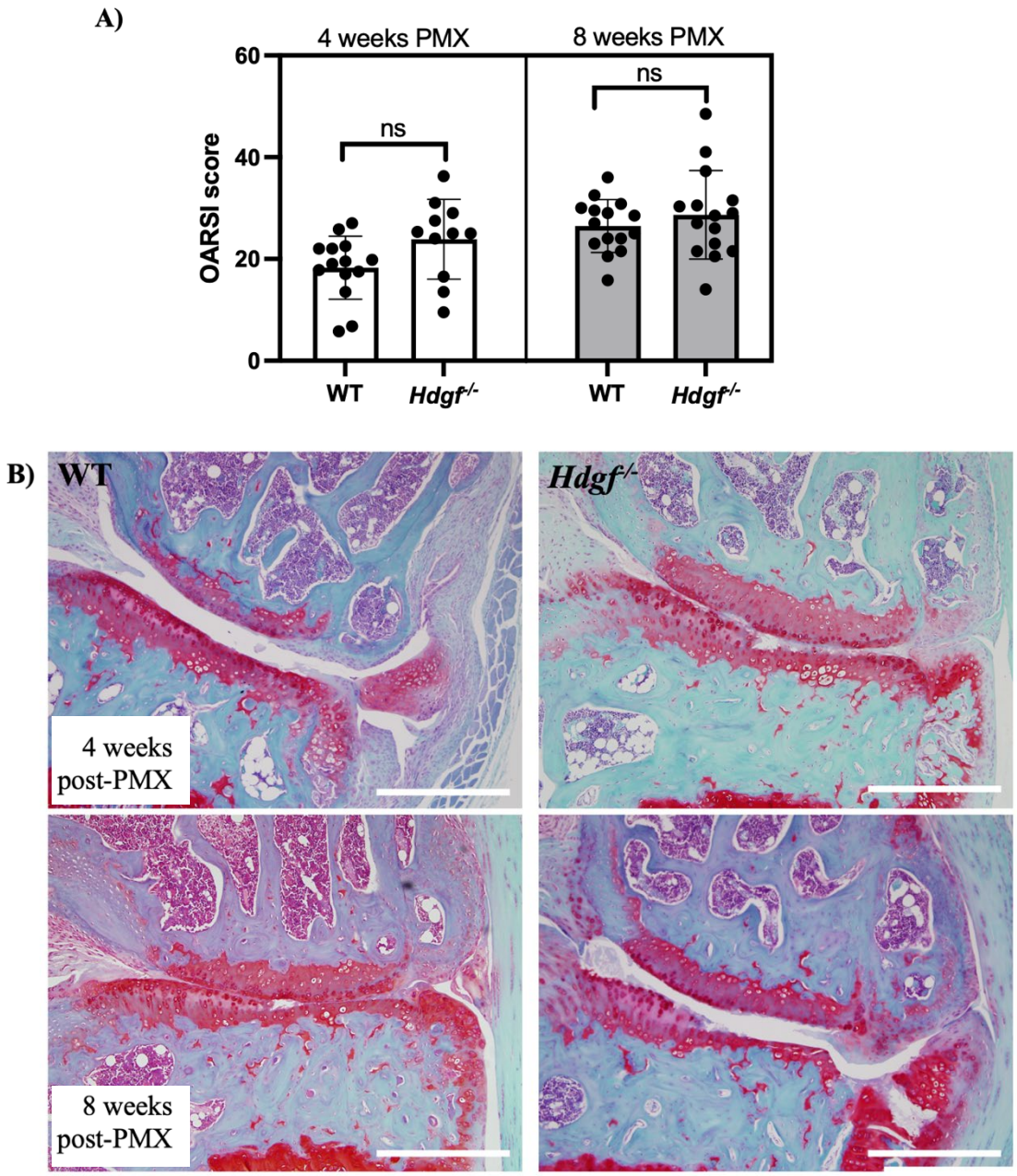

Figure 5.1. The degree of cartilage degradation was similar between WT and *Hdgf*$^{-/-}$ mice following PMX surgery. A) Modified OARSI scores of WT and *Hdgf*$^{-/-}$ mice at 4- and 8-weeks post-PMX surgery. Each dot represents a mouse. Mean ± SD, unpaired two-tailed t-test with Mann-Whitney correction, n=14 (WT 4 weeks), n=11 (*Hdgf*$^{-/-}$ 4 weeks), n=15 (WT 8 weeks), n=15 (*Hdgf*$^{-/-}$ 8 weeks), ns - not significant. B) Representative Saf O-stained histology images of the knee joints for each genotype. 10X magnification, scale bar = 500 μm.

5.3.2. *Hdgf*$^{-/-}$ male mice demonstrated delayed skin healing that was age-dependent

As mentioned previously, other PCM-derived growth factors, like FGF2 and CTGF, are important in response of skin to injury. Mice with knocked out FGF2 demonstrated a slight delay in wound healing, whereas CTGF has been shown to be an important modulator of granulation tissue formation and fibrosis post-wounding.[152 156] I therefore established a skin wounding assay to study the role of HDGF in skin repair. First, I compared WT and *Hdgf*$^{-/-}$ male mice at the age of 10 weeks, the same timepoint when PMX surgery was performed. I did not observe any statistically significant difference in wound healing between the two genotypes at that age (Figure 5.2A). On visual examination, the wounds looked very similar at day 7 post-wounding (Figure 5.2B). It is, however, well-established that response to injury is delayed with ageing in both mice and humans.[265] Thus, I decided to perform the skin wounding assay in 15- and 26-week-old WT and *Hdgf*$^{-/-}$ male mice.

When skin wounding was performed in older mice (15- and 26-week-old), *Hdgf*$^{-/-}$ animals demonstrated delayed skin wound healing compared to the WT mice (Figure 5.3A). Wound healing was similar between 15- and 26-week-old *Hdgf*$^{-/-}$ animals, whereas it was significantly faster in 10-week-old *Hdgf*$^{-/-}$ animals. WT animals showed similar degree of wound healing across all tested age groups. In 15- and 26-week-old animals, the delay in healing in *Hdgf*$^{-/-}$ mice was more evident in the first 4 days following skin wounding, although, percent of wound area closed at day 7 was still significantly higher in WT animals (Figure 5.3A). Visual inspection of wounds at day 7 revealed bigger wounds with some scabbing and flaky skin in *Hdgf*$^{-/-}$ mice at both 15 and 26 weeks of age. Wounds in age-matched WT animals at day 7 were smaller and scabs were mostly absent (Figure 5.3B).

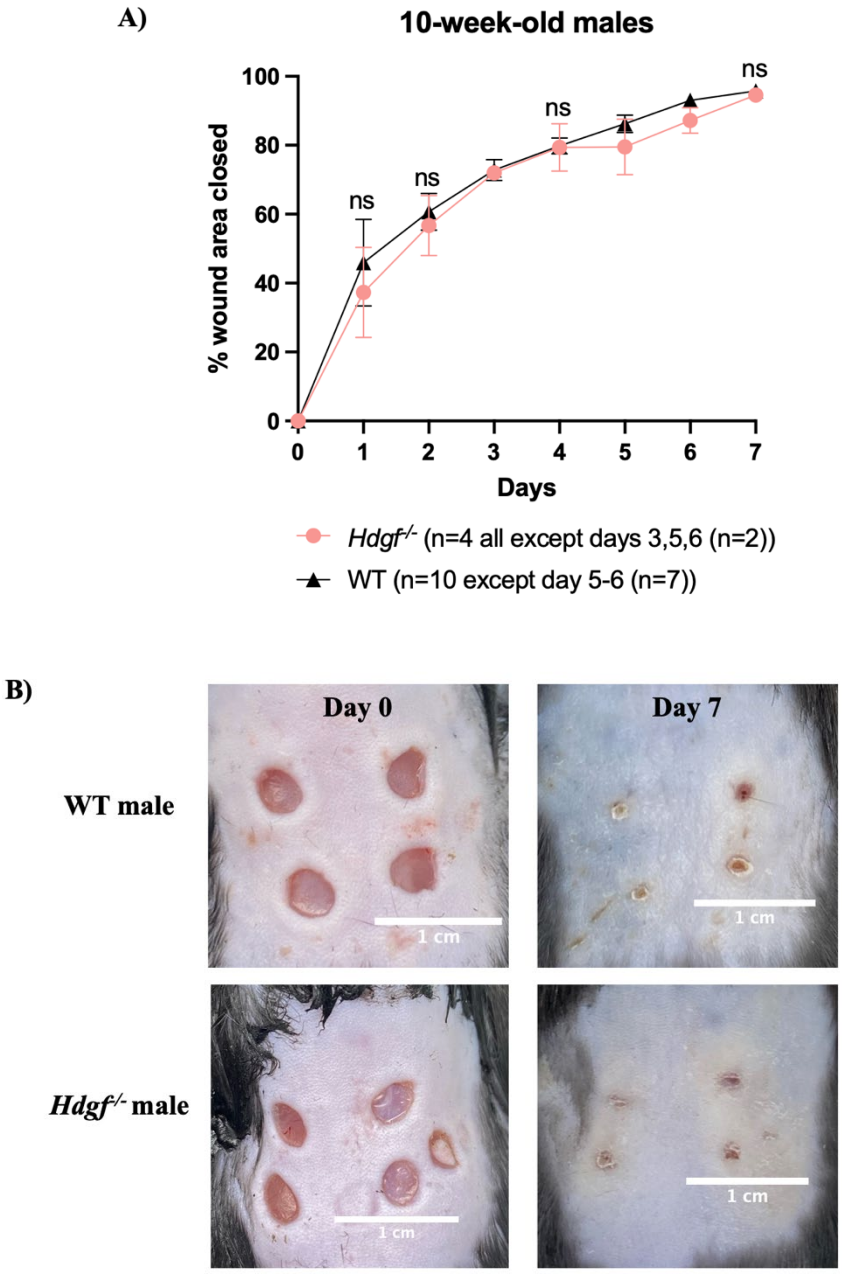

Figure 5.2. No differences were observed in skin wound healing in 10-week-old male mice. A) A graph plotting percent wound area closed over 7 days post-wounding in WT and *Hdgf*$^{-/-}$ mice. Mean ± SD, unpaired two-tailed t-test with Mann-Whitney correction applied for comparing wound area on days with more than 2 mice per group, ns - not significant. B) Representative images of wounded WT and *Hdgf*$^{-/-}$ mice on the day of wounding (day 0) and day 7 post-wounding, scale bar = 1 cm.

A)

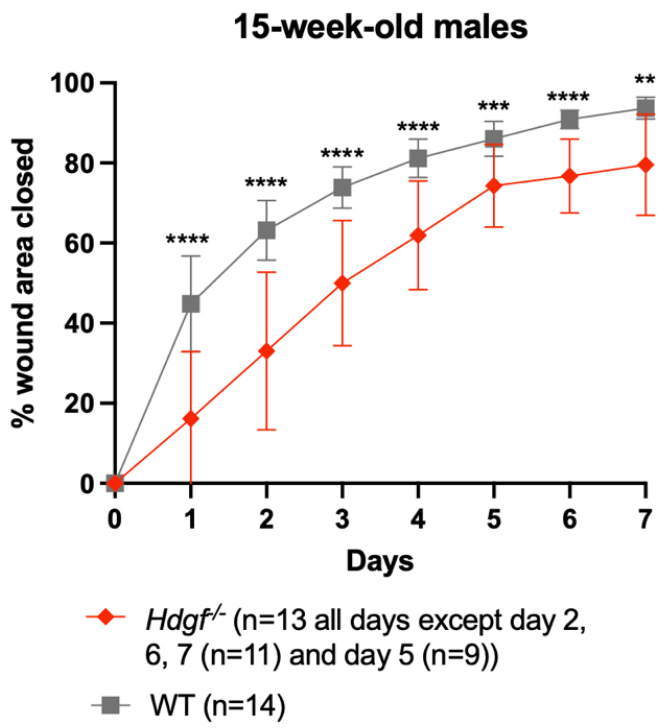
15-week-old males
% wound area closed
100
80
60
40
20
0
0
1
2
3
4
5
6
7
Days
****
****
****
****
***
****
**
Hdgf-/- (n=13 all days except day 2, 6, 7 (n=11) and day 5 (n=9))
WT (n=14)

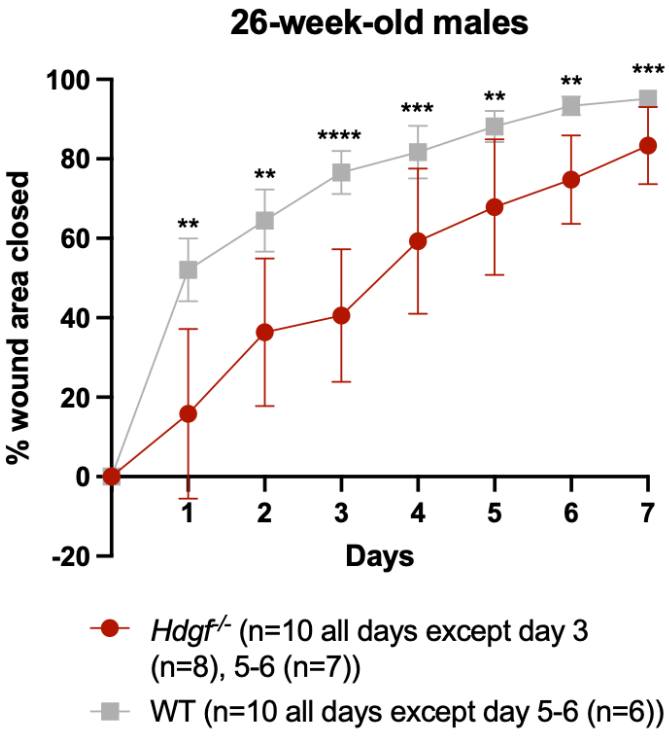
26-week-old males
% wound area closed
100
80
60
40
20
0
-20
1
2
3
4
5
6
7
Days
**
**
****
***
**
**
***
Hdgf-/- (n=10 all days except day 3 (n=8), 5-6 (n=7))
WT (n=10 all days except day 5-6 (n=6))

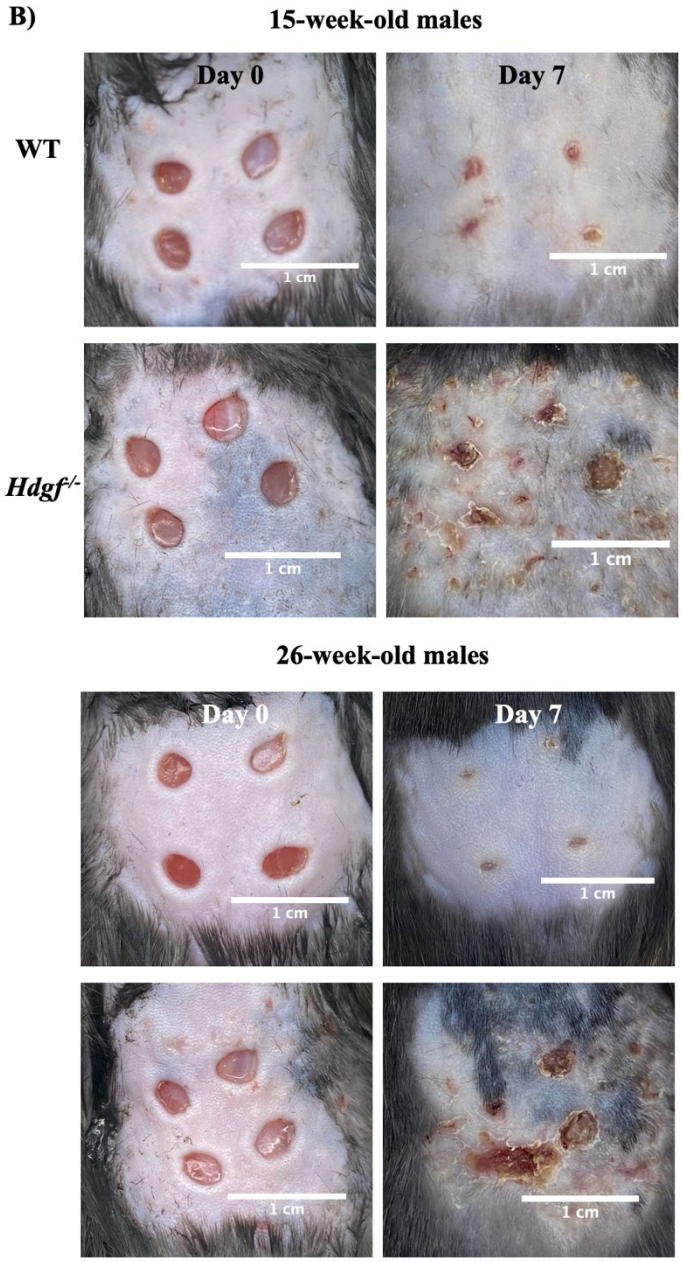

Figure 5.3. HDGF-mediated skin healing delay is age-dependent. A) A graph plotting percent wound area closed over 7 days post-wounding in 15- and 26-week-old WT and *Hdgf*$^{-/-}$ male mice. Mean ± SD, unpaired two-tailed t-test with Mann-Whitney correction, ****p<0.0001, ***p<0.001, **p<0.01, ns - not significant. B) Representative images of wounded 15- and 26-week-old WT and *Hdgf*$^{-/-}$ male mice on the day of wounding (day 0) and day 7 post-wounding, scale bar = 1 cm.

5.3.3. HDGF might be important for both epidermal and dermal aspects of skin wound healing

Histological examination of the wounds of 15-week-old male mice was performed to on days 3, 5, 7, and 10 post-wounding. As described in the methods section of this chapter, the main features that were examined were re-epithelialization of the wound, epidermal thickness of newly formed epithelium, granulation tissue width, and degree of dermal remodelling/reconstruction. As described by van de Vyver et al, the initial stage of murine wound healing is the formation of new epithelium on the sides of the wound that slowly converge in the middle to fully re-epithelialize the wounded area.[263] Examination of re-epithelialization in scars of WT and *Hdgf*$^{-/-}$ male mice revealed a slight delay in re-epithelialization in *Hdgf*$^{-/-}$ animals compared to WT. A visual representation of the way re-epithelialization was measured on day 5 post-wounding is shown in Figure 5.4A. Due to sample size limitations, statistical analysis was performed only on days 5, 7, and 10 post-wounding. While there was a trend towards slower re-epithelialization in *Hdgf*$^{-/-}$, the data showed statistical significance only on day 7, which was also the timepoint with the largest sample size (n = 6 WT and n = 8 *Hdgf*$^{-/-}$) (Figure 5.4B). Epidermal index (the ratio of thickness of newly formed epidermis to thickness of unwounded epidermis), which was only measured for wounds that were 100% re-epithelialized, was similar between the two genotypes on day 7 and 10 post-wounding (Figure 5.4C). This suggests no difference in the degree of epithelial thickening in response to injury between genotypes. In addition to delayed re-epithelialization, keratinised scabs were more apparent in the wounds of *Hdgf*$^{-/-}$ animals compared to WT (Figure 5.5).

A)

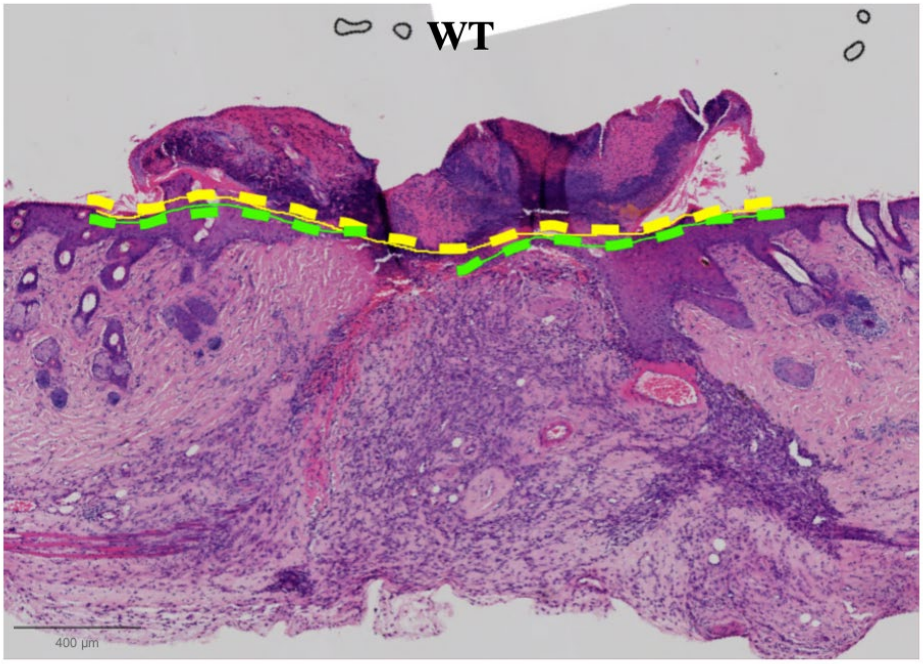

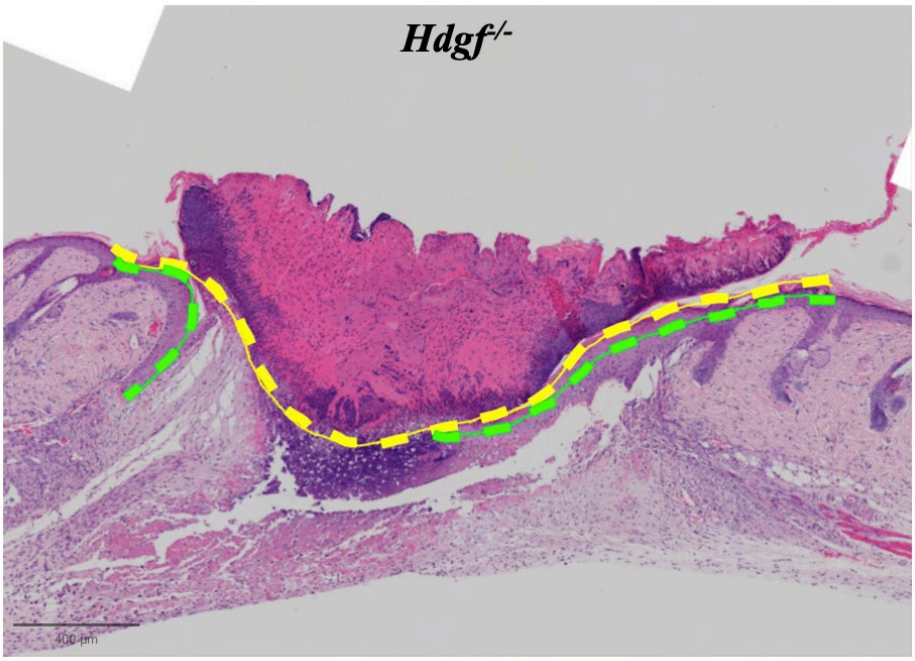

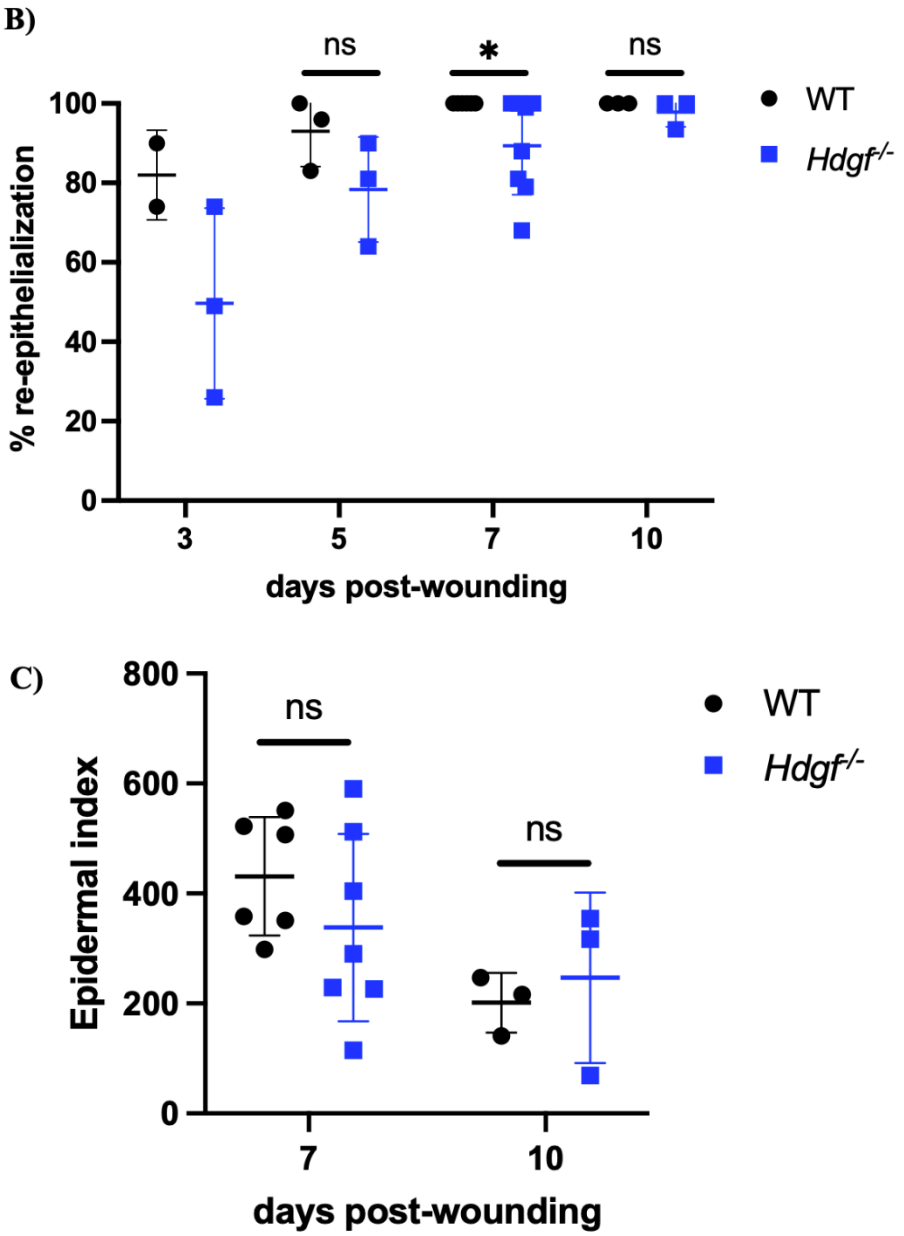

Figure 5.4. Re-epithelialization was slightly delayed in 15-week-old *Hdgf*$^{-/-}$ mice compared to WT. A) Images of wounds on day 5 showing measurements of re-epithelialization. Yellow dotted line represents the distance between the edges of the wound; green dotted lines represent the distance covered by newly formed epithelium. H&E staining, 10X magnification, scale bar = 400 µm. B) Percent re-epithelialization of wounds over 10 days post-wounding. Each dot represents a mouse, mean ± SD is displayed. N = 2 (WT day 3), n = 3 (*Hdgf*$^{-/-}$ day 3), n = 3 (WT and *Hdgf*$^{-/-}$ day 5), n = 6 (WT day 7), n = 8 (*Hdgf*$^{-/-}$ day 7), n = 3 (WT and *Hdgf*$^{-/-}$ day 10). Statistical comparison performed on groups with n>2, unpaired two-tailed t-test with Mann-Whitney correction, *p<0.05, ns - not significant. C) Epidermal index (ratio of thickness of newly formed epithelium to unwounded epithelium) at days 7 and 10 post-wounding, mean ± SD, n = 6 (WT day 7), n = 7 (*Hdgf*$^{-/-}$ day 7), n = 3 (WT and *Hdgf*$^{-/-}$ day 10), unpaired two-tailed t-test with Mann-Whitney correction, ns - not significant.

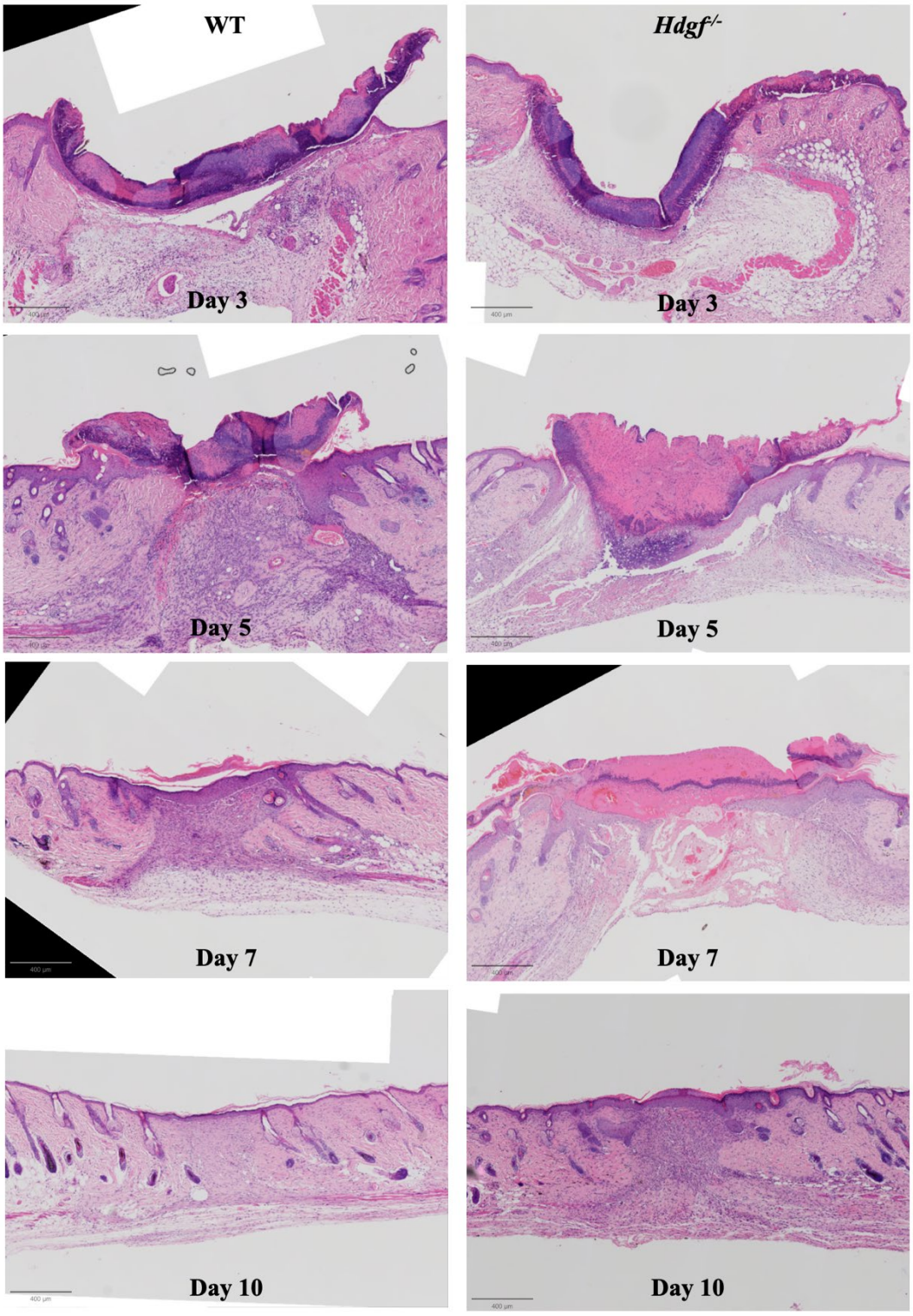

Figure 5.5. Re-epithelialization was slightly delayed in 15-week-old *Hdgf*$^{-/-}$ mice compared to WT. Representative images of wounds over 10 days post-wounding. H&E staining, 10X magnification, scale bar = 400 μm.

Granulation tissue (GT) width was assessed only in samples where fully remodelled dermis with visible collagen fibres was formed on both sides of the wound, no breaks in the tissue were present, and a continuous line could be drawn through the granulation tissue bed to obtain its width. A representative image showing the way GT width was measured is available in Figure 5.6A. Examination of representative GT images revealed significantly wider GT bed in *Hdgf*$^{-/-}$ mice compared to WT, reflected by a greater distance between fully remodelled parts of the dermis (defined by visible blue collagen fibres on Masson's trichrome stain) on both sides of the wounded area (Figure 5.6A). Analysis revealed significantly wider GT in *Hdgf*$^{-/-}$ mice (p-value = 0.0007) on day 7 post-wounding, which was the only timepoint with sufficient sample size (n = 6 WT and n = 8 *Hdgf*$^{-/-}$) for statistical analysis (Figure 5.6B). Wider GT suggests lesser degree of dermal remodelling in *Hdgf*$^{-/-}$ male mice compared to WT males. Taken together with the observed re-epithelialization delay, these results suggest that HDGF might be important for both epidermal and dermal aspects of skin wound healing, as both re-epithelialization and dermal remodelling were affected to some extent in *Hdgf*$^{-/-}$ animals.

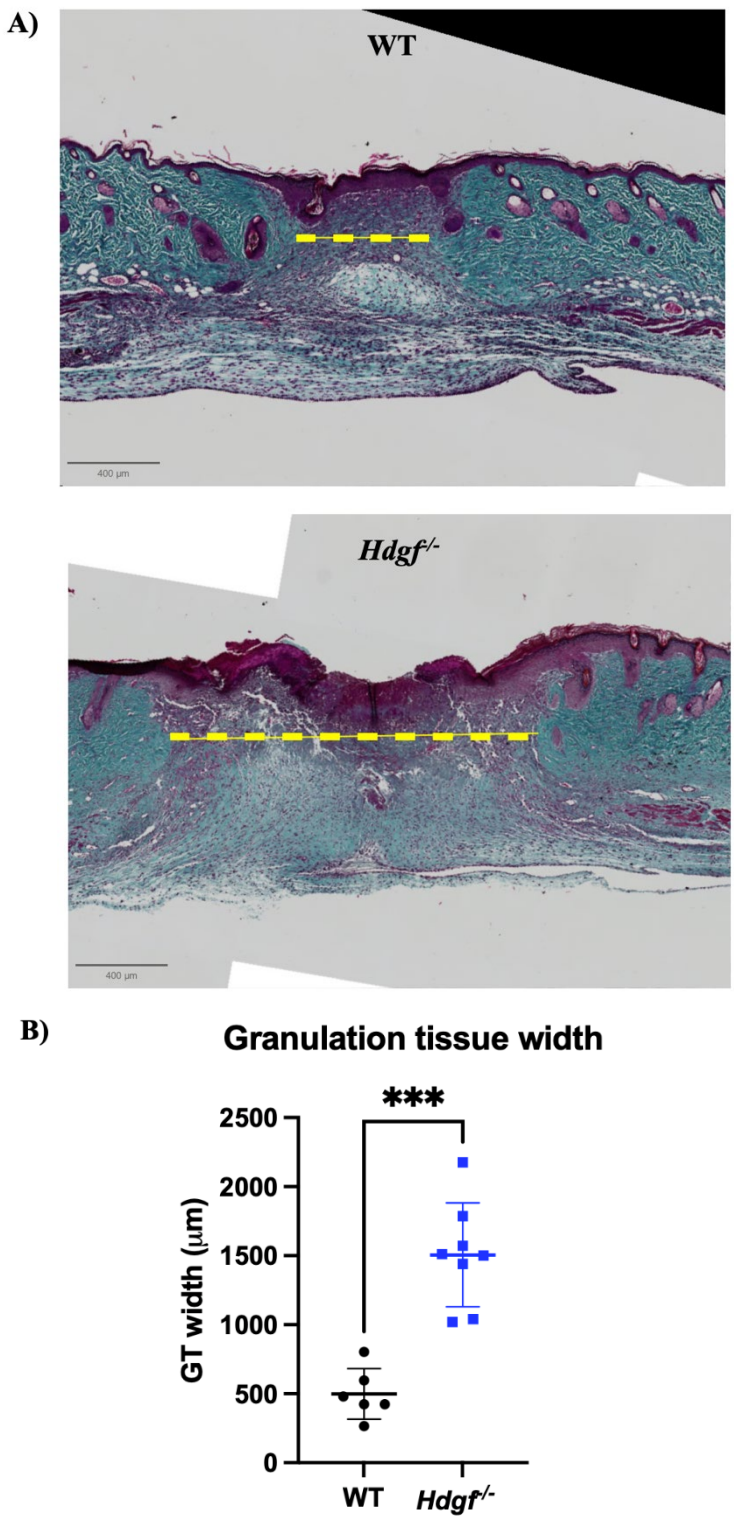

Figure 5.6. HDGF is likely important for the dermal aspect of skin wound healing. A) Images of wounds on day 7 showing measurements of GT width. Yellow dotted line represents the distance between the edges of fully remodelled dermis with visible blue collagen fibres. Masson's trichrome staining, 10X magnification, scale bar = 400 µm. B) Granulation tissue (GT) width in WT and *Hdgf*$^{-/-}$ animals at day 7 post-wounding. Each dot represents a mouse, mean ± SD, n = 6 (WT), n = 8 (*Hdgf*$^{-/-}$). Unpaired two-tailed t-test with Mann-Whitney correction, ***p<0.001.

In order to examine whether observed differences in skin wound healing between the two genotypes were only apparent during tissue injury, I collected and analysed skin from unwounded 15-week-old WT and *Hdgf*$^{-/-}$ male mice. In these uninjured animals, I measured thickness of both epidermis and dermis with the aim to understand potential structural differences between the genotypes. I took six measurements for both epidermis and dermis in various locations of a skin section from each mouse and averaged them to obtain one value per animal. Epidermal thickness was defined as the distance between the top layer of the epidermis and the epidermal-dermal junction (Figure 5.7A), whereas dermal thickness was defined as the distance between the epidermal-dermal junction and panniculus carnosus muscle (Figure 5.7B). I observed a trend towards thinner epidermis and dermis in *Hdgf*$^{-/-}$ mice; however, these differences did not reach statistical significance (n = 3 for each genotype) (Figure 5.7A, B).

As no significant structural differences in the skin were noted between the two genotypes at the baseline (no injury), but I discovered a delay in skin wound healing, increased visible scabbing and a trend towards thinner epidermis and dermis in *Hdgf*$^{-/-}$ mice, I wanted to test whether *Hdgf*$^{-/-}$ mice were more sensitive to milder types of skin injury. As skin wounding procedure involved hair trimming and application of a shaving cream, which can cause skin irritation on its own, I wanted to test whether WT and *Hdgf*$^{-/-}$ mice reacted differently when subjected only to trimming and shaving cream. Due to limitations in the number of animals available, I was only able to conduct this experiment on 3 WT mice and 2 *Hdgf*$^{-/-}$ mice (15-week-old animals). On day 7 post-trimming and shaving cream application, one out of three WT animals had a small scab (Figure 5.8A), whereas one out of two *Hdgf*$^{-/-}$ mice developed larger irritation with scabbing (Figure 5.8B).

A)

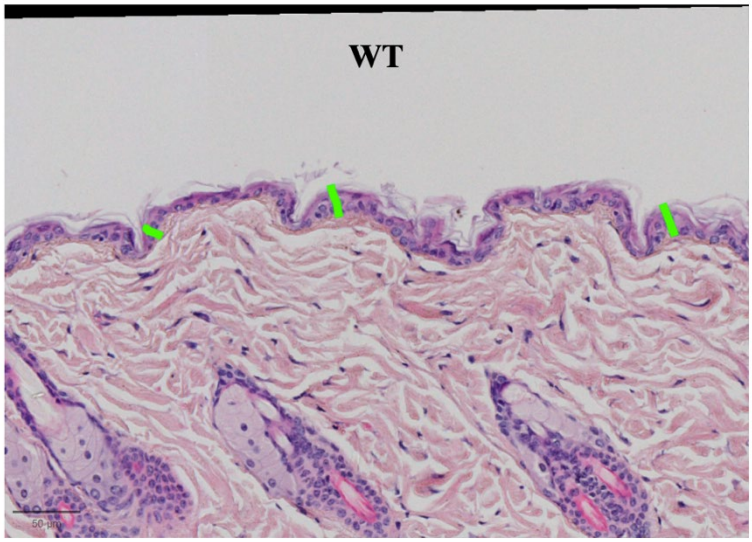

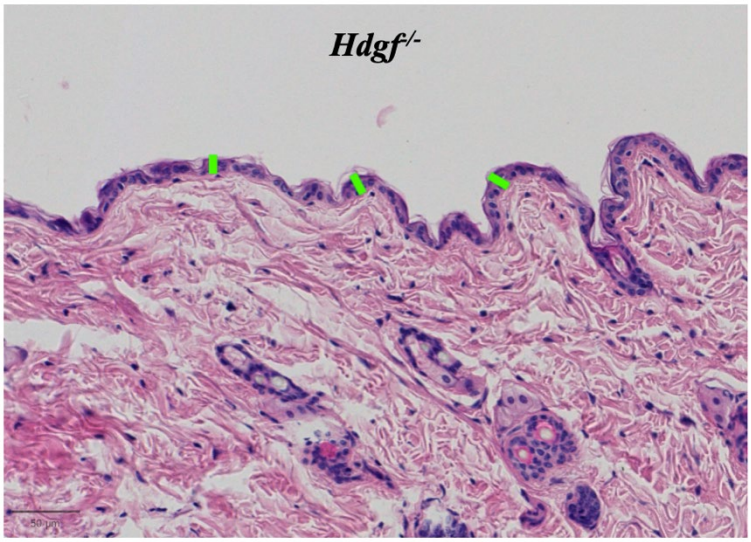

Unwounded epidermis thickness

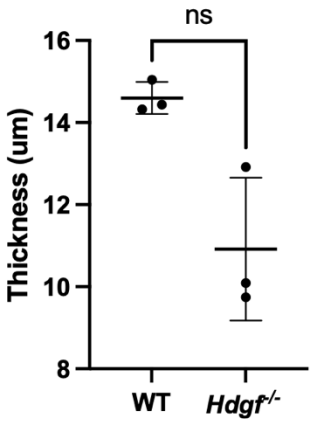

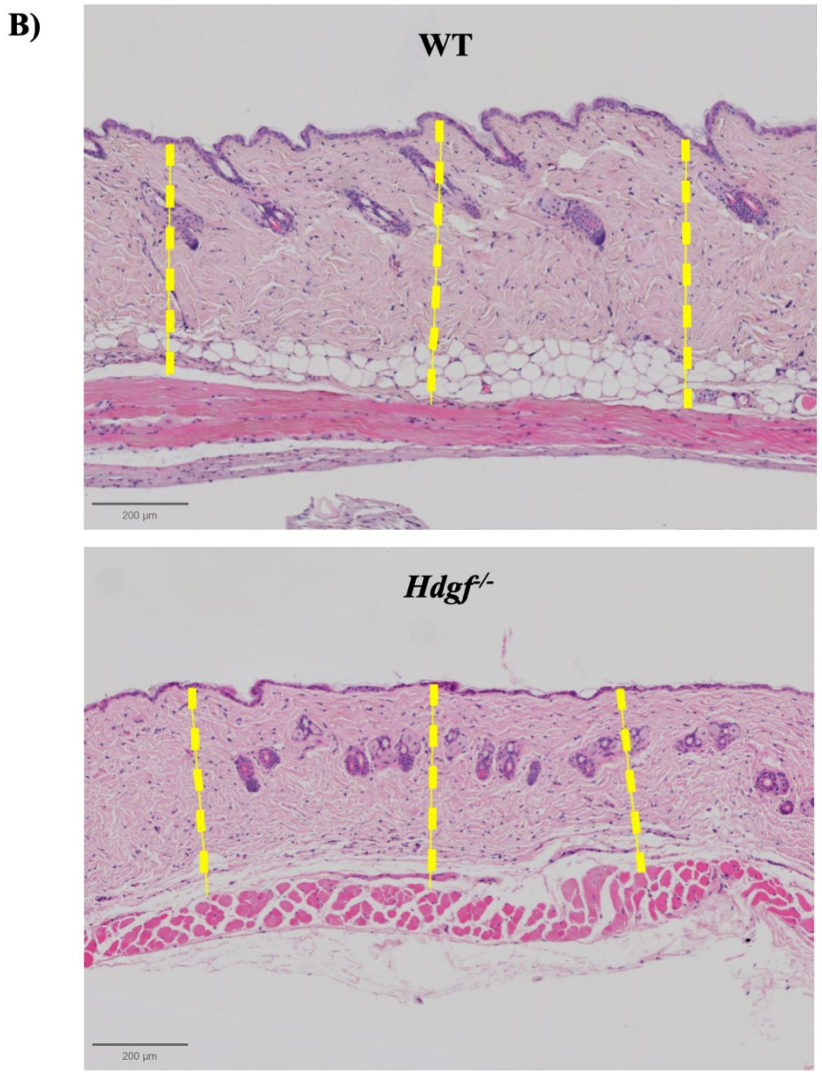

Figure 5.7. Comparison of unwounded 15-week-old male WT and *Hdgf*$^{-/-}$ animals revealed a trend towards thinner epidermis and dermis in *Hdgf*$^{-/-}$. A) Representative images of epidermal thickness measurements: green lines label epidermal thickness, H&E staining, 10X magnification, scale bar = 50 µm. Statistical comparison of epidermal thickness of WT and *Hdgf*$^{-/-}$ mice, each dot represents a mouse, mean ± SD, n = 3 in each genotype. Unpaired two-tailed t-test

with Mann-Whitney correction, ns - not significant. B) Representative images of dermal thickness measurements: yellow dotted lines label dermal thickness, H&E staining, 10X magnification, scale bar = 200 μm. Statistical comparison of dermal thickness of WT and *Hdgf*$^{-/-}$ animals, each dot represents a mouse, mean ± SD, n = 3 in each genotype. Unpaired two-tailed t-test with Mann-Whitney correction, ns - not significant.

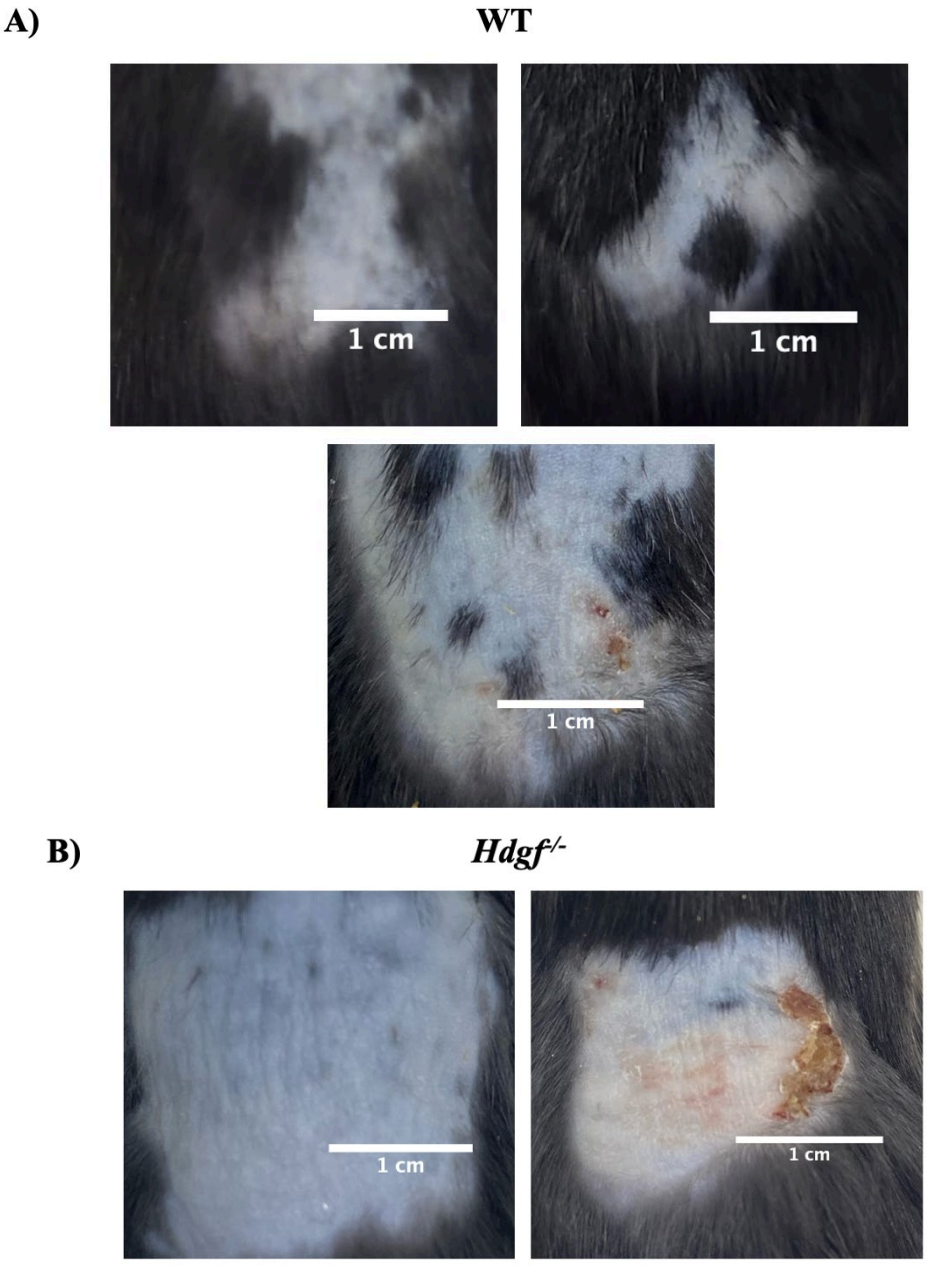

Figure 5.8. Trimming and shaving cream experiment in 15-week-old male WT and *Hdgf*$^{-/-}$ animals. A) WT mice day 7 post-trimming and shaving cream application, each picture is an individual mouse, n = 3, scale bar = 1cm. B) *Hdgf*$^{-/-}$ mice day 7 post-trimming and shaving cream application, each picture is an individual mouse, n = 2, scale bar = 1cm.

5.4. Discussion

This chapter provides the first *in vivo* characterisation of injury responses in *Hdgf*$^{-/-}$ animals. The standard OA induction model - PMX surgery - carried out in 10-week-old skeletally mature animals did not show any statistically significant differences between the genotypes, although there was a trend towards increased disease in *Hdgf*$^{-/-}$ animals. I also examined injury responses in the skin, which had previously been used to demonstrate reduced healing in FGF2 knockout animals, as well as other PCM-bound growth factors.[152 156] I was able to show for the first time that *Hdgf*$^{-/-}$ male animals demonstrated an age-dependent skin wound healing delay, which was only apparent from 15 weeks of age. This prompted us to set up the PMX surgeries in older animals (15-week-old), the results of which are awaited. HDGF-dependent delayed skin healing was age-dependent, but it is worth remembering that a 15-week-old mouse is considered a young adult, whereas 24-month-old mice are classically used for studying age-associated pathologies.[266] Thus, it may be that the HDGF-dependent skin healing delay is not necessarily associated with ageing, but rather with reaching full skeletal maturity. It is known that skin healing in mice is delayed with age, but most of those studies were conducted in animals older than 20 months. For instance, one study found skin healing delay in 20-months-old compared to 2-months-old C57BL/6 mice due to neutrophil depletion.[267] Another study examined ear wounding in "middle-aged" 40-week-old compared to 8-week-old C57BL/6 mice. It found that re-epithelialization, chondrogenesis, myogenesis, and collagen deposition were delayed in 40-week-old mice.[268] Therefore, the identified delay in *Hdgf*$^{-/-}$ cannot, strictly speaking, be called a phenotype of ageing. Furthermore, in *Hdgf*$^{-/-}$ mice there was not much difference between skin healing in 15- and 26-week-old male mice,

suggesting that the HDGF-mediated effect might not be getting progressively worse with age, but is rather constant once animals reach skeletal maturity. To test this hypothesis, one would need to carry out histological analysis of wounds of 15- and 26-week-old animals and see if similar features of skin healing (e.g. delayed re-epithelialization and dermal remodelling) are present in both to a similar level.

Though I was unable to produce statistically robust results for all of the measured metrics, the histological examination of the wounds performed so far has given us some clues about the potential mechanism. Although delayed re-epithelialization observed in *Hdgf*$^{-/-}$ mice over the first 10 days following full-thickness wounding needs to be validated in a larger sample size, it might point to a specific function of HDGF. For instance, re-epithelialization of wounds can be affected by various factors such as excessive inflammation, bacterial infections, or tissue hypoxia. The fact that *Hdgf*$^{-/-}$ mice developed more scabbing and more visible skin irritation (dermatitis-like features) upon wounding might indicate that these mice have a more inflammatory response to injury. One of the conditions known in dermatology is the Koebner phenomenon, which was originally used to describe formation of psoriasiform lesions on uninvolved skin of psoriatic patients in response to trauma and later was extended to include formation of such lesions in response to injury in various other diseases, including vitiligo, Lichen planus, and warts.[269] Although the exact biology behind Koebner phenomenon is not known, its triggers include trauma, mechanical stress, chemical stimulation, and infections. In various skin conditions, Koebner phenomenon development is linked to several processes such as enhanced inflammatory infiltration, increased keratinocyte proliferation, and mechano-transduction-related properties (e.g. tissues with stronger mechanical tension, increased stretching, activation of mechano-sensitive

pathways such as Wnt and Notch).[270] To test whether *Hdgf*$^{-/-}$ mice might have a Koebner phenomenon-like response to trauma, I observed their response to superficial skin trauma. For this, I performed a "trimming and cream" experiment where I trimmed back hair of mice and applied shaving cream in order to see if this type of superficial trauma was enough to trigger the scabbing and redness I observed in *Hdgf*$^{-/-}$ mice after wounding. Due to sample size limitations, it was difficult to make any conclusions, as one out of two *Hdgf*$^{-/-}$ and one out of three WT (albeit mild in the WT animal) mice developed dermatitis-like features. Increasing sample size for this type of experiment is essential to understand whether *Hdgf*$^{-/-}$ mice are more sensitive to trauma per se and might help explain the Koebner-like response to wounding in these mice.

Koebner phenomenon can lead to increased keratinocyte proliferation and keratinocyte hyperplasia. The initial step of wound healing is activation of keratinocytes into proliferative and migrating cells that make their way to the wound centre, leading to wound re-epithelialization. Reverting these activated keratinocytes back to the basal phenotype aids completing the cycle of re-epithelialization.[271] In psoriasis, downregulation of the N-methyl-D-aspartic acid receptor 2C subunit (NMDA-R2C) makes keratinocytes insensitive to TNFα, which normally inhibits migration and proliferation, leading to continued proliferation and hyperplasia.[272] Thus, I wanted to see if *Hdgf*$^{-/-}$ mice were more susceptible to keratinocyte hyperplasia post-wounding. For this, I calculated epidermal index, defined as the ratio between thicknesses of newly formed epidermis and unwounded epidermis. I saw no difference in epidermal index between WT and *Hdgf*$^{-/-}$ mice on days 7 and 10 post-wounding, potentially suggesting that epidermal hyperplasia is not associated with the dermatitis-like

response and decreased healing. The trend towards delayed re-epithelialization observed in *Hdgf*$^{-/-}$ mice over 10 days post-wounding might be pointing to delayed keratinocyte migration or dermal contraction in *Hdgf*$^{-/-}$. These will need to be investigated separately. To explore further the question of epidermal hyperplasia, I measured epidermal thickness in unwounded 15-week-old WT and *Hdgf*$^{-/-}$ mice. Although not statistically significant, *Hdgf*$^{-/-}$ mice showed a trend towards thinner epidermis at the baseline (no injury) compared to the WT.

There was also a trend towards lower dermal thickness in the *Hdgf*$^{-/-}$ mice. It is important to note that the way these measurements were performed has significant technical limitations, as I took six measurements per mouse in random locations within each skin section. To obtain more robust results, it would be better to perform image segmentation analysis that would provide a readout of epidermal and dermal thickness across the whole section. The significance of a trend towards thinner skin thickness in *Hdgf*$^{-/-}$ mice is not clear, but another study that identified thinner epidermal and dermal thickness (in embryos of *Runx2*-deficient mice) found these to be associated with less proliferation and impaired hair follicle development.[273] It is critical to mention that measuring skin thickness in isolated sections was shown to be a potentially unreliable metric due to skin elasticity and potential shrinkage during sectioning.[274] Thus, a more reliable way to measure skin thickness has been suggested by pinning excised fragments to original size on a template before fixing the tissue or measuring it without detaching it from the body (e.g. whole embryo sections in murine development studies).[273 274]

Finally, increased granulation tissue (GT) at day 7 post-wounding in 15-week-old *Hdgf*$^{-/-}$ mice suggested potential involvement of HDGF in dermal remodelling. GT covers the wound and provides scaffolding for new tissue

deposition. Initially filled with macrophages, endothelial cells, and fibroblasts, it undergoes remodelling and provides space for newly formed fibroblasts, collagen, matrix deposition, and angiogenesis. In final stages, myofibroblasts from the edges of the wound cause matrix and collagen retraction that reduces GT area and new collagen fibres are deposited in the area previously occupied by GT.[275] Staining with Masson's trichrome reflected the degree of collagen fibre maturation, thus, the measurement of GT width reflected the degree of dermal remodelling, which is one of the final stages of wound healing. As described in the introduction, murine wounds are mainly healed through contraction of panniculus carnosus muscle and myofibroblast activity, whereas human wounds are healed through GT formation.[275] Thus, although the metric used in this study was GT width, it could be that GT width reflected the degree of dermal contraction rather than the GT contribution to healing. To test this, one could consider staining for myofibroblast markers.

For the skin wounding results to be more translatable to clinic, one can consider changing the skin wounding protocol to mimic human skin healing. An established procedure for creating "human-like" wound healing in mice is via creating an excisional wound (usually over 2 cm^2) that is too large to close by contraction and assessing the degree of both wound closure and regeneration (defined by the formation of new hair follicles).[276]

Lastly, the discovered skin healing delay was validated in male mice only. I have since completed a skin wounding experiment in 15-week-old female mice that has shown no difference in percent wound area closure. Histological confirmation of these findings is awaited. Sex differences in murine wound closure have been reported before and are strain dependent.[262 277 278] Thus, it would be interesting to

learn whether there is a different molecular response to injury in female *Hdgf*$^{-/-}$ mice.

Taken together, this chapter showed for the first time the presence of delayed skin healing phenotype in *Hdgf*$^{-/-}$ male mice that is only evident post skeletal maturity. Potential suggested mechanisms behind this delay could be delayed re-epithelialization and dermal remodelling. We have recently carried out a pilot spatial transcriptomics characterisation on wounded and unwounded skin of 15-week-old WT and *Hdgf*$^{-/-}$ males. This will uncover gene expression differences in the context of skin architecture that might help with understanding the mechanism behind skin healing delay in *Hdgf*$^{-/-}$ animals.

6. Discussion

In this work, I set out to investigate three major questions relating to the role of HDGF in tissue injury and repair: 1) characterisation of HDGF release and biological activity *in vitro*, 2) molecular changes in the *Hdgf*$^{-/-}$ tissues, and 3) the role of HDGF in injury *in vivo*. I was able to answer each of these questions to some extent and will summarise my major findings and comment on the wider implications below.

I demonstrated that HDGF is released immediately following cartilage injury from explanted porcine and murine wild-type (WT) cartilage, confirming results previously published by our group.[99] In addition, I showed that it is released from another connective tissue - the skin - following injury of WT mice, which has not been described before. I have successfully validated the *Hdgf*$^{-/-}$ mice by showing the lack of HDGF protein release (by western blot) from their cartilage and skin following injury. This is the description of HDGF's release in response to injury across multiple tissues. I then attempted to study the role of HDGF in chondrocyte injury response using *in vitro* gap and low-density assays. The gap assay measures 2D migration and allows to examine de-differentiation, migration, and, to some extent, proliferation. To fully characterise chondrocyte response to injury *in vitro*, a 3D invasion assay with a Boyden chamber-like design would be a more suitable system to assess chemotaxis, invasion, and matrix remodelling properties of de-differentiated cells. I found that depleting injury CM of all heparin-binding factors, including HDGF, did not elicit an injury-associated phenotype change of chondrocytes in the gap assay. I then attempted to apply exogenous HDGF to isolated chondrocytes, but did not see any response, which could be because the commercially available HDGF was a plant derivative and did not have the post-

translational modifications necessary to be biologically active in mammalian cells. I performed an experimental trial with other PCM-derived growth factors – FGF2 and MDK – in an attempt to test whether these specific factors alone or in combination could elicit the change of chondrocytes into elongated fibroblast-like cells. In hindsight, that experiment could have benefitted from addition of other PCM-derived recombinant growth factors, such as CTGF and TGFβ. At the time, I did not pursue further *in vitro* assays with recombinant growth factors because they could not answer what the role of HDGF was specifically, so I moved to *in vivo* work on *Hdgf*$^{-/-}$ mice. I could have integrated *in vivo* and *in vitro* parts better by generating injury CM not only from hips, but also from the skin of WT and *Hdgf*$^{-/-}$ animals and applied it onto the gap assay. However, I started looking into skin injury CM only after I had discovered a wound healing delay in *Hdgf*$^{-/-}$ animals, so I did not have time to go back to *in vitro* experimentation at that point. Although I did not decipher the role of HDGF in this part of my work, one important outcome of my *in vitro* experiments is the establishment of gap- and low-density assays for chondrocytes that, to my knowledge, were not done widely in chondrocytes before. Now, these *in vitro* assays can be used by others to study various aspects of chondrocyte biology.

Molecular characterisation of WT and *Hdgf*$^{-/-}$ cartilage before and after injury revealed a similar transcriptional response to injury (at 4 hours). Five genes were differentially expressed between genotypes and across tissues (cartilage and skin) at baseline. These included *Hdgf* itself, three ribosomal subunit genes (*Rps3a1*, *Rps3a2*, *Rps3a3)*, and *Hprt1*. As mentioned earlier, I expected to see a bigger log-fold change for the *Hdgf* gene in knock-out tissues. Current data suggested knock-out efficiency of 81.3% in cartilage and 91.3% in skin. While low

RIN numbers can affect DESeq2 results, cartilage samples had high RIN numbers ranging from 6.9 to 8.9 that fall around the recommended "good" quality RIN of 7 (Supplementary Table 1). It is important to acknowledge that skin samples had lower RIN numbers (4.2-6.1) that is less than a generally accepted "good" RIN value (Supplementary Table 1). However, Novogene's WOBI workflow uses 150 base pair paired-end reads, which are more tolerant of fragmented RNA, with evidence from Novogene that gene expression remains reliable for RNAs with RIN numbers down to 4. Since only part of the *Hdgf* gene was deleted in the knock-out construct, it is possible that exon 1 is still being picked up during sequencing as part of 150 base pair reads, especially because exon 1 is one of the longest exons of the *Hdgf* gene (Figure 1.5).[166] Ordering an exon-level analysis from Novogene would provide a definitive answer to this question. In the meantime, a quantitative PCR with primers spanning exon 1 and another region of the *Hdgf* gene can provide a quick validation of the knock-out and can be done in the future.

Transcriptional analysis of "difference of differences" of cartilage response to injury identified an interesting potential compensatory mechanism in *Hdgf*$^{-/-}$ tissues. Many mitochondrial genes upregulated upon injury in WT cartilage and downregulated in *Hdgf*$^{-/-}$ were potentially compensated for by the upregulation of cell signalling and differentiation-related genes. This suggests a potential role of HDGF in mitochondrial metabolism during stress response and illustrates a possible functional adaptation of *Hdgf*$^{-/-}$ tissues to this loss by upregulating other stress-mediating pathways. SILAC labelled proteomic analysis of the skin, which was prompted by differential regulation of ribosomal subunit genes, showed a global decrease in protein synthesis in *Hdgf*$^{-/-}$ mice following injury. It also showed a

specific reduction in the synthesis of many ribosomal proteins, further suggesting a role of HDGF in protein translation.

In vivo skin injury demonstrated an age-dependent delay in wound healing in *Hdgf*$^{-/-}$ mice that was apparent from 15 weeks of age, but not at 10 weeks of age. This may reflect skeletal maturity rather than age per se as the wound phenotype did not worsen with age. This may be why in 10-week-old *Hdgf*$^{-/-}$ mice there was no OA phenotype after joint destabilisation. Bringing these findings together with transcriptional and proteomic analyses, it is possible to hypothesise that the observed wound healing delay demonstrates impaired ability of *Hdgf*$^{-/-}$ tissues to respond to stress due to downregulation of mitochondrial-related genes and insufficiency of functional adaptive response to fully compensate for this loss (as suggested by the "difference of differences" transcriptional analysis of the cartilage). Additionally, global decrease in translation can be one of the determinants of delayed wound healing in *Hdgf*$^{-/-}$ tissues. To test this hypothesis *in vivo*, one could apply rapamycin (or direct ribosome inhibitors like cycloheximide) to the skin of WT mice to suppress translation and see if that results in wound healing patterns similar to those observed in *Hdgf*$^{-/-}$ animals. Another set of experiments could involve utilising quantitative PCR, immunostaining, and western blots to probe for specific translation-related genes and proteins identified by RNA-seq and proteomic analysis. This type of analysis can be performed in different age groups (10-, 15- and 26-week-old animals) and will give quantifiable results of temporal expressions patterns that may be important for understanding the mechanisms of tissue healing delay. Further examination of specific genes and proteins known to be relevant for wound healing, senescence, and proliferation can yield insights into how HDGF knock-out affects tissue injury response. One could

also try to increase translational efficiency in *Hdgf*$^{-/-}$ animals (e.g. by activating mTORC1 signalling, enhancing rRNA and ribosomal protein synthesis) and examine whether that would improve wound healing. It is important to note that tissue injury response can vary depending on tissue type, therefore, it is possible that the effect of HDGF in injury response can be slightly different in skin versus cartilage. While an excisional wound in the skin, similar to a wound in the cartilage, activates local repair cells, injury response depends on the tissue environment. The skin is a vascular tissue and has the ability to mount a strong immune and inflammatory response to injury. In the cartilage, the likely mechanism of injury response is through the "reprogramming" of chondrocytes in the vicinity of the wound that gain the ability to migrate and proliferate to restore the tissue. These differences might mean that the effect of HDGF on injury response might be tissue specific. Pathway analysis of RNA from cartilage and skin would support this hypothesis, as there was not much overlap between significantly enriched pathways in cartilage and skin, suggesting that the effect of HDGF might be through regulating how specific cell types respond to their environment, rather than affecting any specific pathway. Ongoing PMX studies in 15-week-old animals will reveal whether cartilage injury leads to more severe cartilage degradation in *Hdgf*$^{-/-}$ animals compared to WT.

The demonstration that HDGF is released upon injury from multiple tissues suggests that it may be a general mechanism for sensing injury and triggering a repair response throughout the body. This finding could support the classification of HDGF as an alarmin that had been suggested earlier.[279] Alarmins are soluble factors that are released from injured tissues or cells to alert neighbouring cells to activate an injury response. This can include recruitment and activation of immune

cells of the adaptive and innate systems, as well as repair cells.[279] It is not clear whether HDGF has a direct influence on immune-mediated tissue injury responses. In the skin, inflammatory pathways were differentially expressed (higher) in *Hdgf*$^{-/-}$ compared with WT mice and dermatitis-like features appeared to be more common in *Hdgf*$^{-/-}$ mice following injury, although I was underpowered to test this formally. To investigate this further I would have liked to examine the circulating immune profile of *Hdgf*$^{-/-}$ and WT animals, both at baseline and after a challenge e.g. trauma, infection. There are no known described clinical mutations in *HDGF*.

I have identified a potential role for HDGF as a regulator of protein translation through ribosomal protein synthesis. Some ribosomal proteins, such as rpS6, have been shown to play important roles in skin wound healing. An mTOR mediated phosphorylation of rpS6 occurred following stimulation with cell injury medium, presumed to contain danger-associated molecular patterns (DAMPs) (or alarmins). Mice lacking rpS6 showed an initial acceleration of wound closure but later excessive fibrosis and reduced angiogenesis.[280]

Chronic wound repair and osteoarthritis are two of the most common age-related diseases for which very limited treatments are available. Our group has previously shown that newly synthesised HDGF is reduced in articular cartilage in 45-week-old mice compared with 10-week-old animals. This was also true for other growth factors suggesting that the bioavailability of growth factors in connective tissues changes with age and this may contribute to the repair response in patients.[281] Growth factors in cartilage are bound to the heparan sulfate proteoglycan, perlecan, in the pericellular matrix of chondrocytes.[99] In skin, the extracellular store for HDGF is unknown, although, the basement membrane is rich in perlecan and could be the location. My attempts at immunohistochemistry of the

skin were unfortunately unsuccessful. It is tempting to speculate that breaching the basement membrane at the time of injury may release HDGF locally where it could contribute to activation of keratinocytes to promote their migration. This region is also adjacent to crypts containing stem cells. In cartilage, our group has now established that the growth factors act together in an orchestrated fashion to activate chondroprogenitors of cartilage. Each of the growth factors is likely to have a different role in this process, from "dedifferentiation" to migration, proliferation and "redifferentiation".[102] Further studies are ongoing to try to discern what HDGF is doing in this assay. Renewed attempts to make injury conditioned medium from WT and *Hdgf*$^{-/-}$ cartilage and or/skin will be tried.

All of our tissues come under mechanical stress either through repeated low-grade stress or due to trauma. The question of whether HDGF is also important after bone fracture, in chronic lung disease, or renal fibrosis is unexplored. Additional planned experiments will include spatial transcriptomics of WT and *Hdgf*$^{-/-}$ wounded and unwounded skin. These experiments may help to establish the cells that are making *Hdgf* in the tissue and what else is regulated in them. It may also show more specific gene regulation that is genotype- and injury-dependent albeit in a subset of cells.

To conclude, the main novel outcomes of this work include the establishment of gap- and low-density assays for chondrocyte *in vitro* culture, demonstration of HDGF's release upon injury from multiple connective tissues (skin and cartilage), suggestion of the role of HDGF in regulating protein translation, and discovery of a delayed wound healing response in *Hdgf*$^{-/-}$ skin. Further *in vivo* work on cartilage injury will reveal whether HDGF's effect on tissue healing is similar in cartilage. Both skin and cartilage injury *in vivo* assays need to

be carried out in female mice to determine whether the observed effect is sex dependent. Secondary validation of transcriptomics and proteomics results by quantitative PCR and western blot would yield quantifiable data to supplement bioinformatic analysis. Further *in vitro* experiments in the gap- and low-density assays with injury CM generated from the skin of WT and *Hdgf*$^{-/-}$ animals can be performed to attempt to decipher a specific role of HDGF in injury-associated chondrocyte phenotype change. If these experiments support the role of HDGF as an important mediator of injury response, further work can focus on purifying it from injury CM and obtaining a biologically active recombinant protein that can be trialled as a therapy for enhancing wound healing or cartilage repair.

7. Bibliography

1. Krafts KP. Tissue repair: The hidden drama. *Organogenesis* 2010;6(4):225-33. doi: 10.4161/org.6.4.12555
2. Eming SA, Martin P, Tomic-Canic M. Wound repair and regeneration: mechanisms, signaling, and translation. *Sci Transl Med* 2014;6(265):265sr6. doi: 10.1126/scitranslmed.3009337
3. Padgett DA, Marucha PT, Sheridan JF. CHAPTER 39 - Stress and Wound Healing: Animal Models. In: Ader R, ed. Psychoneuroimmunology (Fourth Edition). Burlington: Academic Press 2007:837-50.
4. Tumbar T, Guasch G, Greco V, et al. Defining the epithelial stem cell niche in skin. *Science* 2004;303(5656):359-63.
5. Losner J, Courtemanche K, Whited JL. A cross-species analysis of systemic mediators of repair and complex tissue regeneration. *npj Regenerative Medicine* 2021;6(1):21. doi: 10.1038/s41536-021-00130-6
6. Anitua E, Andia I, Ardanza B, et al. Autologous platelets as a source of proteins for healing and tissue regeneration. *Thrombosis and haemostasis* 2004;91(01):4-15.
7. Gillitzer R, Goebeler M. Chemokines in cutaneous wound healing. *Journal of leukocyte biology* 2001;69(4):513-21.
8. Croce MA, Dyne K, Boraldi F, et al. Hyaluronan affects protein and collagen synthesis by in vitro human skin fibroblasts. *Tissue and Cell* 2001;33(4):326-31.
9. Metz C. Fibrocytes: a unique cell population implicated in wound healing. *Cellular and Molecular Life Sciences CMLS* 2003;60(7):1342-50.
10. Carlson MA, Longaker MT. The fibroblast-populated collagen matrix as a model of wound healing: a review of the evidence. *Wound repair and regeneration* 2004;12(2):134-47.
11. Raghow R. The role of extracellular matrix in postinflammatory wound healing and fibrosis. *The FASEB journal* 1994;8(11):823-31.
12. Diegelmann RF, Evans MC. Wound healing: an overview of acute, fibrotic and delayed healing. *Front biosci* 2004;9(1):283-89.
13. Vos T, Lim SS, Abbafati C, et al. Global burden of 369 diseases and injuries in 204 countries and territories, 1990–2019: a systematic analysis for the Global Burden of Disease Study 2019. *The Lancet* 2020;396(10258):1204-22.
14. Steinmetz JD, Culbreth GT, Haile LM, et al. Global, regional, and national burden of osteoarthritis, 1990–2020 and projections to 2050: a systematic analysis for the Global Burden of Disease Study 2021. *The Lancet Rheumatology* 2023;5(9):e508-e22. doi: 10.1016/S2665-9913(23)00163-7
15. ARPA-H. ARPA-H launches program to help joints heal themselves. Biden Harris Administration's ARPA-H initiative launches new program to help joints heal themselves: Advanced Research Projects Agency for Health, 2023.
16. Ma W, Chen H, Yuan Q, et al. Global, regional, and national epidemiology of osteoarthritis in working-age individuals: insights from the global burden of disease study 1990-2021. *Sci Rep* 2025;15(1):7907. doi: 10.1038/s41598-025-91783-6 [published Online First: 20250306]

17. Kim EH, Jeon S, Park J, et al. Progressing future osteoarthritis treatment toward precision medicine: integrating regenerative medicine, gene therapy and circadian biology. *Exp Mol Med* 2025;57(6):1133-42. doi: 10.1038/s12276-025-01481-6 [published Online First: 20250630]
18. Vincent T, Hermansson M, Bolton M, et al. Basic FGF mediates an immediate response of articular cartilage to mechanical injury. *Proc Natl Acad Sci U S A* 2002;99(12):8259-64. doi: 10.1073/pnas.122033199 [published Online First: 2002/05/30]
19. Vincent TL. Mechanoflammation in osteoarthritis pathogenesis. *Semin Arthritis Rheum* 2019;49(3s):S36-s38. doi: 10.1016/j.semarthrit.2019.09.018
20. Sen CK. Human Wound and Its Burden: Updated 2025 Compendium of Estimates. *Adv Wound Care (New Rochelle)* 2025 doi: 10.1177/21621918251359554 [published Online First: 20250714]
21. Finnerty CC, Jeschke MG, Branski LK, et al. Hypertrophic scarring: the greatest unmet challenge after burn injury. *The Lancet* 2016;388(10052):1427-36.
22. desJardins-Park HE, Gurtner GC, Wan DC, Longaker MT. From Chronic Wounds to Scarring: The Growing Health Care Burden of Under- and Over-Healing Wounds. *Adv Wound Care (New Rochelle)* 2022;11(9):496-510. doi: 10.1089/wound.2021.0039 [published Online First: 20211115]
23. Chang LR, Marston G, Martin A. Anatomy, Cartilage. StatPearls. Treasure Island (FL): StatPearls Publishing

24. Sophia Fox AJ, Bedi A, Rodeo SA. The basic science of articular cartilage: structure, composition, and function. *Sports Health* 2009;1(6):461-8. doi: 10.1177/1941738109350438 [published Online First: 2009/11/01]
25. Vincent TL, McLean CJ, Full LE, et al. FGF-2 is bound to perlecan in the pericellular matrix of articular cartilage, where it acts as a chondrocyte mechanotransducer. *Osteoarthritis Cartilage* 2007;15(7):752-63. doi: 10.1016/j.joca.2007.01.021 [published Online First: 2007/03/21]
26. Di Matteo A, Bathon JM, Emery P. Rheumatoid arthritis. *The Lancet* 2023;402(10416):2019-33. doi: 10.1016/S0140-6736(23)01525-8
27. Gregersen PA, Savarirayan R. Type II collagen disorders overview. 2019
28. Konarski W, Poboży T, Konarska K, et al. Understanding Osteochondritis Dissecans: A Narrative Review of the Disease Commonly Affecting Children and Adolescents. *Children (Basel)* 2024;11(4) doi: 10.3390/children11040498 [published Online First: 20240422]
29. Mertz P, Costedoat-Chalumeau N, Ferrada MA, et al. Relapsing polychondritis: clinical updates and new differential diagnoses. *Nature Reviews Rheumatology* 2024;20(6):347-60. doi: 10.1038/s41584-024-01113-9
30. Kim SY, Afroz S, Gillespie H, Downey C. A Narrative Review of Chondrocalcinosis: Clinical Presentation, Diagnosis, and Therapies. *Cureus* 2024;16(5):e60434. doi: 10.7759/cureus.60434 [published Online First: 20240516]
31. Gomez-Pena S, Rueda de Eusebio Á, Arrazola García J, et al. Update of cartilaginous tumours according to the WHO classification 2020. *Radiología (English Edition)* 2024;66(1):57-69. doi: https://doi.org/10.1016/j.rxeng.2023.05.006
32. Vincent TL, Wann AKT. Mechanoadaptation: articular cartilage through thick and thin. *The Journal of Physiology* 2019;597(5):1271-81. doi: https://doi.org/10.1113/JP275451

33. Hunter W. VI. Of the structure and diseases of articu-lating cartilages. *Philosophical Transactions of the Royal Society of London* 1743;42(470):514-21. doi: doi:10.1098/rstl.1742.0079
34. Redfern. Observations on the Development and Nutrition of Bone and Cartilage, and on the Relations of Connective Tissues to each other in Health and Disease. *J Anat Physiol* 1897;32(Pt 1):96-108. [published Online First: 1897/10/01]
35. Haas S. Regeneration of cartilage and bone with a special study of these processes as they occur at the chondrocostal junction. *Surg Gynecol Obstet* 1914;19(604):17.
36. Shands A. The regeneration of hyaline cartilage in joints: an experimental study. *Archives of Surgery* 1931;22(1):137-78.
37. Bennett GA, Bauer W, Maddock SJ. A Study of the Repair of Articular Cartilage and the Reaction of Normal Joints of Adult Dogs to Surgically Created Defects of Articular Cartilage,"Joint Mice" and Patellar Displacement. *Am J Pathol* 1932;8(5):499-524.21. [published Online First: 1932/09/01]
38. Buckwalter JA, Mankin HJ. Instructional Course Lectures, The American Academy of Orthopaedic Surgeons - Articular Cartilage. Part II: Degeneration and Osteoarthrosis, Repair, Regeneration, and Transplantation*†. *JBJS* 1997;79(4)
39. Dowthwaite GP, Bishop JC, Redman SN, et al. The surface of articular cartilage contains a progenitor cell population. *Journal of cell science* 2004;117(6):889-97.
40. Mankin HJ. Localization of Tritiated Thymidine in Articular Cartilage of Rabbits: I. Growth In Immature Cartilage. *JBJS* 1962;44(4)
41. Mankin HJ. Localization of tritiated thymidine in articular cartilage of rabbits: II. Repair in immature cartilage. *JBJS* 1962;44(4):688-98.
42. Calandruccio RA, Gilmer WS. Proliferation, regeneration, and repair of articular cartilage of immature animals. *JBJS* 1962;44(3):431-55.
43. Meachim G. The effect of scarification on articular cartilage in the rabbit. *The Journal of Bone & Joint Surgery British Volume* 1963;45(1):150-61.
44. DePalma AF, McKeever CD, Subin DK. Process of repair of articular cartilage demonstrated by histology and autoradiography with tritiated thymidine. *Clinical orthopaedics and related research* 1966;48:229-42. doi: doi:
45. Kim HK, Moran ME, Salter RB. The potential for regeneration of articular cartilage in defects created by chondral shaving and subchondral abrasion. An experimental investigation in rabbits. *JBJS* 1991;73(9)
46. Bos PK, Kops N, Verhaar JAN, van Osch GJVM. Cellular origin of neocartilage formed at wound edges of articular cartilage in a tissue culture experiment. *Osteoarthritis and cartilage* 2008;16(2):204-11. doi: doi:
47. Cheung HS, Cottrell WH, Stephenson K, Nimni ME. In vitro collagen biosynthesis in healing and normal rabbit articular cartilage. *JBJS* 1978;60(8)
48. Ghadially FN, Thomas I, Oryschak AF, Lalonde JM. Long-term results of superficial defects in articular cartilage: a scanning electron-microscope study. *J Pathol* 1977;121(4):213-7. doi: 10.1002/path.1711210404 [published Online First: 1977/04/01]
49. Thompson Jr RC. An experimental study of surface injury to articular cartilage and enzyme responses within the joint. *CLINORTHOP* 1975:239-48. doi: doi:https://dx.doi.org/10.1097/00003086-197503000-00028

50. Frost GE. Cartilage healing and regeneration. *Journal of the South African Veterinary Association* 1979;50(3):181-7. doi: doi:
51. Namba RS, Meuli M, Sullivan KM, et al. Spontaneous repair of superficial defects in articular cartilage in a fetal lamb model. *The Journal of bone and joint surgery American volume* 1998;80(1):4-10. doi: doi:
52. Tew S, Redman S, Kwan A, et al. Differences in repair responses between immature and mature cartilage. *Clinical Orthopaedics and Related Research* 2001;391:S142-S52. doi: doi:http://dx.doi.org/10.1097/00003086-200110001-00014
53. Tew SR, Kwan AP, Hann A, et al. The reactions of articular cartilage to experimental wounding: role of apoptosis. *Arthritis and rheumatism* 2000;43(1):215-25. doi: doi:
54. Wei X, Gao J, Messner K. Maturation-dependent repair of untreated osteochondral defects in the rabbit knee joint. *Journal of biomedical materials research* 1997;34(1):63-72. doi: doi:
55. Wagner W, Reichl J, Wehrmann M, Zenner HP. Neonatal rat cartilage has the capacity for tissue regeneration. *Wound Repair Regen* 2001;9(6):531-6. doi: 10.1046/j.1524-475x.2001.00531.x [published Online First: 2002/03/19]
56. Cheung HS, Lynch KL, Johnson RP, Brewer BJ. In vitro synthesis of tissue-specific type II collagen by healing cartilage: I. Short-term repair of cartilage by mature rabbits. *Arthritis and Rheumatism* 1980;23(2):211-19. doi: doi:https://dx.doi.org/10.1002/art.1780230212
57. Hanie EA, Sullins KE, Powers BE, Nelson PR. Healing of full-thickness cartilage compared with full-thickness cartilage and subchondral bone defects in the equine third carpal bone. *Equine veterinary journal* 1992;24(5):382-6. doi: doi:
58. Chen H, Chevrier A, Hoemann CD, et al. Characterization of subchondral bone repair for marrow-stimulated chondral defects and its relationship to articular cartilage resurfacing. *The American journal of sports medicine* 2011;39(8):1731-40. doi: doi:https://dx.doi.org/10.1177/0363546511403282
59. Anraku Y, Mizuta H, Sei A, et al. Analyses of early events during chondrogenic repair in rat full-thickness articular cartilage defects. *Journal of bone and mineral metabolism* 2009;27(3):272-86. doi: doi:https://dx.doi.org/10.1007/s00774-009-0038-x
60. Müller B, Kohn D. [Indication for and performance of articular cartilage drilling using the Pridie method]. *Orthopade* 1999;28(1):4-10. doi: 10.1007/s001320050315
61. Milgram JW. Injury to articular cartilage joint surfaces. I. Chondral injury produced by patellar shaving: a histopathologic study of human tissue specimens. *Clinical orthopaedics and related research* 1985(192):168-73. doi: doi:
62. Kaul G, Cucchiarini M, Remberger K, et al. Failed cartilage repair for early osteoarthritis defects: a biochemical, histological and immunohistochemical analysis of the repair tissue after treatment with marrow-stimulation techniques. *Knee surgery, sports traumatology, arthroscopy : official journal of the ESSKA* 2012;20(11):2315-24. doi: doi:https://dx.doi.org/10.1007/s00167-011-1853-x
63. Meachim G, Roberts C. Repair of the joint surface from subarticular tissue in the rabbit knee. *Journal of anatomy* 1971;109(Pt 2):317.

64. Baker B, Spadaro J, Marino A, Becker RO. Electrical stimulation of articular cartilage regeneration. *Annals of the New York Academy of Sciences* 1974;238:491-9. doi: doi:
65. Mitchell N, Shepard N. The resurfacing of adult rabbit articular cartilage by multiple perforations through the subchondral bone. *The Journal of bone and joint surgery American volume* 1976;58(2):230-3. doi: doi:
66. Shapiro F, Koide S, Glimcher MJ. Cell origin and differentiation in the repair of full-thickness defects of articular cartilage. *The Journal of bone and joint surgery American volume* 1993;75(4):532-53. doi: doi:
67. Dell'accio F, Vincent TL. Joint surface defects: clinical course and cellular response in spontaneous and experimental lesions. *Eur Cell Mater* 2010;20:210-7. doi: 10.22203/ecm.v020a17 [published Online First: 20100928]
68. Dowthwaite GP, Bishop JC, Redman SN, et al. The surface of articular cartilage contains a progenitor cell population. *Journal of Cell Science* 2004;117(6):889-97. doi: 10.1242/jcs.00912
69. Koelling S, Kruegel J, Irmer M, et al. Migratory Chondrogenic Progenitor Cells from Repair Tissue during the Later Stages of Human Osteoarthritis. *Cell Stem Cell* 2009;4(4):324-35. doi: 10.1016/j.stem.2009.01.015
70. Khan IM, Williams R, Archer CW. One Flew over the Progenitor's Nest: Migratory Cells Find a Home in Osteoarthritic Cartilage. *Cell Stem Cell* 2009;4(4):282-84. doi: https://doi.org/10.1016/j.stem.2009.03.007
71. McCarthy HE, Bara JJ, Brakspear K, et al. The comparison of equine articular cartilage progenitor cells and bone marrow-derived stromal cells as potential cell sources for cartilage repair in the horse. *Vet J* 2012;192(3):345-51. doi: 10.1016/j.tvjl.2011.08.036 [published Online First: 20111002]
72. Collins DH, Mc ET. Sulphate (35SO4) uptake by chondrocytes in relation to histological changes in osteoarthritic human articular cartilage. *Ann Rheum Dis* 1960;19(4):318-30. doi: 10.1136/ard.19.4.318 [published Online First: 1960/12/01]
73. Mankin HJ, Dorfman H, Lippiello L, Zarins A. Biochemical and Metabolic Abnormalities in Articular Cartilage from Osteo-Arthritic Human Hips: II. CORRELATION OF MORPHOLOGY WITH BIOCHEMICAL AND METABOLIC DATA. *JBJS* 1971;53(3)
74. Kurose R, Ichinohe S, Tajima G, et al. Characterization of human synovial fluid cells of 26 patients with osteoarthritis knee for cartilage repair therapy. *International journal of rheumatic diseases* 2010;13(1):68-74. doi: doi:https://dx.doi.org/10.1111/j.1756-185X.2009.01456.x
75. Seol D, McCabe DJ, Choe H, et al. Chondrogenic progenitor cells respond to cartilage injury. *Arthritis & Rheumatism* 2012;64(11):3626-37. doi: https://doi.org/10.1002/art.34613
76. Ogata Y, Mabuchi Y, Yoshida M, et al. Purified Human Synovium Mesenchymal Stem Cells as a Good Resource for Cartilage Regeneration. *PloS one* 2015;10(6):e0129096. doi: doi:https://dx.doi.org/10.1371/journal.pone.0129096
77. Riegger J, Palm HG, Brenner RE. The functional role of chondrogenic stem/progenitor cells: novel evidence for immunomodulatory properties and regenerative potential after cartilage injury. *European cells & materials* 2018;36:110-27. doi: doi:https://dx.doi.org/10.22203/eCM.v036a09

78. Sivasubramaniyan K, Koevoet WJLM, Hakimiyan AA, et al. Cell-surface markers identify tissue resident multipotential stem/stromal cell subsets in synovial intimal and sub-intimal compartments with distinct chondrogenic properties. *Osteoarthritis and cartilage* 2019;27(12):1831-40. doi: doi:https://dx.doi.org/10.1016/j.joca.2019.08.006
79. Bi R, Yin Q, Mei J, et al. Identification of Human Temporomandibular Joint Fibrocartilage Stem Cells with Distinct Chondrogenic Capacity. *Osteoarthritis and cartilage* 2020 doi: doi:https://dx.doi.org/10.1016/j.joca.2020.02.835
80. Vinod E, Johnson NN, Kumar S, et al. Migratory chondroprogenitors retain superior intrinsic chondrogenic potential for regenerative cartilage repair as compared to human fibronectin derived chondroprogenitors. *Scientific reports* 2021;11(1):23685. doi: doi:https://dx.doi.org/10.1038/s41598-021-03082-5
81. Vinod E, Parameswaran R, Amirtham SM, et al. Comparative analysis of human bone marrow mesenchymal stem cells, articular cartilage derived chondroprogenitors and chondrocytes to determine cell superiority for cartilage regeneration. *Acta histochemica* 2021;123(4):151713. doi: doi:https://dx.doi.org/10.1016/j.acthis.2021.151713
82. Roelofs AJ, Zupan J, Riemen AHK, et al. Joint morphogenetic cells in the adult mammalian synovium. *Nature communications* 2017;8:15040. doi: doi:https://dx.doi.org/10.1038/ncomms15040
83. Intema F, Van Roermund PM, Marijnissen AC, et al. Tissue structure modification in knee osteoarthritis by use of joint distraction: an open 1-year pilot study. *Annals of the rheumatic diseases* 2011;70(8):1441-46.
84. Wiegant K, van Roermund PM, Intema F, et al. Sustained clinical and structural benefit after joint distraction in the treatment of severe knee osteoarthritis. *Osteoarthritis and Cartilage* 2013;21(11):1660-67. doi: 10.1016/j.joca.2013.08.006
85. van der Woude JAD, Wiegant K, van Roermund PM, et al. Five-Year Follow-up of Knee Joint Distraction: Clinical Benefit and Cartilaginous Tissue Repair in an Open Uncontrolled Prospective Study. *Cartilage* 2017;8(3):263-71. doi: 10.1177/1947603516665442 [published Online First: 20160826]
86. Jansen MP, Mastbergen SC, MacKay JW, et al. Knee joint distraction results in MRI cartilage thickness increase up to 10 years after treatment. *Rheumatology* 2021;61(3):974-82. doi: 10.1093/rheumatology/keab456
87. Watt FE, Hamid B, Garriga C, et al. The molecular profile of synovial fluid changes upon joint distraction and is associated with clinical response in knee osteoarthritis. *Osteoarthritis Cartilage* 2020;28(3):324-33. doi: 10.1016/j.joca.2019.12.005 [published Online First: 20200102]
88. Sabzevari S, Ebrahimpour A, Roudi MK, Kachooei AR. High Tibial Osteotomy: A Systematic Review and Current Concept. *Arch Bone Jt Surg* 2016;4(3):204-12.
89. Thambiah MD, Tan MKL, Hui JHP. Role of High Tibial Osteotomy in Cartilage Regeneration - Is Correction of Malalignment Mandatory for Success? *Indian J Orthop* 2017;51(5):588-99. doi: 10.4103/ortho.IJOrtho_260_17
90. Steijns J, Green D, Peeters LCW, et al. Proteomic characterization of regenerated cartilage following knee joint distraction; a human case-study.

Connect Tissue Res 2024;65(6):486-96. doi: 10.1080/03008207.2024.2440716 [published Online First: 20241217]
91. Gerwin N, Scotti C, Halleux C, et al. Angiopoietin-like 3-derivative LNA043 for cartilage regeneration in osteoarthritis: a randomized phase 1 trial. *Nat Med* 2022;28(12):2633-45. doi: 10.1038/s41591-022-02059-9 [published Online First: 20221201]
92. Hochberg MC, Guermazi A, Guehring H, et al. Effect of Intra-Articular Sprifermin vs Placebo on Femorotibial Joint Cartilage Thickness in Patients With Osteoarthritis: The FORWARD Randomized Clinical Trial. *JAMA* 2019;322(14):1360-70. doi: 10.1001/jama.2019.14735
93. Kim H, Seo J, Lee Y, et al. The current state of the osteoarthritis drug development pipeline: a comprehensive narrative review of the present challenges and future opportunities. *Ther Adv Musculoskelet Dis* 2022;14:1759720x221085952. doi: 10.1177/1759720x221085952 [published Online First: 20221207]
94. Eltawil NM, De Bari C, Achan P, et al. A novel in vivo murine model of cartilage regeneration. Age and strain-dependent outcome after joint surface injury. *Osteoarthritis Cartilage* 2009;17(6):695-704. doi: 10.1016/j.joca.2008.11.003 [published Online First: 20081113]
95. Rai MF, Sandell LJ. Regeneration of articular cartilage in healer and non-healer mice. *Matrix Biol* 2014;39:50-5. doi: 10.1016/j.matbio.2014.08.011 [published Online First: 20140828]
96. Eldridge SE, Barawi A, Wang H, et al. Agrin induces long-term osteochondral regeneration by supporting repair morphogenesis. *Science Translational Medicine* 2020;12(559):eaax9086. doi: doi:10.1126/scitranslmed.aax9086
97. Hou M, Zhang Y, Zhou X, et al. Kartogenin prevents cartilage degradation and alleviates osteoarthritis progression in mice via the miR-146a/NRF2 axis. *Cell Death Dis* 2021;12(5):483. doi: 10.1038/s41419-021-03765-x [published Online First: 20210513]
98. Johnson K, Zhu S, Tremblay MS, et al. A Stem Cell–Based Approach to Cartilage Repair. *Science* 2012;336(6082):717-21. doi: doi:10.1126/science.1215157
99. Keppie SJ, Mansfield JC, Tang X, et al. Matrix-Bound Growth Factors are Released upon Cartilage Compression by an Aggrecan-Dependent Sodium Flux that is Lost in Osteoarthritis. *Function (Oxf)* 2021;2(5):zqab037. doi: 10.1093/function/zqab037 [published Online First: 2021/08/24]
100. Chia SL, Sawaji Y, Burleigh A, et al. Fibroblast growth factor 2 is an intrinsic chondroprotective agent that suppresses ADAMTS-5 and delays cartilage degradation in murine osteoarthritis. *Arthritis Rheum* 2009;60(7):2019-27. doi: 10.1002/art.24654 [published Online First: 2009/07/01]
101. Tang X, Muhammad H, McLean C, et al. Connective tissue growth factor contributes to joint homeostasis and osteoarthritis severity by controlling the matrix sequestration and activation of latent TGFβ. *Ann Rheum Dis* 2018;77(9):1372-80. doi: 10.1136/annrheumdis-2018-212964 [published Online First: 2018/06/22]
102. Zhu L, Muhammad H, Perry TA, et al. Mechano-activated chondroprogenitors (MACs) drive intrinsic cartilage repair; a process that is arrested in osteoarthritis. *bioRxiv* 2025:2025.08.21.671507. doi: 10.1101/2025.08.21.671507

103. de Kroon LM, Narcisi R, Blaney Davidson EN, et al. Activin receptor-like kinase receptors ALK5 and ALK1 are both required for TGFβ-induced chondrogenic differentiation of human bone marrow-derived mesenchymal stem cells. *PloS one* 2015;10(12):e0146124.
104. Bougault C, Aubert-Foucher E, Paumier A, et al. Dynamic compression of chondrocyte-agarose constructs reveals new candidate mechanosensitive genes. *PloS one* 2012;7(5):e36964.
105. Furumatsu T, Matsumoto E, Kanazawa T, et al. Tensile strain increases expression of CCN2 and COL2A1 by activating TGF-β-Smad2/3 pathway in chondrocytic cells. *Journal of biomechanics* 2013;46(9):1508-15.
106. Tachmazidou I, Hatzikotoulas K, Southam L, et al. Identification of new therapeutic targets for osteoarthritis through genome-wide analyses of UK Biobank data. *Nature Genetics* 2019;51(2):230-36. doi: 10.1038/s41588-018-0327-1
107. Gardiner MD, Vincent TL, Driscoll C, et al. Transcriptional analysis of micro-dissected articular cartilage in post-traumatic murine osteoarthritis. *Osteoarthritis and Cartilage* 2015;23(4):616-28. doi: https://doi.org/10.1016/j.joca.2014.12.014
108. Bakker A, Van De Loo F, Van Beuningen H, et al. Overexpression of active TGF-beta-1 in the murine knee joint: evidence for synovial-layer-dependent chondro-osteophyte formation. *Osteoarthritis and cartilage* 2001;9(2):128-36.
109. van Beuningen HM, Glansbeek HL, van der Kraan PM, van den Berg WB. Differential effects of local application of BMP-2 or TGF-β1 on both articular cartilage composition and osteophyte formation. *Osteoarthritis and Cartilage* 1998;6(5):306-17.
110. Scharstuhl A, Vitters EL, van der Kraan PM, van den Berg WB. Reduction of osteophyte formation and synovial thickening by adenoviral overexpression of transforming growth factor β/bone morphogenetic protein inhibitors during experimental osteoarthritis. *Arthritis & Rheumatism: Official Journal of the American College of Rheumatology* 2003;48(12):3442-51.
111. Zhen G, Wen C, Jia X, et al. Inhibition of TGF-β signaling in mesenchymal stem cells of subchondral bone attenuates osteoarthritis. *Nature medicine* 2013;19(6):704-12.
112. Shen J, Li J, Wang B, et al. Deletion of the transforming growth factor β receptor type II gene in articular chondrocytes leads to a progressive osteoarthritis-like phenotype in mice. *Arthritis Rheum* 2013;65(12):3107-19. doi: 10.1002/art.38122
113. Tan Q, Wang Q, Kuang L, et al. TGF-β/Alk5 signaling prevents osteoarthritis initiation via regulating the senescence of articular cartilage stem cells. *J Cell Physiol* 2021;236(7):5278-92. doi: 10.1002/jcp.30231 [published Online First: 20210116]
114. Dell'Accio F, De Bari C, El Tawil NMF, et al. Activation of WNT and BMP signaling in adult human articular cartilage following mechanical injury. *Arthritis Research & Therapy* 2006;8(5):R139. doi: 10.1186/ar2029
115. Papathanasiou I, Malizos KN, Tsezou A. Bone morphogenetic protein-2-induced Wnt/β-catenin signaling pathway activation through enhanced low-density-lipoprotein receptor-related protein 5 catabolic activity contributes to hypertrophy in osteoarthritic chondrocytes. *Arthritis Res Ther* 2012;14(2):R82. doi: 10.1186/ar3805 [published Online First: 20120418]

116. Zhou T, Gao B, Fan Y, et al. Piezo1/2 mediate mechanotransduction essential for bone formation through concerted activation of NFAT-YAP1-ß-catenin. *elife* 2020;9:e52779.
117. Wang S, Li W, Zhang P, et al. Mechanical overloading induces GPX4-regulated chondrocyte ferroptosis in osteoarthritis via Piezo1 channel facilitated calcium influx. *Journal of advanced research* 2022;41:63-75.
118. Gan D, Tao C, Jin X, et al. Piezo1 activation accelerates osteoarthritis progression and the targeted therapy effect of artemisinin. *Journal of Advanced Research* 2024;62:105-17.
119. Li M, Zhang FJ, Bai RJ. The Hippo-YAP Signaling Pathway in Osteoarthritis and Rheumatoid Arthritis. *J Inflamm Res* 2024;17:1105-20. doi: 10.2147/jir.S444758 [published Online First: 20240219]
120. Yousef H, Alhajj M, Fakoya AO, Sharma S. Anatomy, Skin (Integument), Epidermis. StatPearls. Treasure Island (FL): StatPearls Publishing

121. Chu DH, Loomis CA. 48 - Structure and Development of the Skin and Cutaneous Appendages. In: Polin RA, Abman SH, Rowitch DH, et al., eds. Fetal and Neonatal Physiology (Fifth Edition): Elsevier 2017:490-98.e1.
122. Clayton K, Vallejo AF, Davies J, et al. Langerhans Cells-Programmed by the Epidermis. *Front Immunol* 2017;8:1676. doi: 10.3389/fimmu.2017.01676 [published Online First: 20171129]
123. Zhao R, Jackson CJ, Xue M. Extracellular Matrix and Other Factors that Impact on Cutaneous Scarring. In: Shiffman MA, Low M, eds. Chronic Wounds, Wound Dressings and Wound Healing. Cham: Springer International Publishing 2021:135-78.
124. Smith LT, Holbrook KA, Madri JA. Collagen types I, III, and V in human embryonic and fetal skin. *Am J Anat* 1986;175(4):507-21. doi: 10.1002/aja.1001750409
125. Burd DA, Longaker MT, Adzick NS, et al. Foetal wound healing in a large animal model: the deposition of collagen is confirmed. *Br J Plast Surg* 1990;43(5):571-7. doi: 10.1016/0007-1226(90)90122-g
126. Syed F, Ahmadi E, Iqbal SA, et al. Fibroblasts from the growing margin of keloid scars produce higher levels of collagen I and III compared with intralesional and extralesional sites: clinical implications for lesional site-directed therapy. *Br J Dermatol* 2011;164(1):83-96. doi: 10.1111/j.1365-2133.2010.10048.x
127. Behrens DT, Villone D, Koch M, et al. The epidermal basement membrane is a composite of separate laminin- or collagen IV-containing networks connected by aggregated perlecan, but not by nidogens. *J Biol Chem* 2012;287(22):18700-9. doi: 10.1074/jbc.M111.336073 [published Online First: 20120409]
128. Sugawara K, Tsuruta D, Ishii M, et al. Laminin-332 and -511 in skin. *Experimental Dermatology* 2008;17(6):473-80. doi: https://doi.org/10.1111/j.1600-0625.2008.00721.x
129. Baumann L, Bernstein EF, Weiss AS, et al. Clinical Relevance of Elastin in the Structure and Function of Skin. *Aesthet Surg J Open Forum* 2021;3(3):ojab019. doi: 10.1093/asjof/ojab019 [published Online First: 20210514]

130. du Crest D, Madhumita M, Enbiale W, et al. Skin and Digital–The 2024 Narrative. *Mayo Clinic Proceedings: Digital Health* 2024;2(3):322-30. doi: https://doi.org/10.1016/j.mcpdig.2024.05.008
131. Yakupu A, Aimaier R, Yuan B, et al. The burden of skin and subcutaneous diseases: findings from the global burden of disease study 2019. *Front Public Health* 2023;11:1145513. doi: 10.3389/fpubh.2023.1145513 [published Online First: 20230417]
132. Richard MA, Paul C, Nijsten T, et al. Prevalence of most common skin diseases in Europe: a population-based study. *J Eur Acad Dermatol Venereol* 2022;36(7):1088-96. doi: 10.1111/jdv.18050 [published Online First: 20220322]
133. Shah JB. The history of wound care. *J Am Col Certif Wound Spec* 2011;3(3):65-6. doi: 10.1016/j.jcws.2012.04.002
134. Bhattacharya S. Wound healing through the ages. *Indian J Plast Surg* 2012;45(2):177-9. doi: 10.4103/0970-0358.101255
135. George Broughton I, Janis JE, Attinger CE. A brief history of wound care. *Plastic and reconstructive surgery* 2006;117(7S):6S-11S.
136. Georgiadis J, Nascimento VB, Donat C, et al. Dakin's Solution: "One of the most important and far-reaching contributions to the armamentarium of the surgeons". *Burns* 2019;45(7):1509-17. doi: https://doi.org/10.1016/j.burns.2018.12.001
137. Bryan J. Moist wound healing: a concept that changed our practice. *J Wound Care* 2004;13(6):227-8. doi: 10.12968/jowc.2004.13.6.26625
138. Ozgok Kangal MK, Kopitnik NL. Physiology, Wound Healing. StatPearls. Treasure Island (FL): StatPearls Publishing

139. Pierce GF, Mustoe TA, Lingelbach J, et al. Platelet-derived growth factor and transforming growth factor-beta enhance tissue repair activities by unique mechanisms. *J Cell Biol* 1989;109(1):429-40. doi: 10.1083/jcb.109.1.429
140. Ellis S, Lin EJ, Tartar D. Immunology of Wound Healing. *Curr Dermatol Rep* 2018;7(4):350-58. doi: 10.1007/s13671-018-0234-9 [published Online First: 20180928]
141. Broughton G, 2nd, Janis JE, Attinger CE. The basic science of wound healing. *Plast Reconstr Surg* 2006;117(7 Suppl):12s-34s. doi: 10.1097/01.prs.0000225430.42531.c2
142. Zomer HD, Trentin AG. Skin wound healing in humans and mice: Challenges in translational research. *J Dermatol Sci* 2018;90(1):3-12. doi: 10.1016/j.jdermsci.2017.12.009 [published Online First: 20171226]
143. Ito M, Yang Z, Andl T, et al. Wnt-dependent de novo hair follicle regeneration in adult mouse skin after wounding. *Nature* 2007;447(7142):316-20.
144. Martinot V, Mitchell V, Fevrier P, et al. Comparative study of split thickness skin grafts taken from the scalp and thigh in children. *Burns* 1994;20(2):146-50.
145. Levy V, Lindon C, Zheng Y, et al. Epidermal stem cells arise from the hair follicle after wounding. *Faseb j* 2007;21(7):1358-66. doi: 10.1096/fj.06-6926com [published Online First: 20070125]
146. Brownell I, Guevara E, Bai CB, et al. Nerve-derived sonic hedgehog defines a niche for hair follicle stem cells capable of becoming epidermal stem cells. *Cell Stem Cell* 2011;8(5):552-65. doi: 10.1016/j.stem.2011.02.021

147. Jensen UB, Lowell S, Watt FM. The spatial relationship between stem cells and their progeny in the basal layer of human epidermis: a new view based on whole-mount labelling and lineage analysis. *Development* 1999;126(11):2409-18.
148. Lu CP, Polak L, Rocha AS, et al. Identification of stem cell populations in sweat glands and ducts reveals roles in homeostasis and wound repair. *Cell* 2012;150(1):136-50. doi: 10.1016/j.cell.2012.04.045
149. Wang M, Zhang J, Qiao C, et al. Comparative analysis of human and mouse transcriptomes during skin wound healing. *Front Cell Dev Biol* 2024;12:1486493. doi: 10.3389/fcell.2024.1486493 [published Online First: 20241029]
150. Callaghan MJ, Chang EI, Seiser N, et al. Pulsed Electromagnetic Fields Accelerate Normal and Diabetic Wound Healing by Increasing Endogenous FGF-2 Release. *Plastic and Reconstructive Surgery* 2008;121(1)
151. Monaco CF, Plewes MR, Przygrodzka E, et al. Basic fibroblast growth factor induces proliferation and collagen production by fibroblasts derived from the bovine corpus luteum†. *Biology of Reproduction* 2023;109(3):367-80. doi: 10.1093/biolre/ioad065
152. Ortega S, Ittmann M, Tsang SH, et al. Neuronal defects and delayed wound healing in mice lacking fibroblast growth factor 2. *Proc Natl Acad Sci U S A* 1998;95(10):5672-7. doi: 10.1073/pnas.95.10.5672
153. Koike Y, Yozaki M, Utani A, Murota H. Fibroblast growth factor 2 accelerates the epithelial-mesenchymal transition in keratinocytes during wound healing process. *Sci Rep* 2020;10(1):18545. doi: 10.1038/s41598-020-75584-7 [published Online First: 20201029]
154. Penn JW, Grobbelaar AO, Rolfe KJ. The role of the TGF-β family in wound healing, burns and scarring: a review. *Int J Burns Trauma* 2012;2(1):18-28. [published Online First: 20120205]
155. Shah M, Foreman DM, Ferguson MW. Neutralisation of TGF-beta 1 and TGF-beta 2 or exogenous addition of TGF-beta 3 to cutaneous rat wounds reduces scarring. *J Cell Sci* 1995;108 (Pt 3):985-1002. doi: 10.1242/jcs.108.3.985
156. Lipson KE, Wong C, Teng Y, Spong S. CTGF is a central mediator of tissue remodeling and fibrosis and its inhibition can reverse the process of fibrosis. *Fibrogenesis & Tissue Repair* 2012;5(1):S24. doi: 10.1186/1755-1536-5-S1-S24
157. Brewer CM, Nelson BR, Wakenight P, et al. Adaptations in Hippo-Yap signaling and myofibroblast fate underlie scar-free ear appendage wound healing in spiny mice. *Dev Cell* 2021;56(19):2722-40.e6. doi: 10.1016/j.devcel.2021.09.008 [published Online First: 20211004]
158. Lee M-J, Byun MR, Furutani-Seiki M, et al. YAP and TAZ Regulate Skin Wound Healing. *Journal of Investigative Dermatology* 2014;134(2):518-25. doi: https://doi.org/10.1038/jid.2013.339
159. Coste B, Mathur J, Schmidt M, et al. Piezo1 and Piezo2 are essential components of distinct mechanically activated cation channels. *Science* 2010;330(6000):55-60. doi: 10.1126/science.1193270 [published Online First: 20100902]
160. Solis AG, Bielecki P, Steach HR, et al. Mechanosensation of cyclical force by PIEZO1 is essential for innate immunity. *Nature* 2019;573(7772):69-74. doi: 10.1038/s41586-019-1485-8 [published Online First: 20190821]

161. Kang H, Hong Z, Zhong M, et al. Piezo1 mediates angiogenesis through activation of MT1-MMP signaling. *Am J Physiol Cell Physiol* 2019;316(1):C92-c103. doi: 10.1152/ajpcell.00346.2018 [published Online First: 20181114]
162. He J, Fang B, Shan S, et al. Mechanical stretch promotes hypertrophic scar formation through mechanically activated cation channel Piezo1. *Cell Death Dis* 2021;12(3):226. doi: 10.1038/s41419-021-03481-6 [published Online First: 20210301]
163. Griffin M, Wan D, Longaker M. Piezo Inhibition Prevents and Rescues Scarring by Targeting the Adipocyte to Fibroblast Transition. *Plast Reconstr Surg Glob Open* 2024;12(Suppl 8) doi: 10.1097/01.GOX.0001063984.58514.f7 [published Online First: 20240918]
164. Nakamura H, Izumoto Y, Kambe H, et al. Molecular cloning of complementary DNA for a novel human hepatoma-derived growth factor. Its homology with high mobility group-1 protein. *J Biol Chem* 1994;269(40):25143-9.
165. Yang J, Everett AD. Hepatoma derived growth factor binds DNA through the N-terminal PWWP domain. *BMC Molecular Biology* 2007;8(1):101. doi: 10.1186/1471-2199-8-101
166. Hu TH, Wu JC, Huang ST, et al. HDGF stimulates liver tumorigenesis by enhancing reactive oxygen species generation in mitochondria. *J Biol Chem* 2023;299(11):105335. doi: 10.1016/j.jbc.2023.105335 [published Online First: 20231010]
167. Enomoto H, Nakamura H, Liu W, Nishiguchi S. Hepatoma-Derived Growth Factor: Its Possible Involvement in the Progression of Hepatocellular Carcinoma. *International Journal of Molecular Sciences* 2015;16(6):14086-97.
168. Lukasik SM, Cierpicki T, Borloz M, et al. High resolution structure of the HDGF PWWP domain: a potential DNA binding domain. *Protein Sci* 2006;15(2):314-23. doi: 10.1110/ps.051751706 [published Online First: 20051229]
169. Kishima Y, Yamamoto H, Izumoto Y, et al. Hepatoma-derived Growth Factor Stimulates Cell Growth after Translocation to the Nucleus by Nuclear Localization Signals*. *Journal of Biological Chemistry* 2002;277(12):10315-22. doi: https://doi.org/10.1074/jbc.M111122200
170. Shinohara T, Singh DP, Fatma N. LEDGF, a survival factor, activates stress-related genes. *Progress in Retinal and Eye Research* 2002;21(3):341-58. doi: https://doi.org/10.1016/S1350-9462(02)00007-1
171. Shun MC, Raghavendra NK, Vandegraaff N, et al. LEDGF/p75 functions downstream from preintegration complex formation to effect gene-specific HIV-1 integration. *Genes Dev* 2007;21(14):1767-78. doi: 10.1101/gad.1565107
172. Daugaard M, Baude A, Fugger K, et al. LEDGF (p75) promotes DNA-end resection and homologous recombination. *Nature Structural & Molecular Biology* 2012;19(8):803-10. doi: 10.1038/nsmb.2314
173. Izumoto Y, Kuroda T, Harada H, et al. Hepatoma-Derived Growth Factor Belongs to a Gene Family in Mice Showing Significant Homology in the Amino Terminus. *Biochemical and Biophysical Research Communications* 1997;238(1):26-32. doi: https://doi.org/10.1006/bbrc.1997.7233

174. Baude A, Aaes TL, Zhai B, et al. Hepatoma-derived growth factor-related protein 2 promotes DNA repair by homologous recombination. *Nucleic Acids Res* 2016;44(5):2214-26. doi: 10.1093/nar/gkv1526 [published Online First: 20151231]
175. Gao K, Xu C, Jin X, et al. HDGF-related protein-2 (HRP-2) acts as an oncogene to promote cell growth in hepatocellular carcinoma. *Biochem Biophys Res Commun* 2015;458(4):849-55. doi: 10.1016/j.bbrc.2015.02.042 [published Online First: 20150214]
176. Zhu X, Lan B, Yi X, et al. HRP2-DPF3a-BAF complex coordinates histone modification and chromatin remodeling to regulate myogenic gene transcription. *Nucleic Acids Res* 2020;48(12):6563-82. doi: 10.1093/nar/gkaa441
177. Ikegame K, Yamamoto M, Kishima Y, et al. A New Member of a Hepatoma-Derived Growth Factor Gene Family Can Translocate to the Nucleus. *Biochemical and Biophysical Research Communications* 1999;266(1):81-87. doi: https://doi.org/10.1006/bbrc.1999.1733
178. DIETZ F, FRANKEN S, YOSHIDA K, et al. The family of hepatoma-derived growth factor proteins: characterization of a new member HRP-4 and classification of its subfamilies. *Biochemical Journal* 2002;366(2):491-500. doi: 10.1042/bj20011811
179. Uhlén M, Fagerberg L, Hallström BM, et al. Tissue-based map of the human proteome. *Science* 2015;347(6220):1260419. doi: doi:10.1126/science.1260419
180. Yoshida K, Nakamura H, Okuda Y, et al. Expression of hepatoma-derived growth factor in hepatocarcinogenesis. *J Gastroenterol Hepatol* 2003;18(11):1293-301. doi: 10.1046/j.1440-1746.2003.03191.x
181. Yoshida K, Tomita Y, Okuda Y, et al. Hepatoma-Derived Growth Factor Is a Novel Prognostic Factor for Hepatocellular Carcinoma. *Annals of Surgical Oncology* 2006;13(2):159-67. doi: 10.1245/ASO.2006.11.035
182. Enomoto H, Nakamura H, Liu W, et al. Hepatoma-derived growth factor is induced in liver regeneration. *Hepatol Res* 2009;39(10):988-97. doi: 10.1111/j.1872-034X.2009.00532.x [published Online First: 20090713]
183. Uyama H, Tomita Y, Nakamura H, et al. Hepatoma-derived growth factor is a novel prognostic factor for patients with pancreatic cancer. *Clin Cancer Res* 2006;12(20 Pt 1):6043-8. doi: 10.1158/1078-0432.Ccr-06-1064
184. Chen YT, Chen FW, Chang TH, et al. Hepatoma-derived growth factor supports the antiapoptosis and profibrosis of pancreatic stellate cells. *Cancer Lett* 2019;457:180-90. doi: 10.1016/j.canlet.2019.05.001 [published Online First: 20190509]
185. Liu Y, Wang J, Dong L, et al. Long Noncoding RNA HCP5 Regulates Pancreatic Cancer Gemcitabine (GEM) Resistance By Sponging Hsa-miR-214-3p To Target HDGF. *Onco Targets Ther* 2019;12:8207-16. doi: 10.2147/ott.S222703 [published Online First: 20191004]
186. Han Y, Zhang W, Liu Y. Identification of hepatoma-derived growth factor as a potential prognostic and diagnostic marker for extrahepatic cholangiocarcinoma. *World J Surg* 2013;37(10):2419-27. doi: 10.1007/s00268-013-2132-4
187. Tao F, Ye MF, Sun AJ, et al. Prognostic significance of nuclear hepatoma-derived growth factor expression in gallbladder cancer. *World J Gastroenterol* 2014;20(28):9564-9. doi: 10.3748/wjg.v20.i28.9564

188. Matsuyama A, Inoue H, Shibuta K, et al. Hepatoma-derived growth factor is associated with reduced sensitivity to irradiation in esophageal cancer. *Cancer Res* 2001;61(15):5714-7.
189. Yamamoto S, Tomita Y, Hoshida Y, et al. Expression level of hepatoma-derived growth factor correlates with tumor recurrence of esophageal carcinoma. *Ann Surg Oncol* 2007;14(7):2141-9. doi: 10.1245/s10434-007-9369-9 [published Online First: 20070502]
190. Bao CH, Wang XT, Ma W, et al. Irradiated fibroblasts promote epithelial-mesenchymal transition and HDGF expression of esophageal squamous cell carcinoma. *Biochem Biophys Res Commun* 2015;458(2):441-7. doi: 10.1016/j.bbrc.2015.02.001 [published Online First: 20150210]
191. Lee KH, Choi EY, Kim MK, et al. Hepatoma-derived growth factor regulates the bad-mediated apoptotic pathway and induction of vascular endothelial growth factor in stomach cancer cells. *Oncol Res* 2010;19(2):67-76. doi: 10.3727/096504010x12864748215043
192. Yamamoto S, Tomita Y, Hoshida Y, et al. Expression of hepatoma-derived growth factor is correlated with lymph node metastasis and prognosis of gastric carcinoma. *Clin Cancer Res* 2006;12(1):117-22. doi: 10.1158/1078-0432.Ccr-05-1347
193. Wang Q, Chen C, Ding Q, et al. METTL3-mediated m(6)A modification of HDGF mRNA promotes gastric cancer progression and has prognostic significance. *Gut* 2020;69(7):1193-205. doi: 10.1136/gutjnl-2019-319639 [published Online First: 20191003]
194. Liao F, Dong W, Fan L. Apoptosis of human colorectal carcinoma cells is induced by blocking hepatoma-derived growth factor. *Med Oncol* 2010;27(4):1219-26. doi: 10.1007/s12032-009-9362-1 [published Online First: 20091119]
195. Chang KC, Tai MH, Lin JW, et al. Hepatoma-derived growth factor is a novel prognostic factor for gastrointestinal stromal tumors. *Int J Cancer* 2007;121(5):1059-65. doi: 10.1002/ijc.22803
196. Hu TH, Lin JW, Chen HH, et al. The expression and prognostic role of hepatoma-derived growth factor in colorectal stromal tumors. *Dis Colon Rectum* 2009;52(2):319-26. doi: 10.1007/DCR.0b013e31819d1666
197. Lepourcelet M, Tou L, Cai L, et al. Insights into developmental mechanisms and cancers in the mammalian intestine derived from serial analysis of gene expression and study of the hepatoma-derived growth factor (HDGF). *Development* 2005;132(2):415-27. doi: 10.1242/dev.01579 [published Online First: 20041216]
198. Tsai H-E, Wu J-C, Kung M-L, et al. Up-Regulation of Hepatoma-Derived Growth Factor Facilities Tumor Progression in Malignant Melanoma. *PLOS ONE* 2013;8(3):e59345. doi: 10.1371/journal.pone.0059345
199. Sedlmaier A, Wernert N, Gallitzendörfer R, et al. Overexpression of hepatoma-derived growth factor in melanocytes does not lead to oncogenic transformation. *BMC Cancer* 2011;11:457. doi: 10.1186/1471-2407-11-457 [published Online First: 20111020]
200. Chen S-C, Kung M-L, Hu T-H, et al. Hepatoma-derived growth factor regulates breast cancer cell invasion by modulating epithelial–mesenchymal transition. *The Journal of Pathology* 2012;228(2):158-69. doi: https://doi.org/10.1002/path.3988

201. Han S, Tian Z, Tian H, et al. HDGF promotes gefitinib resistance by activating the PI3K/AKT and MEK/ERK signaling pathways in non-small cell lung cancer. *Cell Death Discov* 2023;9(1):181. doi: 10.1038/s41420-023-01476-0 [published Online First: 20230610]
202. Everett AD, Lobe DR, Matsumura ME, et al. Hepatoma-derived growth factor stimulates smooth muscle cell growth and is expressed in vascular development. *J Clin Invest* 2000;105(5):567-75. doi: 10.1172/jci7497
203. Narron JV, Stoops TD, Barringhaus K, et al. Hepatoma-Derived Growth Factor Is Expressed after Vascular Injury in the Rat and Stimulates Smooth Muscle Cell Migration. *Pediatric Research* 2006;59(6):778-83. doi: 10.1203/01.pdr.0000219299.24435.4f
204. Okuda Y, Nakamura H, Yoshida K, et al. Hepatoma-derived growth factor induces tumorigenesis in vivo through both direct angiogenic activity and induction of vascular endothelial growth factor. *Cancer Sci* 2003;94(12):1034-41. doi: 10.1111/j.1349-7006.2003.tb01397.x
205. Enomoto H, Nakamura H, Liu W, et al. Down-regulation of HDGF Inhibits the Growth of Hepatocellular Carcinoma Cells In Vitro and In Vivo. *Anticancer Res* 2015;35(12):6475-9.
206. Cilley RE, Zgleszewski SE, Chinoy MR. Fetal lung development: airway pressure enhances the expression of developmental genes. *J Pediatr Surg* 2000;35(1):113-8; discussion 19. doi: 10.1016/s0022-3468(00)80026-3
207. Mori M, Morishita H, Nakamura H, et al. Hepatoma-derived growth factor is involved in lung remodeling by stimulating epithelial growth. *Am J Respir Cell Mol Biol* 2004;30(4):459-69. doi: 10.1165/rcmb.2003-0013OC [published Online First: 20030911]
208. Zhou Y, Chen P, Liu Q, et al. Hepatoma-Derived Growth Factor Secreted from Mesenchymal Stem Cells Reduces Myocardial Ischemia-Reperfusion Injury. *Stem Cells Int* 2017;2017:1096980. doi: 10.1155/2017/1096980 [published Online First: 20171114]
209. Ooi BN, Mukhopadhyay A, Masilamani J, et al. Hepatoma-derived growth factor and its role in keloid pathogenesis. *J Cell Mol Med* 2010;14(6a):1328-37. doi: 10.1111/j.1582-4934.2009.00779.x [published Online First: 20090511]
210. Hollander A, D'Onofrio PM, Magharious MM, et al. Quantitative Retinal Protein Analysis after Optic Nerve Transection Reveals a Neuroprotective Role for Hepatoma-Derived Growth Factor on Injured Retinal Ganglion Cells. *Investigative Ophthalmology & Visual Science* 2012;53(7):3973-89. doi: 10.1167/iovs.11-8350
211. Chen SC, Hu TH, Huang CC, et al. Hepatoma-derived growth factor/nucleolin axis as a novel oncogenic pathway in liver carcinogenesis. *Oncotarget* 2015;6(18):16253-70. doi: 10.18632/oncotarget.3608
212. Bremer S, Klein K, Sedlmaier A, et al. Hepatoma-derived growth factor and nucleolin exist in the same ribonucleoprotein complex. *BMC Biochem* 2013;14:2. doi: 10.1186/1471-2091-14-2 [published Online First: 20130110]
213. Zhao J, Yu H, Lin L, et al. Interactome study suggests multiple cellular functions of hepatoma-derived growth factor (HDGF). *Journal of Proteomics* 2011;75(2):588-602. doi: https://doi.org/10.1016/j.jprot.2011.08.021

214. Gallitzendoerfer R, Abouzied MM, Hartmann D, et al. Hepatoma-derived growth factor (HDGF) is dispensable for normal mouse development. *Developmental Dynamics* 2008;237(7):1875-85. doi: https://doi.org/10.1002/dvdy.21589
215. Maddaluno L, Urwyler C, Werner S. Fibroblast growth factors: key players in regeneration and tissue repair. *Development* 2017;144(22):4047-60. doi: 10.1242/dev.152587
216. Alfaro MP, Deskins DL, Wallus M, et al. A physiological role for connective tissue growth factor in early wound healing. *Lab Invest* 2013;93(1):81-95. doi: 10.1038/labinvest.2012.162 [published Online First: 20121119]
217. Narron JV, Stoops TD, Barringhaus K, et al. Hepatoma-derived growth factor is expressed after vascular injury in the rat and stimulates smooth muscle cell migration. *Pediatr Res* 2006;59(6):778-83. doi: 10.1203/01.pdr.0000219299.24435.4f [published Online First: 20060426]
218. Singh S, Zheng JJ, Peiper SC, McLaughlin BJ. Gene expression profile of ARPE-19 during repair of the monolayer. *Graefes Arch Clin Exp Ophthalmol* 2001;239(12):946-51. doi: 10.1007/s004170100371
219. Kessler D, Dethlefsen S, Haase I, et al. Fibroblasts in Mechanically Stressed Collagen Lattices Assume a "Synthetic" Phenotype*. *Journal of Biological Chemistry* 2001;276(39):36575-85. doi: https://doi.org/10.1074/jbc.M101602200
220. Neyman J, Pearson ES. On the use and interpretation of certain test criteria for purposes of statistical inference part I. *Biometrika* 1928;20(1-2):175-240.
221. Hemmings BA, Restuccia DF. PI3K-PKB/Akt pathway. *Cold Spring Harb Perspect Biol* 2012;4(9):a011189. doi: 10.1101/cshperspect.a011189 [published Online First: 2012/09/07]
222. Eswarakumar VP, Lax I, Schlessinger J. Cellular signaling by fibroblast growth factor receptors. *Cytokine & Growth Factor Reviews* 2005;16(2):139-49. doi: https://doi.org/10.1016/j.cytogfr.2005.01.001
223. Schlessinger J. Common and Distinct Elements in Cellular Signaling via EGF and FGF Receptors. *Science* 2004;306(5701):1506-07. doi: 10.1126/science.1105396
224. Hoelzinger DB, Quinton SJ, Walters DK, et al. Extracellular vesicle proteomic analysis leads to the discovery of HDGF as a new factor in multiple myeloma biology. *Blood Advances* 2022;6(11):3458-71. doi: 10.1182/bloodadvances.2021006187
225. Han S, Tian Z, Tian H, et al. HDGF promotes gefitinib resistance by activating the PI3K/AKT and MEK/ERK signaling pathways in non-small cell lung cancer. *Cell Death Discovery* 2023;9(1):181. doi: 10.1038/s41420-023-01476-0
226. Skandalis SS, Karalis T, Heldin P. Intracellular hyaluronan: Importance for cellular functions. *Seminars in Cancer Biology* 2020;62:20-30. doi: https://doi.org/10.1016/j.semcancer.2019.07.002
227. Voelkl K, Gutiérrez-Ángel S, Keeling S, et al. Neuroprotective effects of hepatoma-derived growth factor in models of Huntington's disease. *Life Sci Alliance* 2023;6(11) doi: 10.26508/lsa.202302018 [published Online First: 20230814]
228. Hu B, Qin C, Li L, et al. Midkine promotes glioblastoma progression via PI3K-Akt signaling. *Cancer Cell Int* 2021;21(1):509. doi: 10.1186/s12935-021-02212-3 [published Online First: 2021/09/25]

229. Vincent TL, McClurg O, Troeberg L. The Extracellular Matrix of Articular Cartilage Controls the Bioavailability of Pericellular Matrix-Bound Growth Factors to Drive Tissue Homeostasis and Repair. *Int J Mol Sci* 2022;23(11) doi: 10.3390/ijms23116003 [published Online First: 2022/06/11]
230. Abarca-Buis RF, Mandujano-Tinoco EA, Cabrera-Wrooman A, Krötzsch E. The complexity of TGFβ/activin signaling in regeneration. *J Cell Commun Signal* 2021;15(1):7-23. doi: 10.1007/s12079-021-00605-7 [published Online First: 20210122]
231. Enomoto H, Nakamura H, Nishikawa H, et al. Hepatoma-Derived Growth Factor: An Overview and Its Role as a Potential Therapeutic Target Molecule for Digestive Malignancies. *Int J Mol Sci* 2020;21(12) doi: 10.3390/ijms21124216 [published Online First: 20200613]
232. Nameki N, Tochio N, Koshiba S, et al. Solution structure of the PWWP domain of the hepatoma-derived growth factor family. *Protein Science* 2005;14(3):756-64. doi: https://doi.org/10.1110/ps.04975305
233. LeRoy G, Oksuz O, Descostes N, et al. LEDGF and HDGF2 relieve the nucleosome-induced barrier to transcription in differentiated cells. *Sci Adv* 2019;5(10):eaay3068. doi: 10.1126/sciadv.aay3068 [published Online First: 20191002]
234. Kim D, Langmead B, Salzberg SL. HISAT: a fast spliced aligner with low memory requirements. *Nature Methods* 2015;12(4):357-60. doi: 10.1038/nmeth.3317
235. Liao Y, Smyth GK, Shi W. featureCounts: an efficient general purpose program for assigning sequence reads to genomic features. *Bioinformatics* 2013;30(7):923-30. doi: 10.1093/bioinformatics/btt656
236. Patro R, Duggal G, Love MI, et al. Salmon provides fast and bias-aware quantification of transcript expression. *Nature Methods* 2017;14(4):417-19. doi: 10.1038/nmeth.4197
237. Love MI, Huber W, Anders S. Moderated estimation of fold change and dispersion for RNA-seq data with DESeq2. *Genome Biology* 2014;15(12):550. doi: 10.1186/s13059-014-0550-8
238. Korotkevich G, Sukhov V, Budin N, et al. Fast gene set enrichment analysis. *bioRxiv* 2021:060012. doi: 10.1101/060012
239. Liberzon A, Birger C, Thorvaldsdóttir H, et al. The Molecular Signatures Database (MSigDB) hallmark gene set collection. *Cell Syst* 2015;1(6):417-25. doi: 10.1016/j.cels.2015.12.004
240. Liang Z, Damianou A, Vendrell I, et al. Proximity proteomics reveals UCH-L1 as an essential regulator of NLRP3-mediated IL-1β production in human macrophages and microglia. *Cell Reports* 2024;43(5) doi: 10.1016/j.celrep.2024.114152
241. Howe DG, Blake JA, Bradford YM, et al. Model organism data evolving in support of translational medicine. *Lab Anim (NY)* 2018;47(10):277-89. doi: 10.1038/s41684-018-0150-4 [published Online First: 20180917]
242. Jinnah HA. HPRT1 Disorders. In: Adam MP, Feldman J, Mirzaa GM, et al., eds. GeneReviews(®). Seattle (WA): University of Washington, Seattle

243. Ahmadi M, Eftekhari Kenzerki M, Akrami SM, et al. Overexpression of HPRT1 is associated with poor prognosis in head and neck squamous cell

carcinoma. *FEBS Open Bio* 2021;11(9):2525-40. doi: 10.1002/2211-5463.13250 [published Online First: 20210804]
244. Townsend MH, Felsted AM, Burrup W, et al. Examination of Hypoxanthine Guanine Phosphoribosyltransferase as a biomarker for colorectal cancer patients. *Mol Cell Oncol* 2018;5(4):e1481810. doi: 10.1080/23723556.2018.1481810 [published Online First: 20180801]
245. M JS, E IR, Choudhari R, et al. Hypoxanthine Phosphoribosyl Transferase 1 Is Upregulated, Predicts Clinical Outcome and Controls Gene Expression in Breast Cancer. *Cancers (Basel)* 2020;12(6) doi: 10.3390/cancers12061522 [published Online First: 20200610]
246. Bajad P, Ebner F, Amman F, et al. An internal deletion of ADAR rescued by MAVS deficiency leads to a minute phenotype. *Nucleic Acids Res* 2020;48(6):3286-303. doi: 10.1093/nar/gkaa025
247. O'Donohue MF, Choesmel V, Faubladier M, et al. Functional dichotomy of ribosomal proteins during the synthesis of mammalian 40S ribosomal subunits. *J Cell Biol* 2010;190(5):853-66. doi: 10.1083/jcb.201005117
248. Svoboda AJ, McConkey EH. Crosslinking of proteins to ribosomal RNA in HeLa cell polysomes by sodium periodate. *Biochemical and Biophysical Research Communications* 1978;81(4):1145-52. doi: https://doi.org/10.1016/0006-291X(78)91256-1
249. Tolan DR, Hershey JWB, Traut RT. Crosslinking of eukaryotic initiation factor eIF3 to the 40S ribosomal subunit from rabbit reticulocytes. *Biochimie* 1983;65(7):427-36. doi: https://doi.org/10.1016/S0300-9084(83)80062-5
250. Westermann P, Heumann W, Bommer U-A, et al. Crosslinking of initiation factor eIF-2 to proteins of the small subunit of rat liver ribosomes. *FEBS Letters* 1979;97(1):101-04. doi: https://doi.org/10.1016/0014-5793(79)80061-7
251. Westermann P, Nygård O, Bielka H. Cross-linking of Met-tRNAf to eIF-2 beta and to the ribosomal proteins S3a and S6 within the eukaryotic inhibition complex, eIF-2 .GMPPCP.Met-tRNAf.small ribosomal subunit. *Nucleic Acids Res* 1981;9(10):2387-96. doi: 10.1093/nar/9.10.2387
252. Takahashi Y, Ogata K. Ribosomal proteins cross-linked to natural mRNA by UV irradiation of rat liver polysomes. *J Biochem* 1981;90(5):1549-52. doi: 10.1093/oxfordjournals.jbchem.a133624
253. Naora H, Takai I, Adachi M, Naora H. Altered cellular responses by varying expression of a ribosomal protein gene: sequential coordination of enhancement and suppression of ribosomal protein S3a gene expression induces apoptosis. *J Cell Biol* 1998;141(3):741-53. doi: 10.1083/jcb.141.3.741
254. Russell L, Naora H, Naora H. Down-regulated RPS3a/nbl Expression during Retinoid-induced Differentiation of HL-60 Cells: A Close Association with Diminished Susceptibility to Actinomycin D-stimulated Apoptosis. *Cell Structure and Function* 2000;25(2):103-13. doi: 10.1247/csf.25.103
255. Hu ZB, Minden MD, McCulloch EA. Regulation of drug sensitivity by ribosomal protein S3a. *Blood* 2000;95(3):1047-55. doi: https://doi.org/10.1182/blood.V95.3.1047.003k43_1047_1055
256. Tang Y, He Y, Li C, et al. RPS3A positively regulates the mitochondrial function of human periaortic adipose tissue and is associated with coronary artery diseases. *Cell Discov* 2018;4:52. doi: 10.1038/s41421-018-0041-2 [published Online First: 20180821]

257. Uechi T, Nakajima Y, Nakao A, et al. Ribosomal protein gene knockdown causes developmental defects in zebrafish. *PLoS One* 2006;1(1):e37. doi: 10.1371/journal.pone.0000037 [published Online First: 20061220]
258. Zhou C, Weng J, Liu C, et al. High RPS3A expression correlates with low tumor immune cell infiltration and unfavorable prognosis in hepatocellular carcinoma patients. *Am J Cancer Res* 2020;10(9):2768-84. [published Online First: 20200901]
259. Lim KH, Kim KH, Choi SI, et al. RPS3a over-expressed in HBV-associated hepatocellular carcinoma enhances the HBx-induced NF-κB signaling via its novel chaperoning function. *PLoS One* 2011;6(8):e22258. doi: 10.1371/journal.pone.0022258 [published Online First: 20110816]
260. Chaudhry N, Muhammad H, Seidl C, et al. Highly efficient CRISPR-Cas9-mediated editing identifies novel mechanosensitive microRNA-140 targets in primary human articular chondrocytes. *Osteoarthritis and Cartilage* 2022;30(4):596-604. doi: 10.1016/j.joca.2022.01.005
261. Hu T-H, Huang C-C, Liu L-F, et al. Expression of hepatoma-derived growth factor in hepatocellular carcinoma. *Cancer* 2003;98(7):1444-56. doi: https://doi.org/10.1002/cncr.11653
262. Rowland MB, Moore PE, Bui C, Correll RN. Assessing wound closure in mice using skin-punch biopsy. *STAR Protoc* 2023;4(1):101989. doi: 10.1016/j.xpro.2022.101989 [published Online First: 20230104]
263. van de Vyver M, Boodhoo K, Frazier T, et al. Histology Scoring System for Murine Cutaneous Wounds. *Stem Cells Dev* 2021;30(23):1141-52. doi: 10.1089/scd.2021.0124 [published Online First: 20210714]
264. Bankhead P, Loughrey MB, Fernández JA, et al. QuPath: Open source software for digital pathology image analysis. *Scientific Reports* 2017;7(1):16878. doi: 10.1038/s41598-017-17204-5
265. Vu R, Jin S, Sun P, et al. Wound healing in aged skin exhibits systems-level alterations in cellular composition and cell-cell communication. *Cell Rep* 2022;40(5):111155. doi: 10.1016/j.celrep.2022.111155
266. Jackson SJ, Andrews N, Ball D, et al. Does age matter? The impact of rodent age on study outcomes. *Lab Anim* 2017;51(2):160-69. doi: 10.1177/0023677216653984 [published Online First: 20160710]
267. Nishio N, Okawa Y, Sakurai H, Isobe K. Neutrophil depletion delays wound repair in aged mice. *Age (Dordr)* 2008;30(1):11-9. doi: 10.1007/s11357-007-9043-y [published Online First: 20080108]
268. Costa RA, Ruiz-de-Souza V, Jr. GMA, et al. Effects of strain and age on ear wound healing and regeneration in mice. *Brazilian Journal of Medical and Biological Research* 2009;42(12):1143-49. doi: 10.1590/s0100-879x2009005000042
269. Sagi L, Trau H. The Koebner phenomenon. *Clinics in Dermatology* 2011;29(2):231-36. doi: https://doi.org/10.1016/j.clindermatol.2010.09.014
270. Zhang X, Lei L, Jiang L, et al. Characteristics and pathogenesis of Koebner phenomenon. *Experimental Dermatology* 2023;32(4):310-23. doi: https://doi.org/10.1111/exd.14709
271. Rousselle P, Braye F, Dayan G. Re-epithelialization of adult skin wounds: Cellular mechanisms and therapeutic strategies. *Advanced Drug Delivery Reviews* 2019;146:344-65. doi: https://doi.org/10.1016/j.addr.2018.06.019
272. Morhenn VB, Nahm WJ, Mansbridge JN. Psoriatic keratinocytes are resistant to tumor necrosis factor alpha's induction of mRNA for the NMDA-R2C

subunit. *Experimental Dermatology* 2013;22(11):750-51. doi: https://doi.org/10.1111/exd.12242
273. Glotzer DJ, Zelzer E, Olsen BR. Impaired skin and hair follicle development in Runx2 deficient mice. *Dev Biol* 2008;315(2):459-73. doi: 10.1016/j.ydbio.2008.01.005 [published Online First: 20080116]
274. Hansen LS, Coggle JE, Wells J, Charles MW. The influence of the hair cycle on the thickness of mouse skin. *The Anatomical Record* 1984;210(4):569-73. doi: https://doi.org/10.1002/ar.1092100404
275. León-Sosa A, Castañeda V, Espinosa-Vallejo R, et al. Key points for translating wound regenerative agents from in vivo assays in mice to clinical validation. *Cytotherapy* 2022;24(11):1074-86. doi: https://doi.org/10.1016/j.jcyt.2022.07.004
276. Xue Y, Lim CH, Plikus MV, et al. Wound-Induced Hair Neogenesis Model. *J Invest Dermatol* 2022;142(10):2565-69. doi: 10.1016/j.jid.2022.07.013
277. Rønø B, Engelholm LH, Lund LR, Hald A. Gender Affects Skin Wound Healing in Plasminogen Deficient Mice. *PLOS ONE* 2013;8(3):e59942. doi: 10.1371/journal.pone.0059942
278. Romana-Souza B, Assis de Brito TL, Pereira GR, Monte-Alto-Costa A. Gonadal hormones differently modulate cutaneous wound healing of chronically stressed mice. *Brain, Behavior, and Immunity* 2014;36:101-10. doi: https://doi.org/10.1016/j.bbi.2013.10.015
279. Bianchi ME. DAMPs, PAMPs and alarmins: all we need to know about danger. *Journal of Leukocyte Biology* 2006;81(1):1-5. doi: 10.1189/jlb.0306164
280. Ring NAR, Dworak H, Bachmann B, et al. The p-rpS6-zone delineates wounding responses and the healing process. *Developmental Cell* 2023;58(11):981-92.e6. doi: 10.1016/j.devcel.2023.04.001
281. Ariosa-Morejon Y, Santos A, Fischer R, et al. Age-dependent changes in protein incorporation into collagen-rich tissues of mice by in vivo pulsed SILAC labelling. *eLife* 2021;10:e66635. doi: 10.7554/eLife.66635

8. Supplementary

Supplementary Table 1. Range of RNA integrity numbers (RIN) of samples sent for bulk RNA sequencing

Sample name	Tissue type	RIN
KO_0h_1	cartilage	7.3
KO_0h_2	cartilage	6.9
KO_0h_3	cartilage	7.2
KO_0h_4	cartilage	7.4
KO_4h_1	cartilage	7.6
KO_4h_2	cartilage	7.7
KO_4h_3	cartilage	8
KO_4h_4	cartilage	7.1
WT_0h_1	cartilage	7.6
WT_0h_2	cartilage	6.8
WT_0h_3	cartilage	7.9
WT_0h_4	cartilage	8.2
WT_4h_1	cartilage	7.4
WT_4h_2	cartilage	8.6
WT_4h_3	cartilage	8.9
WT_4h_4	cartilage	8.2
KO_0h_1	skin	4.7
KO_0h_2	skin	5.1
KO_0h_3	skin	5.3
KO_0h_4	skin	5.4
WT_0h_1	skin	5
WT_0h_2	skin	6.1
WT_0h_3	skin	4.9
WT_0h_4	skin	4.2

Abbreviations: wild type (WT), HDGF-knockout (KO), h-hour.

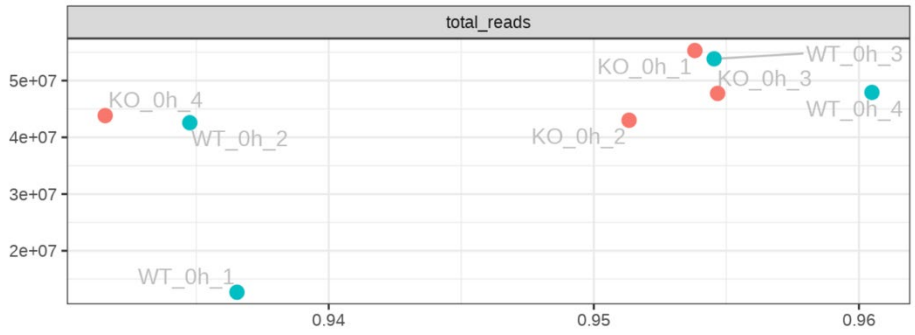

Supplementary Figure 1. Total number of reads detected in skin samples sent for bulk RNA sequencing. WT_0h_1 sample showed significantly less reads than other samples and was excluded from analysis. Abbreviations: wild type (WT), HDGF-knockout (KO), h-hour.